UNIVERSITÄT ZU LÜBECK

From the Institute of Nutritional Medicine
of the University of Lübeck
Director: Prof. Dr. med. Christian Sina

Microbial metabolite butyrate promotes the induction of IL-10^{+}IgM^{+} plasma cells

Dissertation
for Fulfillment of
Requirements
for the Doctoral Degree
of the University of Lübeck

from the Department of Natural Sciences

Submitted by

Bandik Föh
from Kiel, Germany

Lübeck 2022

First referee: Prof. Dr. med. Christian Sina

Second referee: Prof. Dr. rer. nat. Rudolf Manz

Chairman of the board: Prof. Dr. rer. nat. Lars Redecke

Date of oral examination: November 3rd, 2022

Approved for printing. Lübeck, November 9th, 2022

Results of the present work have been published recently in the peer-reviewed scientific journal PLOS ONE [1].

All experiments were planned and performed at the Institute of Nutritional Medicine, University of Lübeck, Germany, or the Division of Immunobiology (Divanovic Lab), Cincinnati Children's Hospital Medical Center, Cincinnati, Ohio, USA. Text passages with no or minor changes were only adopted from published articles if they were originally phrased by the author.

1 ABSTRACT 8

2 ZUSAMMENFASSUNG 9

3 INTRODUCTION 11

3.1 Regulatory B cells 11

3.1.1 Definition 11
3.1.2 Modes of action 11
3.1.3 Milestones in Breg research 12
3.1.4 Origin and Phenotype 14

3.2 Plasma cells - an overview 17

3.2.1 Definition 17
3.2.2 Plasma cell differentiation 17
3.2.3 Murine markers of plasma cells 18
3.2.4 Antibodies 20
3.2.5 Regulatory plasma cells 23

3.3 Short-chain fatty acids 25

3.3.1 Definition 25
3.3.2 Source of SCFAs 26
3.3.3 Energy resource 27
3.3.4 Ligands for G-protein-coupled receptors 27
3.3.5 Inhibitors of histone deacetylases 28
3.3.6 Effects of SCFAs on B cells 29

3.4 Study objectives 30

4 MATERIALS AND METHODS 31

4.1 Animal experiments 31

4.1.1 Mice 31
4.1.2 Immunization and butyrate treatment *in vivo* 32
4.1.3 Dissection and tissue collection 34

4.2 Preparation of single-cell suspensions 34

4.2.1 Single-cell suspension from spleens 34

4.3 Magnetic Activated Cell Sorting of B cells 34

4.3.1 Principle 34
4.3.2 Modified manufacturer's protocol 35

4.4 B cell culture 35

4.5 Flow cytometry 36

4.5.1 Principle 36
4.5.2 Fluidics 36
4.5.3 Optics 37
4.5.4 Electronics 37
4.5.5 General remarks 38
4.5.6 Antibody-labeling 38
4.5.7 Mitochondrial staining 38
4.5.8 Surface staining 39
4.5.9 Intracellular staining 40
4.5.10 Measurements and analyses 41

4.6 RNA-isolation 41

4.6.1 RNA isolation from B cell cultures 41

4.7 cDNA-transcription 43

4.8 Real-time quantitative polymerase chain reaction 44

4.8.1 Principle and analysis 44
4.8.2 Primers 44
4.8.3 Protocol 45

4.9 ELISA 45

4.9.1 Principle of sandwich-ELISAs 45
4.9.2 Protocol 46

4.10 Seahorse analysis 46

4.10.1 Principle 46
4.10.2 Modulators of mitochondrial function used in the Seahorse assay 46
4.10.3 Seahorse analysis of B cells 48
4.10.4 Calculation of mitochondrial parameters 50

4.11 Lists of Materials 51

4.11.1 Buffers, Solutions, and Media 51
4.11.2 Commercially available Kits 52
4.11.3 Instruments 52
4.11.4 Antibodies and dyes for flow cytometry 53
4.11.5 Other reagents 54
4.11.6 Small equipment 55
4.11.7 Primers 56

4.11.8 Software 57

4.12 Statistics 58

4.13 Graphics 58

5 RESULTS 59

5.1 BA induces IL-10^{+}IgM^{+} plasma cells *ex vivo* 59

5.1.1 BA induces splenic CD138^{high} plasma cells ex vivo 59
5.1.2 BA alters the expression of several regulators of plasma cell differentiation . 60
5.1.3 BA but not PA induces gene expression of regulatory cytokines *ex vivo* 62
5.1.4 BA induces the differentiation of IL-10^{+} CD138^{high} plasma cells *ex vivo* 65
5.1.5 IL-10^{+} CD138^{high} plasma cells preferentially express IgM *ex vivo* 67

5.2 BA induces splenic IL-10^{+}IgM^{+} plasma cells *in vivo* 68

5.2.1 BA induces splenic CD138^{high} plasma cells *in vivo* 68
5.2.2 BA administration induces splenic IL-10^{+} plasma cells *in vivo* 69
5.2.3 IL-10^{+} plasma cells preferentially express IgM *in vivo* after BA treatment 71
5.2.4 IgM^{+} plasma cells preferentially express IL-10 *in vivo* after BA treatment 72
5.2.5 BA induces IL-10^{+}IgM^{+} CD138^{high} plasma cells *in vivo* 74
5.2.6 BA promotes antigen-specific plasma cells and IgM *in vivo* 76

5.3 Sialylation capacity of IL-10^{+} plasma cells 78

5.3.1 Splenic IL-10^{+} plasma cells express increased levels of St6gal1 78

5.4 Mechanisms of IL-10 plasma cell induction by BA 80

5.4.1 GPR43 ligands do not induce plasma cells *ex vivo* 80
5.4.2 BA but not PA increases H3K27 acetylation in B cells *ex vivo* 82
5.4.3 HDAC3 inhibition is sufficient to induce plasma cells *ex vivo* 83
5.4.4 HDAC3 inhibition is sufficient to induce regulatory cytokines *ex vivo* 84
5.4.5 Short-term BA treatment increases mitochondrial respiration in isolated murine B cells 86
5.4.6 BA treatment for 24 hours suppresses mitochondrial respiration in B cells ... 88
5.4.7 BA reduces mitochondrial mass and ROS after 24 hours of incubation 90

6 DISCUSSION 97

6.1 Overview 97

6.2 BA induces plasma cell differentiation 99

6.3 BA induces transcription of plasma cell-specific genes 102

6.4 BA induces IL-10 expression in B cells and plasma cells *ex vivo* 103

6.5 BA induces IL-10 expression in plasma cells *in vivo* 104

6.6 IL-10^{+} plasma cells preferentially express IgM 105

6.7 Increased St6gal1 expression in IL-10^{+} plasma cells 107

6.8 HDAC3 inhibition is a possible underlying pathway 108

6.9 Decreased mitochondrial ROS production after HDAC3 inhibition mediates plasma cell differentiation 111

6.10 Additional limitations and outlook 112

7 REFERENCES 114

8 APPENDIX 133

8.1 Abbreviations 133

8.2 List of peer-reviewed publications 136

8.3 Conference contributions 140

8.3.1 Talks 140
8.3.2 Posters 140

8.4 Acknowledgments 141

8.5 Curriculum vitae 142

1 ABSTRACT

The microbial metabolite butyrate belongs to the family of short-chain fatty acids and is produced from dietary fiber by commensal bacteria in the gut. Butyrate has been shown to possess extensive immunosuppressive potential, particularly on macrophages, T, and B lymphocytes. Recently, butyrate has been shown to induce the anti-inflammatory cytokine IL-10 in B cells. However, the IL-10 producing regulatory B cell subtype, as well as the corresponding mechanism remained elusive.

In this study, butyrate, but not the related short-chain fatty acid propionate, was shown to potently induce the differentiation of IL-10^{+} plasma cells in cell culture. Furthermore, *in vivo* administration of butyrate via drinking water or daily intraperitoneal injection increased the frequencies of IL-10^{+} CD138^{high} plasma cells in the spleen of foreign protein antigen (Ovalbumin) plus adjuvant-immunized mice. Anti-inflammatory properties of IL-10^{+} plasma cells had already been described before. Accordingly, the here characterized IL-10^{+} plasma cells were preferentially antigen-unspecific and expressed IgM. Underlying mechanisms most likely include the inhibition of histone deacetylase 3 (HDAC3) and reduced mitochondrial superoxide production for plasma cell differentiation. Additionally, HDAC3 inhibition, but not reduced superoxide production, was sufficient for IL-10 induction.

Taken together, this work characterizes the anti-inflammatory potential of butyrate on B cells. The induction of IgM^{+}IL-10^{+} plasma cells, together with further anti-inflammatory functions of butyrate, underline its great anti-inflammatory potential. HDAC3 inhibition by fiber-induced butyrate generation, butyrate supplementation, or the pharmaceutical provision of specific HDAC3 inhibitors might have the potential to be used as a therapeutic pathway to treat inflammatory (auto-)immune diseases. Butyrate is already approved as a nutritional supplement without known side effects, and might therefore be an easily available therapeutic agent, that should be evaluated in further studies.

2 ZUSAMMENFASSUNG

Butyrat ist ein mikrobieller Metabolit aus der Familie der kurzkettigen Fettsäuren und wird von kommensalen Bakterien im Darm aus Ballaststoffen mittels Fermentation hergestellt. Butyrat besitzt ein umfangreiches immunsuppressives Potenzial, zum Beispiel bei der Regulation von Makrophagen, T- und B-Lymphozyten. Kürzlich wurde zudem gezeigt, dass Butyrat in B-Lymphozyten das anti-inflammatorische Zytokin IL-10 induzieren kann. Der durch Butyrat induzierte IL-10-produzierende regulatorische B Zell Subtyp und der Wirkmechanismus blieben jedoch unklar.

In dieser Studie konnte gezeigt werden, dass Butyrat, aber nicht die verwandte kurzkettige Fettsäure Propionat, die Differenzierung insbesondere von IL-10^{+}-Plasmazellen in Zellkultur induziert. Darüber hinaus erhöhte die *in-vivo*-Applikation von Butyrat über das Trinkwasser oder eine tägliche intraperitoneale Injektion die Häufigkeit von IL-10^{+} CD138^{high} Plasmazellen in der Milz von Fremdprotein-Antigen (Ovalbumin) plus Adjuvant-immunisierten Mäusen. IL-10^{+} Plasmazellen wurden im Vorfeld dieser Arbeit bereits anti-inflammatorische Wirkungen zugeschrieben. Die hier charakterisierten, überwiegend Antigen-unspezifischen IL-10^{+} Plasmazellen exprimierten vorzugsweise IgM. Die Hemmung der Histon-Deacetylase 3 (HDAC3) und eine reduzierte mitochondriale Superoxidproduktion wurden als mögliche Mechanismen von Butyrat für die erhöhte Plasmazelldifferenzierung identifiziert. Die HDAC3-Hemmung war zudem im Gegensatz zur reduzierten Superoxid-Konzentration auch hinreichend für die IL-10-Induktion.

Diese Arbeit konnte einen potentiellen anti-inflammatorischen Wirkmechnismus von Butyrat, die Induktion von IL-10+ IgM+ Plasmazellen, genauer charakterisieren. Zusammen mit weiteren anti-inflammatorischen Wirkungen unterstreichen die Ergebnisse das anti-inflammatorische Potenzial von Butyrat. Die HDAC3-Hemmung durch Ballaststoff-induzierte Butyrat-Produktion, eine geeignete Butyrat-Supplementierung oder die pharmazeutische Bereitstellung spezifischer HDAC3-Inhibitoren könnten basierend auf den Ergebnissen dieser Arbeit das Potenzial besitzen, in einem therapeutischen Ansatz bei inflammatorischen (Auto-)Immunerkrankungen eingesetzt zu werden. Butyrat ist bereits als Nahrungsergänzungsmittel ohne bekannte Nebenwirkungen zugelassen und könnte

daher ein leicht verfügbares Therapeutikum darstellen, das in weiteren Studien evaluiert werden sollte.

3 INTRODUCTION

3.1 Regulatory B cells

3.1.1 Definition

Regulatory B cells (Bregs) are subsets of B lymphocytes with anti-inflammatory, immunosuppressive capacities. Despite considerable efforts to identify a common Breg marker, they are characterized rather by their function than by specific surface antigens or transcription factors [2]. Instead, several subtypes of B cells with regulatory properties have been described [3]. A common similarity between most, but not all Breg subtypes is the production of regulatory cytokines, especially IL-10 [3,4], which is also an important hallmark of other immune cells with immunosuppressive properties including regulatory T cells (Tregs) [5,6].

3.1.2 Modes of action

The result of an effective immune response to injury or pathogens is inflammation, which aims for wound healing and/or the clearance of a pathogen [7]. During inflammation, the immune system is activated in a cascade-like manner, which can lead to detrimental effects, if not resolved properly [7]. In healthy individuals with adequate regulatory mechanisms, however, the immune response is self-limiting and immunosuppressive mediators and cytokines, especially IL-10, IL-35, and TGFβ, play a critical role in that process [8,9]. If the resolution of inflammation fails, autoimmune diseases are a potential consequence [7].

Bregs are a major source of those cytokines that exert anti-inflammatory functions including reduced activation and differentiation of inflammatory immune cells in mice [10,11] and humans [12,13]. Additionally, recent evidence has indicated specific Breg subsets with increased expression of Programmed death-ligand 1 (PD-L1). PD-L1^{hi} Bregs have been shown to efficiently suppress antibody production, T cell activation and to protect against EAE [14]. However, the production of especially IL-10, IL-35, and TGFβ is considered the major mode of action [3].

3.1.3 Milestones in Breg research

3.1.3.1 Animal studies

While Bregs have only recently been recognized as important contributors to immunoregulation and protection against overshooting inflammatory (auto-)immune responses [15], the first evidence of an immunosuppressive role of B cells was already provided decades before:

In 1974, B cells were shown to suppress the immune reaction in a model of delayed hypersensitivity in pigs, although possible underlying mechanisms were not determined and remained elusive for decades [16,17]. The next notable publication on the topic was released in 1996 by *Wolf et al.* and dealt with the consequences of B cell depletion in a murine model of multiple sclerosis (MS) [18]. In this study, B cell-depleted mice showed no significant difference in onset and maximum severity of experimental autoimmune encephalitis (EAE) but, in contrast to non-depleted mice, did not recover from the disease model at all [18]. Similarly, *Mizoguchi et al.* reported a suppressive potential of B cells in a murine model of inflammatory bowel diseases (IBD), although the mechanisms remained unclear [19].

It took another five years until two independent studies showed that IL-10-production specifically is important for the suppression of autoimmunity by B cells in models of MS, IBD, and likely other autoimmune diseases [20,21]. These results were corroborated by *Mauri et al.* in a study from 2003, demonstrating that IL-10-producing B cells prevent the induction of and ameliorate established collagen-induced arthritis in mice [22]. Additionally, protection from allergic hypersensitivity by parasitic helminth infection is linked to increased IL-10-producing B cells [23]. More recently, several elegant studies have provided additional evidence for the significant role of Bregs in IBD pathogenesis. While B cells isolated from a spontaneous mouse model of Crohn's disease displayed reduced production of IL-10 and TGFβ [24], IL-10-producing B cells were independently shown to suppress intestinal inflammation in dextran sodium sulfate (DSS)-induced [25,26], T cell-transfer [27], and IL-$10^{-/-}$ colitis models [26,28]. Furthermore, it was shown that Breg-depleted mice exhibit significantly aggravated intestinal inflammation in a T cell transfer

model of IBD [29] and that *ex vivo* induced Bregs efficiently protected against experimental colitis and EAE [30].

3.1.3.2 Human studies

Importantly, the relevance of Bregs is not limited to mouse models, but has been demonstrated in various human diseases:

Multiple Sclerosis (MS)

B cells participate significantly in the pathogenesis of MS via multiple pathways. Whereas research in the field traditionally focused on the production of autoreactive antibodies as the main culprit, more recent evidence suggests a crucial contribution of antibody-independent mechanisms, including the secretion of various, functionally diverse cytokines [31]. Impaired Breg function correlates with the development and severity of MS and has been suggested as a therapeutic target [15,31]. Notably, IL-10-production by B cells is reduced in MS patients [32–34], while induction of Bregs by helminth infection partially ameliorates MS [35], recapitulating the results of preceding animal studies [20,23]. Furthermore, therapy with Alemtuzumab, Fingolimod, Siponimod, interferon β (IFN-β), and possibly dimethyl-fumarate all promote IL-10$^+$ Bregs in MS patients, indicating that this might be an underlying mechanism for their therapeutic effects [36–43].

Systemic Lupus Erythematosus (SLE)

The data on Breg frequencies in SLE patients are complex. Although most studies found increased frequencies of some subtypes of Bregs in SLE, these increases have been suggested to be of compensatory origin [12,44–46]. In addition, Bregs from SLE patients seem to be functionally impaired indicating that even though they might be numerically increased, Bregs do not exhibit their immunosuppressive capacity adequately in SLE patients, contributing to the disease phenotype [12,47–49]. Supporting evidence stems from severe SLE cases, that were treated with Rituximab leading to a depletion of CD20$^+$ B cells. The repopulation of those patients with B cells of immunosuppressive capacity correlated with a positive clinical outcome after Rituximab-treatment [49–51]. Moreover, PD-L1$^+$ Bregs have been shown to survive Rituximab therapy and effectively inhibit T cell differentiation [14]. These results point towards the re-establishment of functional Bregs

as a major contributor to successful therapy with Rituximab and support the relevance of Bregs in SLE pathology.

Rheumatoid Arthritis (RA)

In patients suffering from RA, Bregs have been reported to be both numerically and functionally impaired [13]. Several independent studies have demonstrated a reduced frequency of IL-10$^+$ Bregs and an inverse correlation of Breg frequency with disease activity and biological markers of inflammation [52–54]. Additionally, PD-L1$^+$ Bregs are reduced in RA patients and increase upon successful treatment [55]. Recapitulating previous animal studies, these results suggest a crucial role of Bregs in RA pathophysiology.

Inflammatory bowel diseases (IBD)

Compared to other autoimmune diseases reports on Breg frequencies and functions in human IBD are limited. Most notably, *Oka et al.* found that CpG-induced IL-10 production by B cells from Crohn's disease (CD)-patients is significantly reduced, corroborating similar findings in mice [29]. Furthermore, *Wang et al.* reported a reduction of IL-10 and Bregs in patients with Ulcerative Colitis (UC) [56]. In this study, Breg frequency and IL-10 levels correlated inversely with disease activity and laboratory parameters of inflammation [56]. On the contrary, IL-35 levels are increased in IBD patients, possibly as part of a counter-regulatory mechanism toward overshooting intestinal inflammation [57]. Taken together, studies in mice and humans combine to indicate an important role for Bregs in maintaining intestinal homeostasis and in the pathophysiology of IBD.

3.1.4 Origin and Phenotype

IL-10 is the main culprit of the immunosuppressive function of most Breg subtypes and has therefore been used as a marker for identifying different Breg subsets [2,3]. Several of these subsets show similar effector functions but differ in the expression of surface antigens, including markers for immature and mature B cells, or plasma cells (**Table 1,** adapted and modified from *Rosser et al.* [3]). Furthermore, a Breg-defining transcription factor similar to Foxp3 for Tregs has not been identified yet, supporting the hypothesis that Bregs are not derived from one dedicated B cell lineage. Most likely, Bregs can rather arise from different B cell populations in response to adequate stimuli. The question of whether

these stimuli are consistent or vary depending on the B cell subpopulation that is affected remains unclear and needs to be elucidated.

Nevertheless, some contributing stimuli have been identified, including the activation of CD40/80 and Toll-like receptors (e.g. TLR9), which leads to increased IL-10 production by B cells [4]. Bregs may also arise in response to some cytokines, esp. IL-1β, IL-6, and IL-21 [3]. In general, it has been discussed that some inflammatory stimuli, that usually lead to inflammatory responses may also promote Breg differentiation, to prevent overshooting inflammation. Finally, recent evidence points towards microbial metabolites being able to induce Bregs [30].

Breg subset	Mouse	Human	Key Features	References
T2-MZP cells	$CD19^+CD21^{hi}$ $CD23^{hi}CD24^{hi}$	–	found in spleen, produce IL-10, induce Treg cells, suppress effector $CD4^+$ and $CD8^+$ T cells, drive Tr1 differentiation through PD1/PD-L1 expression	Evans et al., 2007 [58]; Blair et al., 2009 [59]; Carter et al., 2011 [11]; Said et al. 2018 [60]
MZ(-like) cells	$CD19^+CD21^{hi}C$ $D23^-$	$CD19^+CD27^+$ IgD^+IgM^{high}	found in spleen, produce IL-10, induce Treg cells, suppress effector $CD4^+$ and $CD8^+$ T cells	Gray et al., 2007 [61]; Bankoti et al., 2012 [62]; Miles et al., 2012 [63]; Chagnon-Choquet, 2014 [64]; Huber et al., 2016 [65]; Appelgren et al. 2018 [66]
B10 cells	$CD5^+CD1d^{hi}$	$CD24^{hi}CD27^+$	found in spleen (mice) and blood (humans), produce IL-10, suppress effector $CD4^+$ T cells, monocytes, and DCs	Yanaba et al., 2009 [67]; Matsushita et al., 2010 [68]; Iwata et al., 2011 [45]; Horikawa et al., 2013 [69]; Hasan et al., 2017 [70]; Zheng et al., 2017 [71]; Shi et al., 2020 [72]
Plasma cells	$CD138^+$	$CD138^+Ig^+$	found in spleen, dLNs, and at sites of inflammation, produce IL-10 and IL-35, suppress NK cells, neutrophils, DCs, effector $CD4^+$, and cytotoxic $CD8^+$ T cells, display high IL-10 levels in lesions of MS patients, recirculate from the gut, and protect from EAE	Rafei et al., 2009 [73]; Neves et al., 2010 [74]; Shen et al., 2014 [75]; Matsumoto et al., 2014 [76], Shalapour et al., 2015 [77]; Lino et al., 2018 [78]; Machado-Santos et al., 2018 [79]; Luu et al., 2019 [30], Rojas et al., 2019 [80]
$Tim1^+$ B cells	$Tim\text{-}1^+CD19^+$	$Tim\text{-}1^+CD19^+$	found in spleen, produce IL-10, suppress effector $CD4^+$ T cells, TIM-1 ligation induces IL-10 production	Ding et al., 2011 [81]; Xiao et al., 2012 [82]; Xiao et al., 2015 [83]; Aravena et al., 2017 [84]
Immature B cells	–	$CD19^+CD24^{hi}$ $CD38^{hi}$	found in blood and at the site of inflammation, produce IL-10, induce Treg cells, suppress $CD8^+$, Th1, and Th17 cells	Blair et al., 2010 [12]; Bosma et al., 2012 [51]; Das et al., 2012 [85]; Flores-Borja et al., 2013 [13]; Hasan et al., 2017 [70]; Wang et al., 2020 [86]
Br1 cells	–	$CD19^+CD25^{hi}$ $CD71^{hi}$	found in blood and produce IL-10 and IgG4	Lee et al., 2013 [87]; van de Veen et al., 2013 [88]

Table 1: Overview of Breg subsets identified in murine and human studies. This table has been adapted from *Rosser et al.* [3] and updated by the addition of several recent publications.

3.2 Plasma cells - an overview

3.2.1 Definition

Plasma cells are white blood cells of 10-18 µm diameter originating from the bone marrow. They are differentiated antibody-secreting cells and derive from the B lymphocytic cell line. They are oval in shape and display abundant basophilic cytoplasm and a characteristic, eccentric nucleus with a cartwheel shape [89]. The main canonical function of plasma cells is the production and secretion of large quantities of antibodies [89,90]. To enable large-scale production, modification, and secretion of proteins, plasma cells display a well-developed rough endoplasmatic reticulum and Golgi apparatus [89].

3.2.2 Plasma cell differentiation

The differentiation of B cells towards plasma cells is a complex process that involves a variety of regulatory factors. Activated B cells can be induced toward plasma cells in secondary lymphoid tissues inside and outside of the germinal center (GC) reaction [91].

T cell-independent antigens induce GC-independent plasma cells. T cell-dependent protein antigens can induce GC-independent and –dependent plasma cells. In short, mature B cells continuously circulate through the follicles of secondary lymphoid organs searching for antigens. Upon antigen encounter, B cells process the antigens and present them via MHC class II. When antigen-presenting B cells are recognized by T helper cells activated by the same antigen they receive T cell help. B cells and T helper cells interact through CD40-CD40L recognition and the secretion of cytokines. This interaction drives B cell proliferation and differentiation. The exact mechanisms deciding about a further GC-independent or -dependent B cell differentiation are not completely understood [91]. GC-dependent B cell differentiation is mainly characterized by affinity maturation of the BCR by a process called somatic hypermutation [91]. BCR class switching has long been attributed to GC reactions. However, BCR class switching can also occur GC-independently [92,93]. For this, cytokine signals activate activation-induced cytidine deaminase (AICDA) leading to immunoglobulin class switch recombination (CSR). During this process, BCRs switch from IgM to one of the mature immunoglobulin classes IgA, IgE, or IgG. Subsequently, activated B cells can either differentiate into memory B cells or plasma cells [91,94].

The signals instructing B cells inside and outside of the GC to differentiate into plasma cells are not completely understood, but several mechanisms have been characterized. One critical factor for plasma cell differentiation is the expression of high-affinity B cell receptors (BCR) that exceed the affinity commonly expressed in memory B cell precursors leading to enhanced signaling within plasma cell precursors [91]. High-affinity BCR signaling alone, however, does not suffice for plasma cell differentiation. Strong T follicular helper (Tfh) cell signaling has been demonstrated to promote plasma cell differentiation. Accordingly, Tfh signaling is heavily imprinted in plasma cell precursors [91,95]. Additional instruction for plasma cell differentiation comes from metabolic, more specifically mitochondrial signaling. Plasma cell precursors display reduced mitochondrial mass and ROS-production, and artificial reduction of mitochondrial ROS levels leads to preferential differentiation towards plasma cells, whereas high ROS levels characterize class switch recombination [96].

After B cells have committed to plasma cell differentiation, they essentially undergo a lineage switch, accompanied by vastly altered gene expression patterns [91]. Surprisingly this fundamental change in cellular biology is instructed by only a few transcription factors, the most important of which are interferon regulatory factor 4 (IRF4), B lymphocyte-induced maturation protein-1 (BLIMP-1, also called PR domain zinc finger protein 1; PRDM1), and X-box binding protein 1 (XBP1). IRF4 is upregulated early after B cell activation [97], and high levels of IRF4 induce BLIMP-1 expression [91]. In turn, BLIMP-1 is the master transcriptional regulator of plasma cell differentiation [98,99] and represses mature B cell genes, including AICDA, paired box protein Pax-5 (PAX5), B-cell lymphoma 6 protein (BCL6), and several more [91,100,101]. Furthermore, BLIMP-1 induces genes essential for plasma cell differentiation including IRF4 [101] and XBP1, which instructs the expansion of cellular structures for the secretion of high amounts of antibodies [102].

3.2.3 Murine markers of plasma cells

Terminally differentiated plasma cells usually express high levels of CD138 (= Syndecan-1). It is a surface protein that binds to insoluble extracellular matrix proteins like collagens and fibronectins, through heparan sulfate chains [103,104]. Additionally, it binds soluble growth factors, including epidermal, fibroblast, and hepatocyte growth factors (EGF, FGF, HGF) [103,104]. Although CD138 has not been described as a receptor by itself, it has been

shown that CD138 acts as a co-receptor for EGF, and "a proliferation-inducing ligand" (APRIL) by binding them in the vicinity of their inherent receptors in myeloma cells [104,105]. No other hematopoietic cells are known to express CD138 [105,106]. CD138 is easily accessible for cell surface staining and subsequent flow cytometric analysis and is, therefore, a convenient surface marker of murine plasma cells. In contrast, human plasma cells are frequently identified by their expression of CD38, since only approximately 50% of circulating human plasma cells express CD138 [107,108].

Several other surface markers for murine plasma cells have been suggested but are mostly not as specific and therefore not as suitable to identify plasma cells by themselves. These suggested markers include a group of three surface receptors: (i) B cell maturation antigen (BCMA), (ii) transmembrane activator and CAML (calcium-modulator and cyclophilin ligand) interactor (TACI), and (iii) B cell-activating factor BAFF receptor (BAFF-R), that interact with the common/ related ligands: BAFF and APRIL. BCMA is expressed by plasma cells and GC B lymphocytes. Activation of BCMA by its ligands BAFF and APRIL promotes the survival of plasma cells [109]. TACI is another surface receptor expressed on mature B lymphocytes but upregulated on both activated B cells and plasma cells. Known ligands of TACI are also BAFF and APRIL. TACI plays a complex role in the activation of B cells but is generally also a promoting factor for B cell maturation and plasma cell survival [109]. BAFF-R can be used as a negative marker since it is typically expressed by many subtypes of B cells but not plasma cells. Its main ligand is BAFF, and activation promotes the maturation of immature and survival of mature B cells [109].

Besides surface markers, there are intracellular transcription factors identifying plasma cells. These markers are rather specific but are also more difficult to analyze because of their intracellular location. Flow cytometric analysis of intracellular transcription markers involves cellular permeabilization and fixation, which is time-consuming. Moreover, it can lead to changes in cell morphology and frequently diminishes the signal of intracellular reporter proteins like green fluorescent protein (GFP). One of the intracellular markers for plasma cell identification is BLIMP-1/PRDM1, the master regulator of plasma cell differentiation as described above [98,99]. However, in addition to plasma cells, BLIMP-1 is also expressed by T cells. Here, it is critically involved in the homeostasis of $CD4^+$ and $CD8^+$ T cells [110]. In plasma cells, BLIMP-1 induces increased expression of XBP1, which is

another intracellular plasma cell marker. XBP1 is an essential differentiation factor for plasma cells inducing a secretory phenotype. However, XBP1 is an unspecific marker as it is expressed ubiquitously in adult tissues [111]. IRF4 is another transcription factor crucially involved in PC differentiation and can be used as an additional intracellular marker of PCs [112]. However, IRF4 specificity for PCs is limited as well, since it is expressed in other B cell subtypes, and regulates the differentiation of T cells, and dendritic cells [113].

Due to its plasma cell specificity and convenient accessibility as an abundantly expressed surface antigen in mice, CD138 is widely used as a murine plasma cell marker in research applications and was utilized in most experiments of the present study.

3.2.4 **Antibodies**

The major canonical function of plasma cells is the production and secretion of antibodies [90]. Antibodies are composed of two identical heavy and two identical light chains (**Figure 1A**). These four chains are arranged in three globular regions to form a roughly Y-shaped protein [114]. The three globular regions can be classified as two antigen-binding fragments (Fab) and one crystallizable fragment (Fc). The main function of the Fab regions is the (specific) binding of antigens. As a part of the Fab, the variable domains have highly heterogenic amino acid sequences to allow for the specific binding of a large variety of antigens [114]. While the Fab region is composed of both heavy and light chains the Fc part only contains the constant domains of the antibody heavy chains. The main function of the Fc part is the interaction with the immune system; mainly the interaction with complement factors and classical Fc-receptors. Two major modifications to the constant domain of antibodies control their biological activity: class switching and Fc glycosylation [114].

3.2.4.1 Class switch recombination (CSR)

During CSR, the constant domain of the heavy chain is changed, while the variable domain remains the same. As a result, the antigen specificity remains unchanged but the immunoglobulin class that is expressed as BCR and/or antibody by the B cell or plasma cell is altered. Initially, mature B cells express IgD and IgM. Activation by BCR signaling leads to the proliferation of antigen-specific B cells and T cell help, co-receptors, and/ or cytokines lead to CSR. During CSR, constant fragments of the heavy chain gene locus are removed from the chromosome. AICDA is one of the enzymes essentially involved in this process

[92]. The expression of IgD and IgM by activated B cells is switched to IgA, IgG, or IgE antibodies. Each immunoglobulin class has different biological functions. Additionally, subclasses with distinct biological activity have been identified for IgG and IgA. In humans, these subclasses have been termed IgG1-4 and IgA1-2. Mice have only one IgA subclass and the murine IgG subclasses are termed IgG1, IgG2a (IgG2c in C57BL/6 mice), IgG2b, and IgG3.

The biological activity of IgG antibodies is generally mediated by their affinity towards different classical Fcγ-receptors and molecules of the complement system and differs distinctly between the subclasses [115]. FcγRIIB is a widely expressed Fcγ-receptor and the only one that is classified as an inhibitory receptor [116]. Furthermore, FcγRIIB is the only classical Fcγ-receptor expressed on B cells and is crucially involved in regulating humoral immunity [116]. Crosslinking of FcγRIIB induces inhibitory signaling that increases, during simultaneous BCR signaling, the threshold for B cell activation [117,118]. The absence of FcγRIIB on B cells promotes uncontrolled B cell activation and the development and exacerbation of autoimmune diseases [116,117]. In addition, isolated crosslinking of FcγRIIB on plasma cells may induce apoptotic signals and efficiently decrease the humoral immune response [116,119]. FcγRIIB is further expressed ubiquitously on innate immune cells and its crosslinking leads to a downregulation of innate effector responses, such as phagocytosis, antibody-dependent cell-mediated cytotoxicity, and the release of pro-inflammatory cytokines [116]. Notably, distinct IgG subclasses are especially prone to activate FcγRIIB. In mice, IgG1 has a higher affinity towards FcγRIIB compared to classical activating Fcγ-receptors; and human IgG4 corresponds to murine IgG1 in this regard [120,121]. Accordingly, murine IgG1 and human IgG4 are immunoglobulin subclasses with high anti-inflammatory potential [115,120,121]. On the other hand, murine IgG2a (IgG2c in C57BL/6 mice) and IgG2b subclasses are particularly associated with proinflammatory properties, such as activation of the complement system [115] and various immune cells via high affinity-binding to classical activating Fcγ receptors [115,122–124].

3.2.4.2 Antibody glycosylation

Another way of modifying the Fc activity of antibodies is the type of Fc glycosylation. Although all immunoglobulin isotypes and subclasses are potentially equipped with glycan chains, the relevance for distinct glycosylation patterns is established best for IgG antibodies. This is due to the unique IgG Fc N-glycosylation site at Asn297 of both heavy

chains of all IgG subclasses in different species (e.g. humans and mice) (**Figure 1A**) compared to several glycosylation sites of IgM, IgD, IgA, and IgE glycosylation [125]. The IgG glycan core attached to Asn297 is composed of two N-acetylglucosamine (GlcNAc) residues, followed by three mannose and two additional GlcNAc residues arranged in a biantennary mode. Additional sugars, each with specific effects on the biological activity of the antibody can be added to this core structure: fucose, bisecting GlcNac, galactose, and sialic acid (**Figure 1B)** [121]**.** Sialylation of IgG antibodies is primarily catalyzed by β-galactoside-α-2,6-sialyltransferase 1 (St6gal1) and has decisive effects on IgG activity by holding the IgG in an open conformation [121,125–127]. Terminal sialylation occurs in approximately 10-15% of total human and mouse IgG antibodies; decreasing with age and inflammation [128].

In intravenous immunoglobulin (IVIg) therapy (treatment of patients with inflammatory diseases with high amounts (2g/kg) of pooled serum IgG from healthy donors), sialylated antigen-unspecific IgG has been suggested to be the major anti-inflammatory component ultimately inducing the upregulation of FcγRIIB expression on immune cells [129]. In addition, C-type lectins have been implicated in mediating the immunosuppressive functions of sialylated IgGs on DCs, macrophages, and T helper cells [130–132]. Accordingly, *ex vivo* sialylation of antigen-specific IgG is effective in treating several murine models of autoimmune diseases and is implicated as a promising target for the treatment of autoimmunity [124,132–134]. In addition to the immunosuppressive effects for sialylated IgG, sialylated IgM [135] and IgA antibodies [136] have shown anti-inflammatory potential as well. Thus, increasing the sialylation of antibodies *in vivo* might be an elegant pathway to inhibit inflammatory immune responses that needs to be explored further.

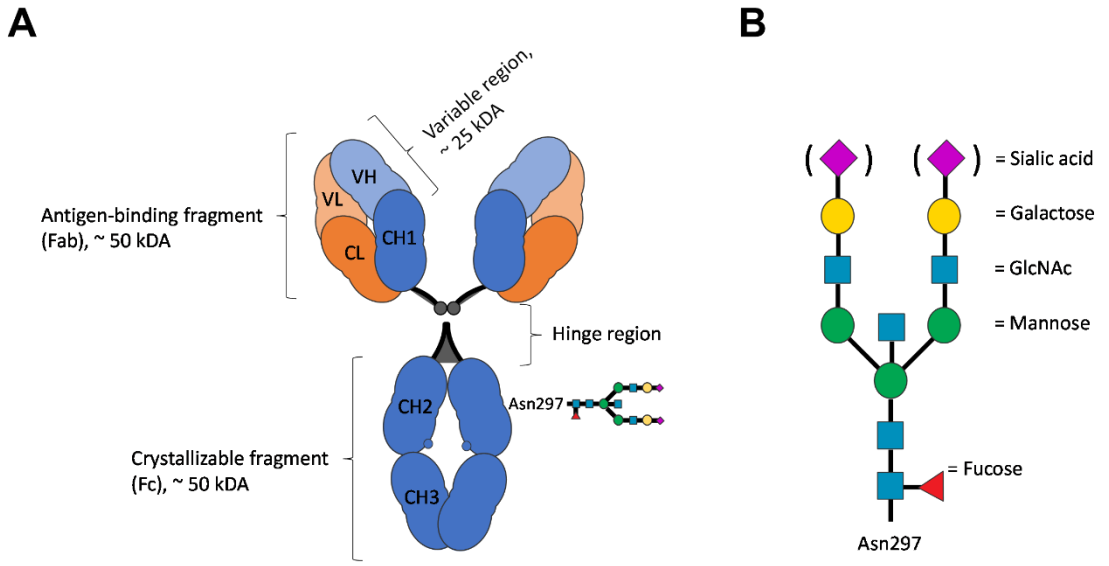

Figure 1: IgG-antibody structure and glycosylation pattern. (A) Schematic representation of the basic structure of IgG-antibodies. Two heavy chains (blue) and two light chains (orange) form three globular domains; one Fc fragment and two Fab-fragments. Fc and Fab fragments are linked by the hinge region (grey/black). Heavy chains and light chains participate in forming the variable regions (Fv), which are crucial for specific antigen recognition. Heavy chains are equipped with glycan chains at Asn297. Asn297 = Asparagine residue 297, CH = constant heavy chain domain, CL = constant light chain domain, Fab = antigen-binding fragment, Fc = crystallizable fragment, VH = variable heavy chain domain, VL = variable light chain domain. **(B)** Schematic representation of a fully equipped glycan at Asn297 of an IgG antibody. The extent of glycosylation of antibodies varies and affects the biological activity and receptor affinity of the antibodies. Particularly, terminal sialylation (purple) leads to a more anti-inflammatory function of IgG antibodies. GlcNAc = N-acetylglycosamine.

3.2.5 Regulatory plasma cells

Beginning in the late 1990s increasing evidence suggested that B cell subsets may act in an immunosuppressive manner on other immune cells and can exert anti-inflammatory functions in autoimmune and infectious diseases (see chapter **3.1**). However, the regulatory role of plasma cells specifically has been investigated only recently. In 2009 it was reported that *ex vivo* treatment of murine B cells with GM-CSF and IL-15 induced the expression of antibodies and CD138 indicative of plasma cells [73]. Notably, CD138 expression occurred in parallel with IL-10 induction, and the resulting IL-10$^+$ CD138$^+$ plasma cells induced complete remission of EAE in mice [73]. Similar effects were observed for gut-derived IgA$^+$ plasma cells that recirculate to the central nervous system in EAE and can

suppress neuroinflammation via the production of IL-10 [80]. The regulatory capacity of IL-10$^+$ CD138^{high} plasma cells is underlined by the suppression of protective immunity during murine *Salmonella typhimurium* infection [74] and the reduction of T cell-dependent immunity [77]. Strikingly, murine CD138^{high} plasma cells have been identified to be the main source of B cell-derived IL-10 in SLE [137], EAE [75], and *Salmonella typhimurium* infection [74,75] indicating a broad role in regulating immunity [138]. In EAE models, CD138^{high} plasma cells were not only the main source of IL-10 but also of IL-35, which was of crucial relevance for the recovery from EAE and for regulating the immune response against *Salmonella* infection [75].

Recently, a natural plasma cell subset expressing LAG3 was identified. These LAG3$^+$ plasma cells were present in naïve mice, expressed IgM, PD-L1, and PD-L2, and strongly upregulated IL-10 upon infection [78]. Expression of the checkpoint ligands PD-L1 and PD-L2 indicates an additional pathway, by which these cells might downregulate cellular immunity. Indeed, studies in solid tumors demonstrate an immunosuppressive role for PD-L1$^+$ Bregs and plasma cells [139]. In three murine prostate cancer models, chemoresistance of tumors against oxaliplatin was mediated by IgA$^+$IL-10$^+$PD-L1$^+$ regulatory plasma cells [77]. These cells inhibited the activation of CD8$^+$ cytotoxic T cells within tumor masses. After eradication of regulatory plasma cells, oxaliplatin therapy was able to induce tumor eradication by CD8$^+$ cytotoxic T cells expressing the PD-L1 receptor PD-1 [77]. Similarly, liver resident IgA$^+$ plasma cells expressing IL-10 and PD-L1 promoted the progression of hepatocellular carcinoma by inducing exhaustion of hepatic CD8$^+$ cytotoxic T cells [140]. Importantly, accumulation of these cells begins in human and murine livers in parallel with fibrosis, but even before the development of hepatocellular carcinoma, indicating a possible role in tumor pathogenesis [140]. In multiple myeloma, CD138$^+$ plasma cells can express PD-L1 as an escape mechanism from cytotoxic T cells [141]. Furthermore, PD-L1 expression in plasma cells from multiple myeloma patients is associated with disease progression [142] and is a possible prognostic biomarker [143].

Overall, there is mounting evidence of a central role of regulatory plasma cells producing different immunosuppressive cytokines, co-receptors, and possibly antibodies in dampening immunity in infection, autoimmune disorders, and cancer.

3.3 Short-chain fatty acids

3.3.1 Definition

Mammals and their microbiome have co-developed to form a complex symbiotic relationship. The largest and most diverse part of the human microbiome is located within the gut. The total catalogued set of genes expressed by gut microbiota amounts to astonishing 10,000,000 genes [144,145] compared to approximately 30,000-40,000 genes in the human genome [146]. The products of these microbial genes provide several functions essential to the host. Among them are host defense and immunoregulatory mechanisms on the one hand, and the digestion of complex food components on the other [147]. Immune regulatory functions of the gut microbiota are often elicited by major microbial constituents like DNA, RNA, proteins, or bacterial wall components that are recognized by the host through pattern-recognition receptors [147]. Those receptors include Toll-like receptors, nucleotide oligomerization receptors, C-type lectin receptors, and RIG-1-like receptors [147]. The digestion of complex macronutrients and the production of micronutrients and vitamins are exerted mostly through a vast array of specialized microbial enzymes which exceeds the human repertoire by far [147].

However, the immune regulatory and digestive functions of microbiota are not mutually exclusive but instead significantly intertwined. Complex food components and intestinal secretions are used by commensal bacteria as energy sources and are converted into microbial metabolites of very diverse structures. Many of these metabolites, exclusively generated by the host's microbiome, have been described to exert immunomodulatory functions through various molecular targets, including intra- and extracellular receptors and enzymes. Based on previous research, microbiome-generated metabolites belonging to the group of short-chain fatty acids (SCFAs) are considered to have the most profound

immunoregulatory impact [148]. By definition, SCFAs are carboxylic acids with an aliphatic chain and fewer than 6 carbon atoms.

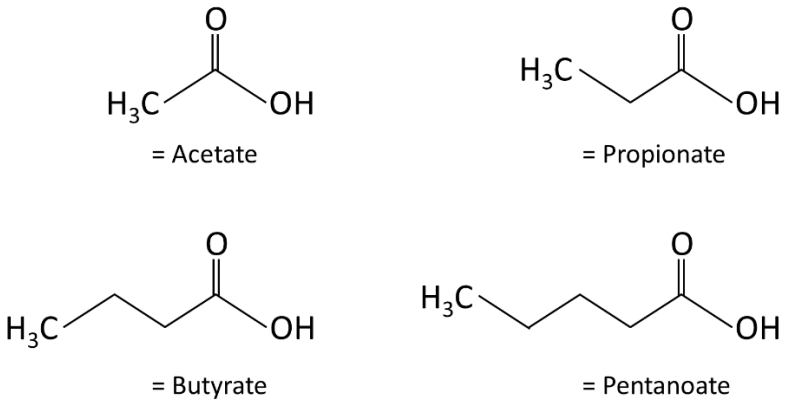

Figure 2: Chemical structures of the immunologically most relevant short-chain fatty acids.

3.3.2 Source of SCFAs

SCFAs are highly abundant in the gut and reach total concentrations of up to 130 mM in the caecum, the majority of which being acetate (AA), propionate (PA), and butyrate (BA) [149] (**Figure 2**). The production of SCFAs is dependent on anaerobic bacterial fermentation of dietary fiber or non-digestible carbohydrates [148]. More specifically, the main substrates for bacterial fermentation and SCFA production are resistant starches, inulin, and pectin. These long-chain molecules are initially degraded to oligosaccharides, monosaccharides, and smaller substrates [148]. The molecular pathways used to generate specific SCFAs and bacterial species involved are different for each SCFA:

AA is mainly produced via Acetyl-CoA or the Wood-Ljungdahl pathway from pyruvate by *Bacteroides, Bifidobacterium, Prevotella, and Ruminococcus* spp. among others [148]. *Akkermansia muciniphilia* is another notable source [148]. PA is a product of lactate, succinate, or propanediol pathways and is produced mainly by members of the Bacteroidetes phylum [148].

Most notably, BA is formed by condensation of two molecules of Acetyl-CoA, which is then reduced to Butyryl-CoA [148]. Two pathways are then employed for the generation of BA. The classical pathway utilizes phospho-transbutyrylase and butyrate kinase and is mainly used by *Coprococcus* spp.. The second pathway uses butyryl-CoA:acetate CoA-transferase and relies on AA or lactate as substrates [150]. It is employed mainly by *Faecalibacterium prausnitzii, Eubacterium rectale,* and *Roseburia spp*. However, there are significantly more bacterial species, that produce SCFAs in relevant amounts [151].

3.3.3 Energy resource

The symbiotic nature of the host-gut microbiome relationship is well exemplified by the use of dietary fiber. Commensal bacteria use the digestion of otherwise indigestible carbohydrates as an energy source. The resulting byproducts, especially BA, are then used also as the main energy source for the host's colonocytes through fatty acid oxidation [152,153]. It has even been proposed that IBD might be caused by an energy deficiency of colonocytes due to a lack of BA [154]. Considering a variety of anti-inflammatory effects of SCFAs, BA treatment is considered a potential option for IBD treatment [155]. Notably, the metabolization of BA leads to higher concentrations of BA in the colonic mucosa than in the portal vein [149]. The hepatic metabolism of SCFAs reduces their levels in peripheral blood even further [149]. However, while concentrations of SCFAs in the systemic circulation are detected only in the micromolar range [149,156], they accumulate in tissues of high immunological relevance, such as mesenteric lymph nodes and the spleen, reaching concentrations between 1 and 1.5 $mmol*kg^{-1}$ in the case of BA [156]. Thus, immunological effects of SCFAs are more likely to occur either in the gastrointestinal tract or in immunological effector organs rather than in the systemic circulation. Despite their role as an energy substrate for colonocytes, oral administration of SCFAs is an effective way of increasing the concentrations of BA and PA in immunological effector organs [156].

3.3.4 Ligands for G-protein-coupled receptors

SCFAs are ligands for several G-protein-coupled receptors (GPRs). Specifically, three GPRs with high affinities for the main SCFAs have been described: GPR43 (free fatty acid receptor 2, FFAR3), GPR41 (FFAR3), and GPR109A. AA, PA, and BA are all ligands for GPR43 (AA = PA > BA) and GPR41 (PA = BA > AA) [151]. While GPR41 is coupled only to $G_{i/o}$-proteins, GPR43

is coupled to both $G_{i/o}$- and G_q-proteins. Interestingly, its functions outside of the intestines are mainly mediated by $G_{i/o}$, whereas G_q-coupling plays an important role inside the gut [157]. There is a third GPCR named GPR109A that binds BA and niacin but not AA, or PA as its main ligands [158].

GPR41 and 43 play a crucial role in regulating host metabolism. In the gut, secretion of glucagon-like peptide-1 by enteroendocrine L-cells is triggered, when GPR41 and 43 are activated, supporting an adequate glucose response to ingested food [157]. Activation of GPR43 in white adipose tissue is involved in regulating satiety, glucose, and lipid metabolism [148]. Moreover, immunomodulatory roles for these GPRs have been described: In the gut, GPR43 mediates neutrophil chemotaxis and affects the severity and resolution of intestinal inflammation [159,160]. GPR41 is involved in microbiota-dependent amelioration of allergic asthma in mice [161]. GPR109A is known for its immunomodulatory effects, whereas its impact on host metabolism seems to be smaller compared to GPR41 and 43 [148]. Stimulation of GPR109A activates anti-inflammatory programs in macrophages and dendritic cells, thereby inducing Tregs and suppressing colonic inflammation and carcinogenesis [162]. Furthermore, both GPR43 and GPR109A expression have been reported to be necessary for the amelioration of experimental colitis by dietary fiber [163].

Most notably, in contrast to the other SCFA-receptors (GPR41, GPR109a), GPR43 is expressed on activated murine B cells [156].

3.3.5 Inhibitors of histone deacetylases

Gene expression is crucially regulated by the acetylation status of DNA-binding histones [164]. Highly acetylated histones are not able to bind DNA tightly and allow for permissive access of transcription factors to their target genes. Deacetylation of histones on the other hand allows them to bind DNA more tightly and repress gene expression [164]. Thereby, acetylation of histones directly affects the transcription of genes. Histone deacetylases (HDACs) are a group of enzymes that is crucially involved in regulating the acetylation status of histones by removing acetyl-groups from ε-N-acetyl-lysine amino acids [165]. The counterpart to HDACs is taken by histone acetyltransferases (HATs), which increase the acetylation of histones. 11 different classical Zn^{2+}-dependent HDACs have been identified

in higher eukaryotes and organized into four classes (class I to IV). Class III additionally features NAD+ dependent sirtuins, that are mechanistically distinct from classical HDACs [165] (**Table 2**).

Class	Members
Class I	HDAC1, HDAC2, HDAC3, HDAC8
Class IIa	HDAC4, HDAC5, HDAC7, HDAC9
Class IIb	HDAC6, HDAC10
Class III (sirtuins)	SIRT1-7
Class IV	HDAC11

Table 2: Classes of HDACs

The first evidence that BA is involved in regulating histone acetylation came from *Riggs et al.* who reported in 1977 that BA caused a rapid and reversible increase in histone acetylation in two distinct cancer cell lines [166]. A year later, it was reported by several groups that inhibition of HDACs by BA was the underlying mechanism [167] and BA remains the most effective HDAC inhibitor among the group of SCFAs. However, PA but not AA has been reported to inhibit HDAC activity as well [167,168]. While both BA and PA inhibit Class I HDACs primarily, the spectrum of inhibition differs between the two SCFAs. While inhibition of Class I HDACs by PA is limited to HDAC1, HDAC2, and HDAC8, BA additionally suppresses HDAC3 activity [169]. Notably, HDAC3 coordinates intestinal homeostasis depending on the presence of commensal bacteria [170]. Furthermore, BA has been shown to promote antimicrobial features in macrophages specifically by inhibiting HDAC3 [171].

3.3.6 Effects of SCFAs on B cells

Multiple immunosuppressive effects of SCFAs have been described, including the differentiation of peripheral regulatory T cells (Tregs) [172,173] and the inhibition of pro-inflammatory cytokine production in peripheral mononuclear blood cells [174], neutrophils [175], macrophages [176], dendritic cells [158,177], and effector $CD4^+$ T cells [30]. However, considering the crucial relevance of B cells in the pathogenesis of autoimmunity and allergy [178], SCFA effects on B cells have not been investigated sufficiently.

In recent years, SCFAs have been shown to mediate antibody secretion in mice supporting antibody responses both in the intestines and systemically [156,179], indicating increased plasma cell activity and/or differentiation. Moreover, recent studies suggest the induction of the anti-inflammatory cytokine IL-10 in B cells by SCFAs, particularly BA and pentanoate [30,180,181]. These studies also demonstrate that these SCFAs protect against experimental mouse models of IBD, multiple sclerosis, sjögren's syndrome, and rheumatoid arthritis [30,180,181]. However, they did not characterize these IL-10-producing B cells further regarding a possible plasma cell phenotype, differential immunoglobulin expression, and antibody sialylation.

3.4 Study objectives

Anti-inflammatory effects of SCFAs on a wide variety of immune cells, including B cells, have been described and recent studies have further suggested that BA can induce IL-10$^+$ regulatory B cells [30,180,181]. However, the IL-10-producing regulatory B cell subtype as well as the corresponding mechanism of BA remained elusive.

Thus, this study aimed to answer the following questions:

1. Does BA, but not PA, induce IL-10$^+$ plasma cells *ex vivo*?
2. Can IL-10$^+$ regulatory plasma cells be induced *in vivo* by the application of BA?
3. What antibodies are generated by BA-induced IL-10$^+$ plasma cells?
4. What are possible underlying mechanisms?

4 MATERIALS AND METHODS

4.1 Animal experiments

4.1.1 Mice

C57BL/6J mice were purchased at 8 weeks of age from Charles River Laboratories for experiments performed at the animal facility of the University of Lübeck, Lübeck, Germany, or from Jackson Laboratories for experiments performed at the animal facility of the Cincinnati Children's Hospital Medical Center, Cincinnati, OH, USA. IL-10 reporter (Vert-X) mice were originally kindly provided by Prof. Christopher L. Karp (Cincinnati Children's Hospital Medical Center, Cincinnati, OH, USA) and bred in-house in both facilities [182]. These mice express green fluorescent protein (GFP) under the IL-10 promoter, thereby enabling the measurement of GFP signals when IL-10 transcription is induced [182]. All animal experiments were approved by the Committee on the Ethics of Animal Experiments of the University of Lübeck (approval number: 51-5/2019) or the Cincinnati Children's Hospital Medical Center's Institutional Animal Care and Use Committee (IACUC 2020-0034) and performed by certified personnel. Mice were kept at a regular light/dark cycle and were provided with food and water *ad libitum*. Monitoring of the health and well-being of the mice was conducted at least daily by a qualified person. 8- to 12-week-old mice were used for *in vivo* experiments. 8- to 16-week-old mice were used for *ex vivo* experiments (approval number 39_2015-06-01_Ehlers). For one experiment animals of the same sex were used. All efforts were made to minimize and alleviate distress and suffering. Refined aspects of study planning, housing, and husbandry were applied. Power analysis was conducted prior to the study to reduce the number of animals to the necessary minimum for reliable results. No harmful noise, vibrations, or lighting were present during the study. Habituation and husbandry handling was combined with handling for research purposes wherever possible. Mice were anesthetized and analgized by injection of ketamine hydrochloride (80 mg/kg body weight; Medistar, Germany) and xylazine hydrochloride (10 mg/kg body weight; Bayer, Germany), and mice were sacrificed by cervical dislocation according to the respective governmental and institutional guidelines.

4.1.2 Immunization and butyrate treatment *in vivo*

To investigate the effect of BA *in vivo*, 8 to 12-week-old C57BL/6J or IL-10-reporter mice were treated with BA and immunized i.p. with Ovalbumin (Ova) in complete Freund's adjuvant (CFA) in a total volume of 200 µl as indicated in **Figure 3**. Ova was purchased from Sigma-Aldrich (USA) and CFA was prepared by adding heat-killed Mtb.H37 RA (BD Biosciences, CA, USA) to incomplete Freund's adjuvant (IFA; Sigma-Aldrich, Germany; 1 mg Mtb/ml). 100 µL of CFA and 100 µl of a 1 mg/ml Ova-PBS stock solution were mixed before immunization.

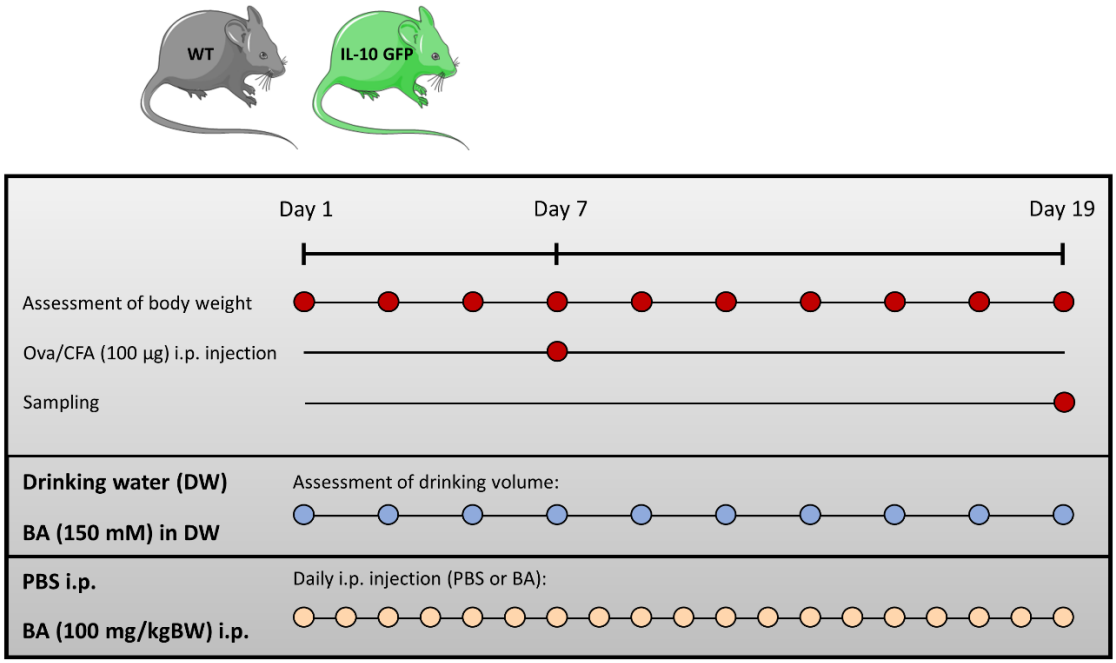

Figure 3: *In vivo* setup for BA treatment and Ova/CFA-immunization. CFA = complete Freund's adjuvant, DW = Drinking water, i.p. = intraperitoneal, kgBW = bodyweight in kilograms, Ova = ovalbumin.

BA or the respective vehicle control were administered to the mice continuously starting 7 days before immunization in two different routes: i) BA was dissolved in designated drinking water of the animal facility (DW) in a concentration of 150 mM and provided *ad libitum*, DW was used as the vehicle control; ii) BA was administered by daily intraperitoneal (i.p.) injection (100 mg/kg body weight), PBS was injected as the vehicle control.

Ova/CFA immunization was used to activate the immune system and elicit an immune response. No significant changes were found for body weight development in any of the experimental groups, while BA in DW did not change drinking volume (**Figure 4**). 12 days after immunization all mice were sacrificed and the spleens were sampled for further analysis.

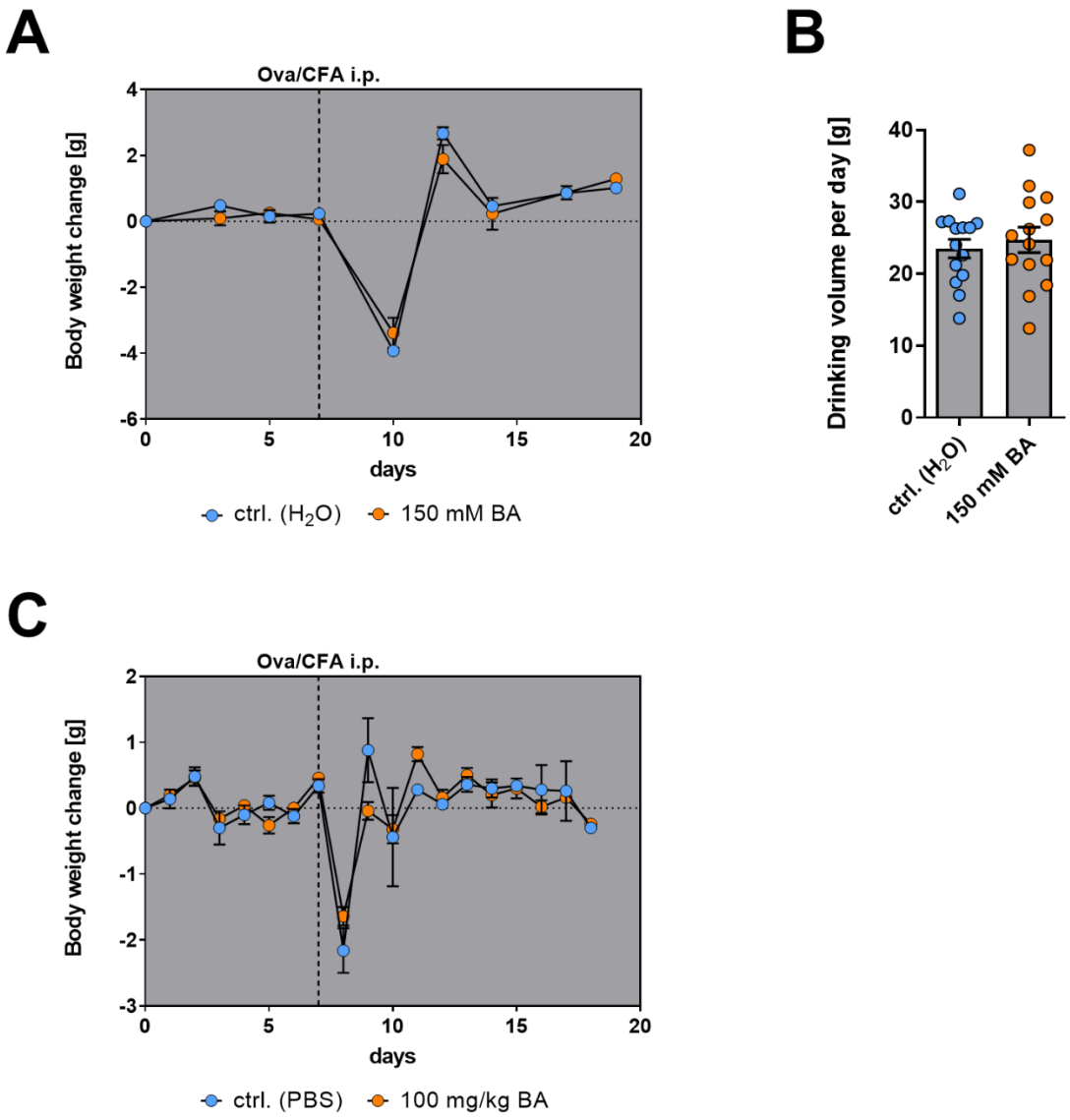

Figure 4: Weight development and drinking volume of the experimental groups treated with/without BA. (A+C) After an initial drop in body weight after the Ova/CFA-immunization, the body weight recovered quickly. No significant differences in body weight were found for BA in DW **(A)**, or i.p. injection of 100 mg/kg BA **(C)** compared to respective controls. **(B)** BA in DW did not change the drinking volume per day.

4.1.3 Dissection and tissue collection

Mice were killed by cervical dislocation. 70% Ethanol was used to sterilize the dissection field and to keep mice hair from contaminating the abdominal contents. Sterilized surgical-grade scissors and forceps were used to open the abdomen and to collect spleens. The surrounding fibrous and fatty tissue was removed carefully. All organs were kept in ice-cold PBS for a maximum of one hour before processing.

4.2 Preparation of single-cell suspensions

4.2.1 Single-cell suspension from spleens

Spleens of untreated mice for *ex vivo* experiments or of treated mice from *in vivo* experiments (see **4.1**) were placed on 70 µm cell strainers on 50 ml Falcon tubes. The tissue was then ground forcefully with the sterile plunger of a 1 ml syringe against the mesh. The cell strainer was subsequently flushed with 25 ml of ice-cold PBS. The cell suspension was spun down (5 min, 4 xg, 4°C), resuspended in 5 ml of ice-cold PBS, and filtered through a new 70 µm cell strainer to remove any remaining tissue debris or cellular aggregates. Single cells were kept in ice-cold PBS for a maximum of one hour before processing.

4.3 Magnetic Activated Cell Sorting of B cells

4.3.1 Principle

Isolation of B cells from murine spleens of untreated mice for *ex vivo* experiments was achieved by depleting non-B cells using a B cell Isolation Kit (Miltenyi Biotec, Germany). This kit uses negative Magnetic Activated Cell Sorting (MACS). For this method, non-B cells are labeled with biotinylated antibodies directed against surface antigens that are expressed by other murine cells, but not B cells. In this case, the targeted antigens are CD43 (Ly48), CD4 (L3T4), and Ter-119. In the next step magnetic beads conjugated with anti-biotin antibodies are added as a secondary labeling agent. The cell suspension is then added to a separation column in a strong magnetic field that captures the magnetic anti-biotin beads and therefore cells labeled with biotinylated antibodies. Non-labeled cells are

collected in the flow-through of the column. Negative MACS was chosen as a sorting technique, because of the relatively short, simple, and highly reliable procedure as well as its ability to sort cells without binding of antibodies to the cells of interest, therefore minimizing artificial sorting-related alterations of cell physiology.

4.3.2 Modified manufacturer's protocol

Single-cell suspensions were gently centrifuged (5 min, 400 x g, 4°C) and the supernatants were discarded. Cells were resuspended in 2 ml cold MACS buffer by gently pipetting up and down. Filtered splenocytes were counted in a hemocytometer using Trypan Blue solution (Thermo Fisher, USA). 10 µl of Biotin-Antibody Cocktail provided in the kit were added per 10^7 cells in MACS buffer and mixed well. After 20 minutes of incubation at 4°C, 20 µl of anti-Biotin MicroBeads were added per 10^7 cells, followed by mixing and an additional 20 minutes of incubation at 4°C. LS columns (Miltenyi Biotec, Germany) were placed in the magnetic field of a QuadroMACS Separator (Miltenyi Biotec, Germany) and primed with 3 ml of MACS Buffer. Subsequently, single-cell suspensions incubated with biotinylated antibodies and Anti-Biotin Microbeads were applied to the columns carefully to prevent the formation of bubbles. Afterward, the columns were flushed with 1 ml of MACS buffer. The flow-through was collected into new 50-ml tubes and 100 µl were taken for purity control. The isolation was considered successful if the percentage of $B220^+/CD3^-$ cells, as determined by flow cytometry, was over 95%.

4.4 B cell culture

Isolated B cells were cultured in RPMI medium with 10% FBS, 100 µM 2-ME, 1 mM HEPES, and 100 U/ml Penicillin/Streptomycin (later referred to as *B cell medium*). B cells were cultured at 10^5 to 10^6 cells per ml. The medium was supplemented with 3 µg/ml LPS and 100 nM all-trans Retinoic Acid (atRA), both of which promote the differentiation of naïve B cells into plasma cells [156,179,183,184]. Further, 10 ng/ml of IL-6 were added to support the potential expression of IL-10 [185]. These conditions were applied in all cell-culture experiments, if not stated otherwise, and are referred to as *plasma cell-inducing conditions* in the following. Cells were cultured at 37°C and 5% CO_2 (Heracell VIOS 160i, Thermo Fisher, Germany) for up to 4 days as described for each experiment. Subsequently, cells were

harvested by gently pipetting up and down and the medium was removed by washing the cells twice with PBS (5 min, 4 x g, 4°C). Sodium butyrate (BA) and sodium propionate (PA) were used in cell culture in physiological concentrations that have been described before for splenic and lymphoid tissues [156]. Single-cell suspensions for flow cytometry were prepared by resuspending B cells in FACS-buffer in indicated concentrations.

4.5 Flow cytometry

Single splenic cells of the *in vivo* experiments and of the B cell culture *ex vivo* experiments were analyzed using flow cytometry.

4.5.1 Principle

Flow cytometry is a laser-based method that facilitates the analysis of cell characteristics and cell populations and is often used in medical sciences, especially Immunology.

In flow cytometry, cells are labeled with antibodies conjugated to fluorochromes, cellular dyes that act as fluorochromes, and/or reporter proteins expressed by the cell itself. Upon excitation by light of a specific spectrum of wavelengths, each fluorochrome emits another specific spectrum of light. Flow cytometry utilizes this characteristic to identify multiple fluorochromes at the surface and within the same cell. Modern flow cytometers are able to detect a range from 1 to more than 30 fluorescent parameters. Applying this technique, it is possible to analyze multiple features of the same cell at the same time, including but not limited to cell viability, proliferation, expression of target proteins, and metabolic characteristics.

4.5.2 Fluidics

The *sample injection port* of a flow cytometer is the part that takes up the suspension of single cells stained with fluorochromes. The cells reach the *flow chamber* where a process called *hydrodynamic focusing* ensures that single cells are moving at approximately the same velocity on the same axis through the system. This is important to have a reliable readout of single cells in the end and is achieved by applying a faster-moving sheath stream that forces the cells into the smaller and slower core stream. This way single cells reach the *interrogation points*, where excitation of the fluorochromes takes place.

4.5.3 Optics

At *interrogation points,* the single cells intersect with monochromatic and coherent *lasers* of different wavelengths. These lasers excite the dyes and fluorochromes with a corresponding excitation spectrum (**Figure 5A-D**). An adjustable system of *mirrors* and *filters* directs the emitted light and divides it into smaller ranges of wavelengths that correspond to the maximal emission wavelength of the fluorochromes. Downstream, *detectors* capture the emitted and filtered photons. The signal is amplified and converted into electrons (so-called *photocurrents*). Additional detectors capture the light that is scattered by the cells, providing information about the size and complexity of each cell (known as forward and side scatter).

4.5.4 Electronics

The electronics part of a flow cytometer digitizes and processes the *photocurrents* from the detectors and records the data for analysis. Each voltage pulse created by *photocurrents* at the *detectors* has three different properties that can be used for analysis: height, width, and area of the pulse (**Figure 5E**). If not stated otherwise, the area of the pulse was used for analyses in this study. Specialized software is used to record, store and analyze the obtained data.

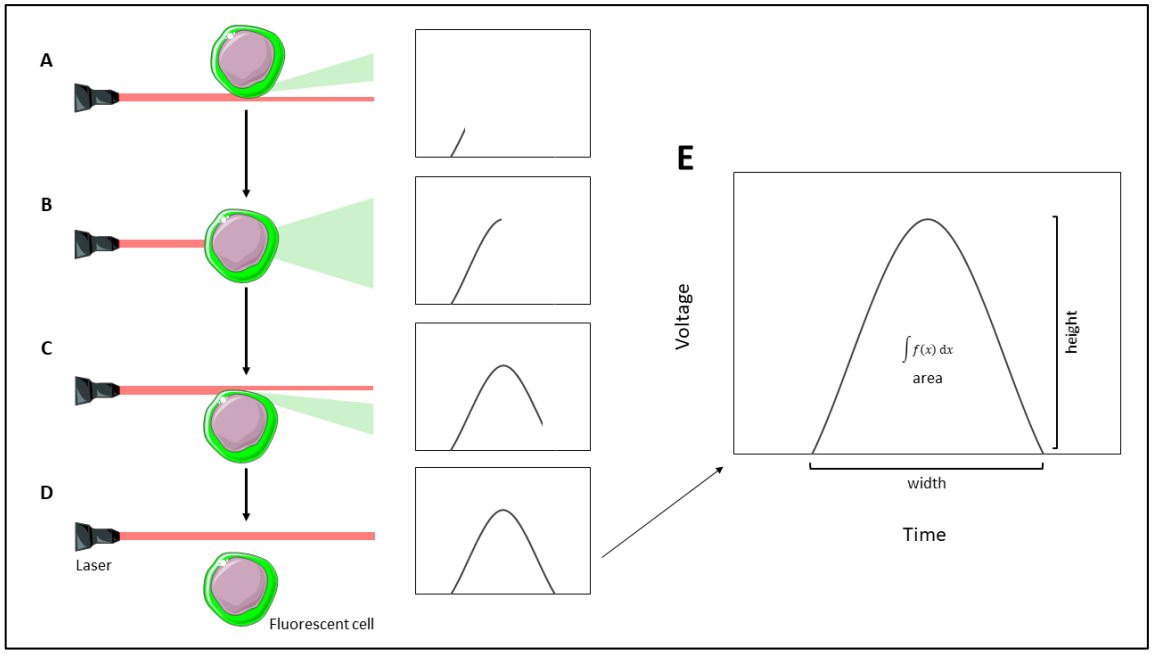

Figure 5: Generation of a voltage pulse by a single cell passing through the interrogation point. (A) The cell reaches the interrogation point and partially intersects with the laser

beam. Excitation of fluorochromes at the surface or within the cell leads to the emission of light of different wavelengths. The emitted light is detected, which leads to an increase in voltage. **(B)** The laser beam hits the maximum diameter of the cell. The voltage signal reaches its maximum intensity. **(C)** As the cell exits the interrogation point, the signal intensity fades. **(D)** The cell has completely exited the interrogation point. Signal intensity reaches baseline level. **(E)** Example of a voltage pulse generated by a cell passing through an interrogation point of a flow cytometer. For analysis, pulse width, height, or area may be used.

4.5.5 General remarks

Tissues and cells used for flow cytometry were processed as fast as possible while thoroughly following the protocols. Fluorochrome-conjugated antibodies, fluorescent dyes, and cells stained with them and/or expressing fluorescent-reporter proteins were protected from light during the process of harvesting, staining, and measurement to ensure the least possible loss of fluorescent signal. Cells expressing fluorescent proteins or stained with mitochondrial dyes were always measured immediately after staining.

4.5.6 Antibody-labeling

Anti-alpha2,6-St6gal1-antibody (#AF5924, ST6GAL1 Antibody, R&D Systems, USA), the corresponding IgG isotype control antibody (#AB-108-C, R&D Systems, USA), and Anti-Mouse H3K27ac-antibody (monoclonal, clone 8173, Cell Signaling Technology, USA) - detecting acetylated lysine residues at the 27th amino acid position in Histone H3 - were fluorophore-conjugated with Alexa Fluor 488 using a commercially available kit following the manufacturer's instructions (#A20181, Thermo Fisher, USA). In brief, after equilibration to room temperature, the antibody was diluted to 1 mg/ml in PBS and 0.1 M sodium bicarbonate buffer. 100 µl of the antibody solution was mixed with the reactive dye provided by the manufacturer, incubated for 1 hour, and gently mixed every 15 minutes as instructed. Purification of the labeled antibody was achieved using several centrifugation steps and spin columns, as described in detail by the manufacturer. Finally, all labeled antibodies were diluted to the desired working concentrations in FACS buffer (see **4.11.1**).

4.5.7 Mitochondrial staining

For experiments where mitochondrial staining was necessary, it preceded surface staining of the cells, and no permeabilization, fixation, and intracellular staining were added

because these steps are not compatible with the mitochondrial dyes. All the dyes used in this work passively diffuse across the plasma membrane and accumulate in active mitochondria. Three different dyes (all Thermo Fisher, USA) were used:

a) *MitoTracker Green FM (MT Green)* is a carbocyanine-based, bright green fluorescent dye that accumulates in the mitochondria of living cells and is not dependent on mitochondrial membrane potential (MMP), making it a useful tool to determine mitochondrial mass [186].
b) *Tetramethylrhodamine-ethylester* (TMRE) is a red fluorescent dye that reversibly accumulates in mitochondria of living cells, is dependent on MMP, and does not affect their function [187–190]. Therefore, it stains active mitochondria rather than mitochondrial mass and can be used in combination with MitoTracker Green FM for normalization to determine mitochondrial potential per mitochondrial mass in arbitrary units [190,191].
c) *MitoSOX Red (MitoSOX)* is a usually non-fluorescent, cationic dye that accumulates in the mitochondria of living cells. Specific oxidation by superoxide, which is the predominant ROS in mitochondria [192,193], leads to the emission of a red fluorescent signal enabling to stain for mitochondrial ROS production of living cells for usage in flow cytometry [194].

Because of overlapping emission spectra of TMRE and MitoSOX Red, they are incompatible for combination in flow cytometry. Instead, one panel was used that combined MitoTracker Green FM with TMRE and another one for MitoSOX Red.

For mitochondrial staining 0.2 x 10^6 cells were seeded into V-shaped 96-well microplates and washed with 200 µl of FACS-buffer (5 min, 400 x g, 4°C). 100 µl staining solution containing RPMI with 100 nM MitoTracker Green FM and 150 nM TMRE or 5 µM MitoSOX Red were added to the cells. After mixing well by gently pipetting up and down, plates were incubated at 37°C in the dark for 15 minutes and washed with 300 µl of FACS-buffer.

4.5.8 Surface staining

Single-cell suspensions in FACS-buffer were prepared from *ex vivo* B cell cultures or from spleens as described in **4.2** or **4.4**. Subsequently, 0.2 to 1 x 10*6 cells were seeded into V-shaped 96-well microplates and washed with 200 µl of FACS buffer (5 min, 400 x g, 4°C). To

block the unspecific binding of antibodies by Fc-receptors present on B cells, 100 µl of a purified antibody against CD16/CD32 (FcγR-Block) in a concentration of 1 µg/ml was added as recommended by the manufacturer. After incubation for 10 minutes on ice, the cells were washed with 200 µl of FACS Buffer (5 min, 400 x g, 4°C).

The Spectrum Viewer from BD Biosciences (available at https://www.bdbiosciences.com/en-us/applications/research-applications/multicolor-flow-cytometry/product-selection-tools/spectrum-viewer) was used to design staining panels. Fluorochromes with highly overlapping emission spectra were avoided to prevent signal spillovers. Surface staining Master Mixes were prepared in FACS buffer following the manufacturer's recommendations and own titrations for optimal staining concentrations. In general, final working concentrations between 1 and 5 µg/ml were used for each antibody. The antibodies that were used are listed in **4.11.4** and are indicated for every experiment in the results section. In all experiments, a fixable Live/Dead staining (eBioscience Fixable Viability Dye, Thermo Fisher, USA) was added in a concentration of 0.5 to 1 µl per 10^6 cells as recommended by the manufacturer's protocol.

100 µl of staining solution were added to 0.2 to 2 x 10^6 cells in the 96 well microplates and mixed well by pipetting gently up and down, followed by incubation for 20 minutes on ice in the dark. The surface staining was followed by three washing steps with 200 µl FACS-buffer each (5 min, 400 x g, 4°C). Cells were then either resuspended in FACS-buffer for direct measurements or intracellular staining was conducted.

4.5.9 Intracellular staining

Fixation and permeabilization for intracellular staining were achieved by adding 150 µl of Fixation and Permeabilization Solution (BD Biosciences, USA), mixing well, and incubating for 30 min at Room Temperature in the dark. Cells were then washed using 200 µl of BD PermWash Buffer (BD Biosciences, USA; 5 min, 400 x g, 4°C). Intracellular staining Master Mixes were prepared in BD PermWash Buffer (BD Biosciences, USA) following the manufacturer's recommendations and own titrations for optimal staining concentrations. In general, 100 µl of Master Mix were used with final working concentrations between 1 and 5 µg/ml of fluorochrome-conjugated antibodies each. The antibodies that were used are listed in **4.11.4** and are indicated in the results for each experiment. After incubation

for 60 min on ice in the dark, cells were washed three times with 200 µl of BD PermWash Buffer (BD Biosciences, USA; 5 min, 400 x g, 4°C), before being resuspended in FACS-buffer for measurements.

4.5.10 Measurements and analyses

Compensation controls were prepared and measured usually on the day of the experiment. Controls for mitochondrial and viability dyes as well as unstained controls of wildtype and IL-10 reporter mice were prepared from the cell populations of the corresponding experiment and UltraComp eBeads (ThermoFisher, USA) were used for reliable single-color compensation controls of antibodies.

For experiments performed at the University of Lübeck (Germany), the AttuneNXT instrument and software (Thermo Fisher, USA) were used. At Cincinnati Children's Hospital (Ohio, USA) measurements were done with BD LSRFortessa flow cytometers and FACSDiva Software (BD Biosciences, USA).

FlowJo software (FlowJo, LLC, USA) was used to analyze the obtained data. Automatically calculated compensation matrices were – only where necessary – carefully adjusted to compensate optimally for spillovers between channels.

4.6 RNA-isolation

4.6.1 RNA isolation from B cell cultures

A commercially available kit was used to isolate RNA from B cell cultures (innuPREP RNA Mini Kit 2.0, Analytik Jena, Germany). The manufacturer's protocol was modified by adding a DNA-digestion step to increase the RNA purity of the final sample. If not otherwise stated, the reagents used in the following protocol (**Table 3**) are contents of the RNA-isolation kit (innuPREP RNA Mini Kit 2.0, Analytik Jena, Germany).

Step	Process
1: Lysis of eukaryotic cells	400 µl of Lysis-Solution RL were added to a maximum of 5 x 10^6 cells, mixed well, and incubated for 3 min at RT. Centrifugation at maximum speed for 1 min.
2: Selective removal of genomic DNA	Spin Filter D was placed in a new receiver tube and the supernatant from step 1 was added to the filter. Centrifugation at 11,000 x g for 2 min. Spin Filter D containing gDNA was discarded and 400 µl of 70% ethanol was added to the filtrate.
3: Selective binding of RNA	Spin Filter R was placed in a new receiver tube and the filtrate from step 2 was added. Centrifugation for 2 min at 11,000 x g.
4: DNA digestion	20 µl of 100mU/µl DNase I in 1X DNase reaction buffer (DNase I, Amplification Grade, Thermo Fisher, USA) was added to Spin Filter R and incubated for 20 min at RT. Centrifugation for 1 min at 11,000 x g.
5: Washing step I	The filtrate was discarded and Spin Filter R was transferred into a new receiver tube. Application of 500 µl of Washing Solution HS to Spin Filter R. Centrifugation at 11,000 x g for 1 min.
6: Washing step II	The filtrate was discarded and 750 µl of Washing Solution LS was added to Spin Filter R. Centrifugation at 11,000 x g for 1 min.
7: Removal of residual ethanol	The filtrate was discarded and Spin Filter R was placed in a new receiver tube. Centrifugation at 11,000 x g for 3 min.
8: Elution of RNA	Spin Filter R was placed in an elution tube (1.5 ml DNase/RNase-free reaction tube). Application of 40 µl of RNase-free water to Spin Filter R and incubation for 20 min at RT. Centrifugation at 11,000 x g for 1 min. The filter was discarded and the RNA sample was either used directly or stored at -80°C.

Table 3: Protocol for the isolation of RNA from eukaryotic cells, adapted and slightly modified from the manufacturer's protocol.

4.7 cDNA-transcription

Isolated RNA was transcribed into complementary DNA (cDNA) by reverse transcriptase (RevertAid H Minus Reverse Transcriptase, Thermo Fisher, USA). Single-stranded oligonucleotides consisting of 20 Thymidine bases (Oligo(dT), biomers.net, Germany) were used as Primers targeting the polyadenylated tail of eukaryotic, post-transcriptional mRNAs. A mixture of dATP, dCTP, dGTP, and dTTP (dNTP set, peqGOLD, VWR International, USA) was added providing the deoxynucleotide substrates for the reaction. The exact protocol is provided in **Table 4**.

Step	Process
1: Normalization of RNA-concentration	RNA-concentration was measured using a NanoDrop 2000 (Thermo Fisher, USA). 1 µg of RNA was added to RNase/DNase-free reaction tubes and RNase/DNase-free water was added up to a volume of 11.5 µl.
2: Addition of Master Mix	Per sample 8.5 µl of freshly prepared Master Mix were added, containing: • 0.5 µl RNase inhibitor, 40 U/µl (Ribolock, Thermo Fisher, USA) • 2 µl dNTP mix, 10 mM each (dNTP set, peqGOLD, VWR International, USA) • 1 µl reverse transcriptase, 200 U/µL (RevertAid H Minus Reverse Transcriptase, Thermo Fisher, USA) • 4 µl 5x Reaction Buffer (RevertAid H Minus Reverse Transcriptase, Thermo Fisher, USA) • 1 µl Oligo(dT) (biomers.net, Germany)
3: Reverse transcription	Incubation at 42°C for 60 min.
4: Enzyme Inactivation	Incubation at 70°C for 10 min.
5: Dilution	1:5 dilution of cDNA samples and storage at -20°C.

Table 4: cDNA-transcription protocol.

4.8 Real-time quantitative polymerase chain reaction

4.8.1 Principle and analysis

In real-time quantitative polymerase chain reaction (qPCR), target cDNA transcribed from mRNA is amplified following the principles of polymerase chain reaction [195]. Additionally, a fluorescent dye is used, that emits light of a specific spectrum after preferentially binding to DNA double-strands. During amplification cycles, the emitted light is detected and recorded in real-time resulting in an amplification curve. The cycle, at which the emitted light intensity reaches a set threshold, is the cycle-threshold (CT)-value. After normalization to a stably expressed reference gene, these values can be used to calculate the relative expression of target genes.

In this study, the $\Delta\Delta CT$-method was used. In short, for every sample, the CT-value of the reference gene was subtracted from the CT-value of each target gene resulting in ΔCT-values. Next, ΔCT of the control samples was subtracted from ΔCT of treated samples resulting in $\Delta\Delta CT$-values. Relative expression levels of treated samples compared to the control sample and normalized for the reference gene resulted from $2^{-\Delta\Delta CT}$. Mathematical formulae for calculating the relative expression are provided below:

$$\Delta CT_{treated} = CT_{target\ gene;treated\ sample} - CT_{reference\ gene;treated\ sample}$$

$$\Delta CT_{control} = CT_{target\ gene;control\ sample} - CT_{reference\ gene;control\ sample}$$

$$\Delta\Delta CT = \Delta CT_{treated} - \Delta CT_{control}$$

$$Relative\ expression = 2^{-\Delta\Delta CT}$$

4.8.2 Primers

Primers for qPCR were designed using the Basic Local Alignment Search Tool (BLAST) provided by the National Center for Biotechnology Information (NCBI, Bethesda, USA) [196] and checked using the in-silico PCR tool provided by the Genomics Institute of the University of California Santa Cruz, USA [197]. Additional checks for product length were performed for all primers using PCR and gel electrophoresis. Forward and reverse primers were used in a concentration of 125 nM each. The primer sequences for target genes are provided in **Table 12**.

4.8.3 Protocol

For qPCR experiments, cDNA was obtained as described in **4.7** and 2 µl per technical replicate were prepared in a 96-well PCR plate (Sarstedt, Germany). PerfeCTa SYBR Green SuperMix (VWR International, USA) and forward and reverse primers (125 nM each) were added following the manufacturer's instructions to a final volume of 20 µl. The StepOnePlus Real-Time PCR System and Software (Thermo Fisher, USA) were used to conduct the qPCR following the manufacturer's recommendations. At least two technical replicates were done for each sample and β-Actin was used as a reference gene. The instrument protocol is shown in **Table 5**.

Step	Temperature	Duration
1: Initial denaturation	95°C	4 min
2: Denaturation	95°C	30 sec
3: Annealing	60°C	30 sec
4: Elongation	72°C	30 sec
Repeat cycles 2-4 an additional 39 times		
5: Melting curve determination	Slowly increasing temperatures	Approx. 30 min

Table 5: Instrument protocol for qPCR.

4.9 ELISA

4.9.1 Principle of sandwich-ELISAs

Sandwich Enzyme-linked Immunosorbent Assay (ELISA) is a technique for measuring protein in liquid samples. ELISA plates are coated with either specific antibodies or antigens. After several washing steps, the sample is then added to the plate leading to the binding of the protein of interest to the antibody or antigen coated on the plate. In the next step, the remaining binding sites are blocked by a blocking buffer containing non-related peptides. Subsequently, enzyme-linked detection antibodies are added to the assay binding to the protein of interest. Finally, colorimetric substrates for the enzymes linked to the detection antibodies are added and the optical density (OD) is measured using an ELISA plate reader.

4.9.2 Protocol

Previously published methods were used for ELISA measurements [198] and slightly modified where necessary. Blocking, serum dilutions, and addition of detection antibodies were conducted in 2.5% milk powder in PBS. For total IgM antibody measurements, an anti-murine IgM antibody from Bethyl Laboratories (Montgomery, USA) was used at a concentration of 5 µg/ml. For detection of antigen-specific antibodies, Ova-coated ELISA-plates were generated by using 10 µg/mL of Ova. The detection antibodies were diluted according to the manufacturer's instructions. Horseradish peroxidase (HRP)-coupled polyclonal goat anti-mouse IgM-specific antibodies purchased from Bethyl Laboratories (Montgomery, USA) were used for the detection of bound antibodies following incubation with diluted serum samples (1:100). The plates were incubated with 3,3´,5,5´-tetramethylbenzidine (TMB) substrate (BD Biosciences, San Diego, USA), and the same volume of 4.2% H_2S0_4 (BD Biosciences, San Diego, USA) was used to stop the reaction. The OD was measured at a wavelength of 450 nm.

4.10 Seahorse analysis

4.10.1 Principle

A real-time assessment of mitochondrial function in B cells was conducted at Cincinnati Children's Hospital (Ohio, USA) using a Seahorse XFe96 Analyzer. The Seahorse assay allows for simultaneous measurements of oxygen consumption rates (OCR) and extracellular acidification rates (ECAR). Multiple modulators of mitochondrial function are consecutively injected into the assay to manipulate mitochondrial function as described in chapter **4.10.2**. The usage of these modulators allows for the calculation of multiple aspects of mitochondrial respiration (**Figure 6**).

4.10.2 Modulators of mitochondrial function used in the Seahorse assay

Oligomycin A (O) is an antibiotic derived from *Streptomyces* and a long-known, efficient inhibitor of ATP-synthase, the crucial enzyme facilitating oxidative phosphorylation (OXPHOS) of ADP to ATP [199]. Because of the coupling of other respiratory chain complexes to ATP-synthase, Oligomycin leads to reduced electron flow and oxygen

consumption in the respiratory chain without completely stopping it. The remaining electron flow is elicited by Proton leaks caused by uncoupling proteins [200]. Thus, sufficient concentrations of Oligomycin abrogate the oxygen consumption that is normally used for ATP production, which then can be calculated from the measurements.

Carbonyl cyanide-4-(trifluoromethoxy)phenylhydrazone (FCCP) is used as an uncoupling agent in the Seahorse assay. It transports Protons across the mitochondrial membrane, uncoupling the rest of the respiratory chain from ATP-synthase [201]. This leads to a maximal increase of Complex I-III activity after FCCP addition and enables measurements of oxygen consumption during maximal mitochondrial respiration in cells of interest.

Finally, Rotenone (Rot) and Antimycin A (AA) are used to inhibit Complex I and Complex III of the respiratory chain, respectively [202,203]. Through the combination of both inhibitors, the respiratory chain is inhibited almost completely. The remaining oxygen consumption measured in the Seahorse assay is ascribed to non-mitochondrial oxygen consumption.

Several parameters of mitochondrial respiration can be calculated from the measurements obtained during the Seahorse assay and are schematically depicted in **Figure 6**.

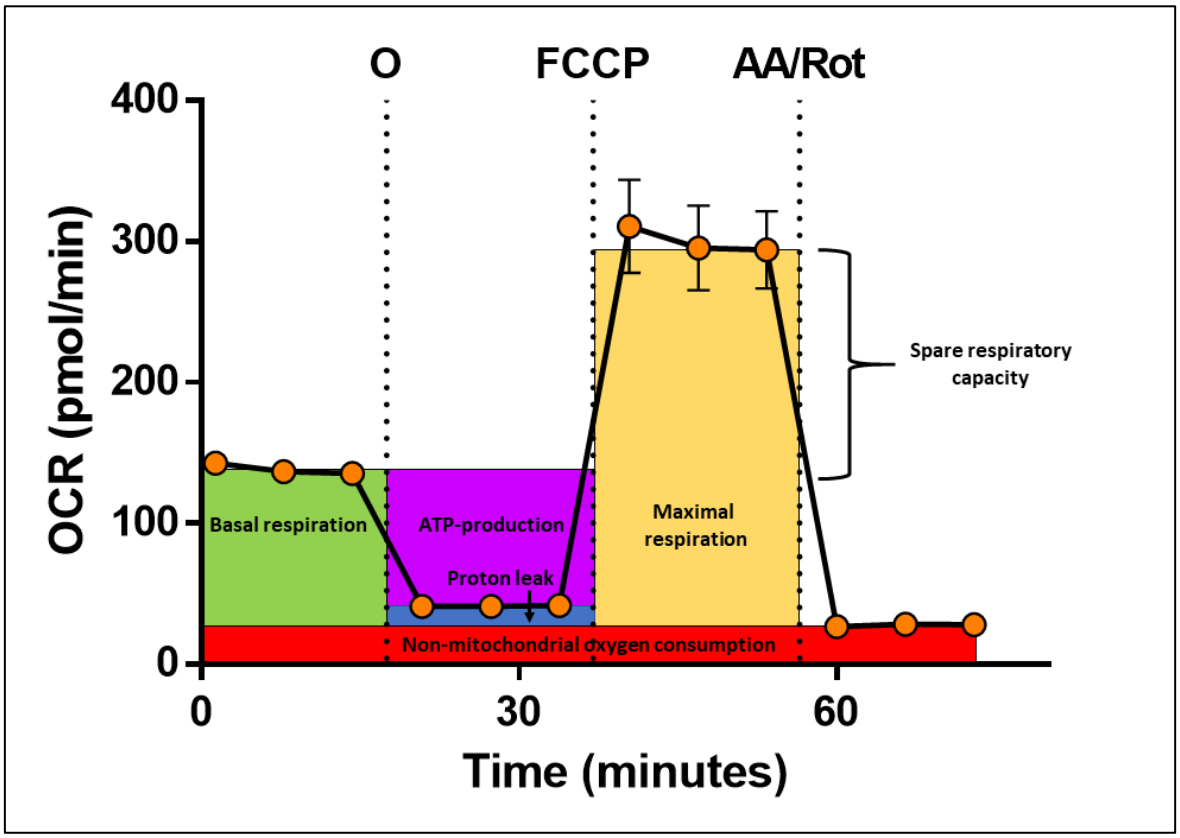

Figure 6: Principles of analyzing a Seahorse assay. Data shown here are from isolated B cells cultured under plasma cell-inducing conditions for one day. Colored boxes schematically illustrate parameters that can be calculated from the raw data. The illustration was fashioned following the manufacturer's guide [204] by using own data. O = Oligomycin injection, FCCP = FCCP injection, AA/Rot = Antimycin A and Rotenone injection.

4.10.3 **Seahorse analysis of B cells**

For Seahorse analysis of B cells, manufacturer's recommendations and published data [205] were used to generate an optimized protocol. Various conditions for cell density, incubation times, and concentrations of mitochondrial modulators, as well as glucose, were tested before the final experiments were performed. For all data shown in the results section, the following protocol was used.

To hydrate the cartridge of the Seahorse XF96e Extracellular Flux Assay (Agilent, USA), its utility plate was filled with 200 µl of sterile water per well. Subsequently, the cartridge was carefully placed on top of the filled utility plate, so that the sensors were submerged in sterile water. The utility plate and cartridge were wrapped in laboratory foil (Parafilm M, Paul Marienfeld, Germany) to prevent evaporation and incubated overnight at 37°C not

supplemented with CO_2. The next day, the water was discarded and 200 µl of Seahorse XF Calibrant Solution was added per well. The cartridge was placed back on top of the utility plate and incubated at 37°C not supplemented with CO_2 for one hour.

B cells were isolated from murine spleens (see **4.2**) or harvested from cell culture (see **4.4**) and washed three times in cold PBS (5 min, 400 x g, 4°C). Cells were then resuspended in RPMI medium and living cells were counted using Trypan blue solution (Thermo Fisher, USA). After the cells had been spun down (5 min, 400 x g, 4°C), RPMI medium was discarded and cells were resuspended in a density of 10^7 cells per ml of Seahorse Mitostress Medium (Seahorse XF Base Medium +10 mM D(+)-Glucose, +1 mM Sodium Pyruvate, +2 mM L-Glutamine). Next, 6 x 10^5 cells per well were seeded in a new Seahorse XF96e Cell Culture Microplate (Agilent, USA) and the volume was adjusted to 175 µl. Cells were then spun down carefully (5 min, 200 x g, Room Temperature) and seeding densities were checked microscopically for 90-95% confluency, followed by incubation for 45 to 60 minutes at 37°C not supplemented with CO_2.

Working solutions of mitochondrial modulators in Seahorse Mitostress Medium were prepared immediately before the assay was loaded. To evaluate the short-term effects of BA on mitochondrial metabolism, the cartridge ports were loaded with 25 µl of working solutions, so that the final concentrations that were added in each well consecutively reached 0.5 mM BA, 2 µM Oligomycin, 2 µM FCCP, and 9 µM/1 µM AA/Rot, respectively. To evaluate more long-term effects of Butyrate, B cells were cultured for one day under plasma cell-inducing conditions with or without 0.5 mM BA, and without additional BA injection during the assay. There were at least 5-6 technical replicates for each condition.

Before every assay, the instrument was calibrated and equilibrated using the Seahorse cartridge and the utility plate with Seahorse XF Calibrant Solution. A standard Mitostress instrument protocol was used for the measurements of the long-term effects of BA. After each injection and at baseline, 3 measurement cycles were conducted, each encompassing 3 minutes of mixing and 3 minutes of measuring OCR and ECAR. For short-term BA effects, 6 additional measurement cycles were conducted directly after BA injection.

4.10.4 **Calculation of mitochondrial parameters**

Parameters of mitochondrial respiration were calculated following the manufacturer's recommendations (Seahorse XF Cell Mito Stress Test Kit, Agilent, USA). The following formulas are adapted from the manufacturer and used during the study (see also **Figure 6**).

$$Non\text{-}mitochondrial\ respiration = Minimum\ rate\ measurement\ after\ AA/Rot\ injection$$

$$Basal\ respiration = (Last\ rate\ measurement\ before\ first\ injection) - (Non\text{-}mitochondrial\ respiration)$$

$$Basal\ respiration\ after\ BA\ injection = (Last\ rate\ measurement\ before\ oligomycin\ injection) - (Non\text{-}mitochondrial\ respiration)$$

$$Acute\ response\ to\ BA = (Last\ rate\ measurement\ before\ oligomycin\ injection) - (Last\ rate\ measurement\ before\ BA\ injection)$$

$$Maximal\ respiration = (Maximum\ rate\ measurement\ after\ FCCP\ injection) - (Non\text{-}mitochondrial\ respiration)$$

$$ATP\ production\ rate = (Last\ rate\ measurement\ before\ oligomycin\ injection) - (Minimum\ rate\ measurement\ after\ oligomycin\ injection)$$

$$Spare\ respiratory\ capacity\ [\%] = \frac{(Maximal\ respiration)}{(Basal\ respiration)} * 100$$

$$Coupling\ efficiency\ [\%] = \frac{(ATP\ production\ rate)}{(Basal\ respiration)} * 100$$

$$Proton\ leak = (Minimum\ rate\ measurement\ after\ oligomycin\ injectio) - (Non\text{-}mitochondrial\ respiration)$$

4.11 Lists of Materials

4.11.1 Buffers, Solutions, and Media

Name	Components (if prepared fresh)	Source	Product No.
B cell Medium	RPMI 1640 Medium +10% FBS +100 µM Dimercaptoethanol +1 mM HEPES +100 U/ml Penicillin/Streptomycin	Thermo Fisher Thermo Fisher Thermo Fisher Sigma-Aldrich Thermo Fisher	21875 10270-106 31350-010 H0887 15140-122
Dulbecco's PBS		Sigma-Aldrich	D8537
FACS Buffer	PBS +2% FBS	Sigma-Aldrich Thermo Fisher	D8537 10270-106
Fixation and Permeabilization Solution		BD Biosciences	554722
MACS Buffer	PBS +1.5% FBS +1 mM EDTA	Sigma-Aldrich Thermo Fisher Corning	D8537 10270-106 46-034-CI
Permeabilization wash buffer (10x)		Biolegend	421002
RPMI 1640 Medium		Thermo Fisher	21875
Seahorse Mitostress Medium	Seahorse XF Base Medium +10 mM D(+)-Glucose +1 mM Sodium Pyruvate +2 mM L-Glutamine	Agilent Sigma-Aldrich Thermo Fisher Sigma-Aldrich	102353-100 G7021-100G 11360070 G8540
Seahorse XF Base Medium Minimal DMEM		Agilent	102353-100
Seahorse XF Calibrant Solution		Agilent	100840-000
UltraPure RNase/DNase-Free Water		Invitrogen	10977-049

Table 6: Buffers, solutions, and media.

4.11.2 **Commercially available Kits**

Method	Name	Source	Product No.
Antibody labeling	PE / R-Phycoerythrin Conjugation Kit - Lightning-Link	Abcam, GB	ab102918
Antibody labeling	Alexa Fluor 488 Antibody Labeling Kit	Thermo Fisher, USA	A20181,
B cell isolation	Mouse B cell isolation kit	Miltenyi Biotec, Germany	130-090-862
Cell Fixation and Permeabilization	Fixation/Permeabilization Solution Kit	BD Biosciences, USA	554714
DNA digestion	DNase I, Amplification Grade	Thermo Fisher, USA	18068015
Extracellular flux analysis	Seahorse XF Cell Mito Stress Test Kit	Agilent, USA	103015-100
RNA isolation	innuPREP RNA Mini Kit 2.0	analytik jena, Germany	845-KS-2040250

Table 7: Commercially available kits.

4.11.3 **Instruments**

Instruments	Manufacturer
Attune NxT Flow Cytometer	Thermo Fisher, Germany
Heracell VIOS 160i	Thermo Fisher, Germany
Heraeus Multifuge X3FR	Thermo Fisher, Germany
Heraeus Multifuge X3R	Thermo Fisher, Germany
LSRFortessa Flow Cytometer	BD Biosciences, USA
NanoDrop 2000	Thermo Fisher, USA
NUAIRE Biosafety Cabinet, NU-425-600E	NUAIRE, USA
QuadroMACS Separator	Miltenyi Biotec, Germany
Seahorse XFe96 Analyzer	Agilent, USA
SIGMA 1-14 Centrifuge	Sigma Laborzentrifugen, Germany

StepOnePlus Real-Time PCR System	Thermo Fisher, Germany
T1 Thermocycler	Biometra, Germany
ZEISS Primovert	ZEISS, Germany

Table 8: Instruments.

4.11.4 Antibodies and dyes for flow cytometry

Target	Conjugate	Source	Product No.
B220/CD45R	BV786	BD Biosciences, USA	563894
CD138/Syndecan-1	BV711	BD Biosciences, USA	563193
CD16/32 (FcγR-Block)	unconjugated	Biolegend, USA	101302
eBioscience Fixable Viability Dye	eFluor 780	Thermo Fisher, USA	65-0865-14
H3K27ac	unconjugated	Cell Signaling Technology, USA	8173
IgG	PE	Biolegend, USA	405307
IgG1	BV421	Biolegend, USA	406616
IgM	PE-cyanine7	Thermo Fisher, USA	25-5890-82
Isotype control, goat IgG	unconjugated	R&D Systems, USA	AB-108-C
MitoSOX Red	-	Thermo Fisher, USA	M36008
MitoTracker Green FM	-	Thermo Fisher, USA	M7514
Ovalbumin, fluorochrome-conjugated	AF647	Thermo Fisher, USA	O34784
Sialyltransferase 1/St6gal1 Antibody	unconjugated	R&D Systems, USA	AF5924
TGF1β	PE	Biolegend, USA	141403
TMRE	-	Thermo Fisher, USA	T669

Table 9: Antibodies and dyes for flow cytometry.

4.11.5 **Other reagents**

Reagent	Source	Product No.
2-Deoxy-D-glucose	Sigma-Aldrich, USA	D8375
All-trans Retinoic acid	Sigma-Aldrich, USA	R2625
Attune Focusing Fluid	Thermo Fisher, USA	A24904
Bovine serum albumin	PAA Laboratories, Germany	K51-001
D-Glucose	Sigma-Aldrich, USA	G8270
DMSO	Sigma-Aldrich, USA	S-002-M
dNTP set, peqGOLD	VWR International, USA	732-2783
Flow Cytometry Sheath Fluid	BD Biosciences, USA	342003
Goat anti-Mouse IgM Antibody	Bethyl Laboratories, USA	A90-101A
Goat anti-Mouse IgM Antibody HRP Conjugated	Bethyl Laboratories, USA	A90-101P
GPR43 (FFA2) Agonist	Merck Millipore, Germany	371725
Ketamine hydrochloride	Medistar, Germany	03048734
Lipopolysaccharides from *Escherichia coli* O111:B4	Sigma-Aldrich, USA	L3024
Metformin (1,1-Dimethylbiguanide hydrochloride)	Sigma-Aldrich, USA	D150959
PerfeCTa SYBR Green SuperMix	VWR International, USA	733-1251
Phorbol-12-myristate-13-acetate (PMA)	Sigma-Aldrich, USA	P1585
Recombinant murine IL-6	PeproTech, USA	216-16
RevertAid H Minus Reverse Transcriptase + 5X Reaction Buffer	Thermo Fisher, USA	EP0452
RGFP966	Sigma-Aldrich, USA	SML1652
RiboLock RNase-Inhibitor	Thermo Fisher, USA	EO0381
Sodium acetate	Sigma-Aldrich, USA	S5636
Sodium butyrate	Sigma-Aldrich, USA	303410
Sodium butyrate solution	Merck Millipore, Germany	TR-1008
Sodium propionate	Sigma-Aldrich, USA	P1880
TGR5-receptor agonist (CCDC)	Cayman Chemicals, USA	16291

TMB Substrate Reagent Set	BD Biosciences, USA	555214
Trichostatin A	Sigma-Aldrich, USA	T8552
Trypan Blue Solution	Thermo Fisher, USA	15250061
UltraComp eBeads Compensation Beads	Thermo Fisher, USA	01-2222-42
Xylazine hydrochloride (Rompun) 2%	Bayer, Germany	1320422

Table 10: Other reagents.

4.11.6 **Small equipment**

Product	Source	Product No.
96 fast PCR plate, half skirt	Sarstedt, Germany	72.1981.202
96-well microwell plates 450 µl	Thermo Fisher Scientific, USA	249944
accu-jet pro, pipettors	BRAND, Germany	26300
Acura manual 855 multichannel pipette	Socorex Isba SA, Switzerland	825.0200
Biosphere filter tips, 10 µl	Sarstedt, Germany	70.1130.210
Biosphere filter tips, 100 µl	Sarstedt, Germany	70.760.212
Biosphere filter tips, 1000 µl	Sarstedt, Germany	70.762.211
Cell culture flasks, 250 ml	Greiner Bio-One International, Austria	658175
Cell culture flasks, 50 ml	Greiner Bio-One International, Austria	690175
Cell strainer, 70 µm	Sigma-Aldrich, USA	CLS431751
Eppendorf Research Plus, 0.5 – 10 µl	Eppendorf, Germany	3123000020
Eppendorf Research Plus, 10 – 100 µl	Eppendorf, Germany	3123000047
Eppendorf Research Plus, 100 – 1000 µl	Eppendorf, Germany	3123000144
LS columns	Miltenyi Biotec, Germany	130-042-401
Micro tube, 1.5 ml	Sarstedt, Germany	72.690.001
Micro tube, 1.5 ml SafeSeal	Sarstedt, Germany	72.706.400
Micro tube, 2 ml SafeSeal	Sarstedt, Germany	72.695.400

Micro tube, 2 ml SafeSeal	Sarstedt, Germany	72.695.500
Multipette M4	Eppendorf, Germany	4982000012
Optical adhesive covers (PCR compatible)	Life Technologies, USA	4360954
Parafilm, M	Paul Marienfeld, Germany	7407505
Pipette tips, 10 µl	Sarstedt, Germany	70.1130
Pipette tips, 1000 µl	Sarstedt, Germany	70.762.010
Pipette tips, 200 µl	Greiner Bio-One International, Austria	739296
Seahorse XF96e Cell Culture Microplate	Agilent, USA	101085-004
Seahorse XF96e Extracellular Flux Assay	Agilent, USA	100850-001
Serological pipette, 10 ml	Sarstedt, Germany	86.1254.001
Serological pipette, 25 ml	Sarstedt, Germany	86.1685.001
Serological pipette, 5 ml	Sarstedt, Germany	86.1253.001
Serological pipette, 50 ml	Sarstedt, Germany	86.1256.001
TC-Flask T75	Sarstedt, Germany	83.3911.002
Tube, 15 ml	Sarstedt, Germany	62.554.502
Tube, 50 ml	Sarstedt, Germany	62.548.004

Table 11: Small equipment.

4.11.7 **Primers**

Target	5’ – 3’ sequence	Product base length	NCBI Reference
Oligo(dT) primer	TTTTTTTTTTTTTTTTTTT		
Aicda (forward)	CATCCTTTTGCCCTTGTACG	382 bp	NM_009645.2
Aicda (reverse)	CACAGGGTGGGTGTAACAAA		
Bcl6 (forward)	GCGGGAACCACGATCC	237 bp	NM_009744.4
Bcl6 (reverse)	TGCTTTAAAACTGGTGTCCG		
Ebi3 (forward)	TCATTGCCACTTACAGGCTC	427bp	NM_015766.2
Ebi3 (reverse)	GCTGACACCTGGATGCAA		

IL-10 (forward)	TGCCTGCTCTTACTGACTGG	217bp	NM_010548.2
IL-10 (reverse)	GGCAACCCAAGTAACCCTTA		
Irf4 (forward)	GGATTGTTCCAGAGGGAGC	274 bp	NM_001347508.1
Irf4 (reverse)	CCTGTCACCTGGCAACC		
Irf8 (forward)	TCTGACCCTCAGGCCTCTT	468bp	NM_001301811.1
Irf8 (reverse)	GTCACACATCCTGCAATCAGA		
p35 (forward)	TGTGTCTCCCAAGGTCAGC	388bp	NM_008351.3
p35 (reverse)	GCTCCCTCTTGTTGTGGAAG		
Tgfβ (forward)	ACCAACTATTGCTTCAGCTCC	275bp	NM_011577.2
Tgfβ (reverse)	TTGCGACCCACGTAGTAGAC		
Xbp1 (forward)	ACACGCTTGGGAATGGACAC	942 bp	NM_001271730.1
Xbp1 (reverse)	CCATGGGAAGATGTTCTGGG		
β-Actin (forward)	GATGCTCCCCGGGCTGTATT	225bp	NM_007393.5
β-Actin (reverse)	GGGGTACTTCAGGGTCAGGA		

Table 12: Primers used for qRT-PCR. Primers were purchased from *metabion international* (Germany), except for Oligo(dT) primers, which were purchased from *biomers.net* (Germany).

4.11.8 **Software**

Software	Developer
Attune NxT software	Thermo Fisher, USA
Office 365	Microsoft, USA
FACSDiva	BD Biosciences, USA
FlowJo Software 10	FlowJo, LLC, USA
GraphPad Prism 9.3.0	GraphPad Software, Inc, USA
Seahorse Wave Desktop Software	Agilent, USA
StepOne Software	Thermo Fisher, USA

Table 13: Software

4.12 **Statistics**

Statistical calculations were performed using GraphPad Prism 9.3.0 (GraphPad Software, Inc, USA). Results were accepted as statistically significant if the p-value was < 0.05. Comparisons of two groups were done using unpaired or paired student's t-tests with Geisser-Greenhouse correction, or Mann-Whitney test where applicable. Multiple comparisons were performed using One-Way-ANOVA, or a mixed-effects model. In the case of multiple comparisons, significant results were followed up by post-hoc testing with Tukey's Honest Significant Difference test. All experiments were replicated independently. Data in plots are depicted as mean ± SEM, if not stated otherwise in the figure legend. Levels of statistical significance are depicted as follows: * $p < 0.05$, ** $p < 0.01$, *** $p < 0.001$.

4.13 **Graphics**

Graphs and plots were prepared with GraphPad Prism Version 9.3.0 (GraphPad Software, Inc, USA). Graphical elements used for figures were adapted from Servier Medical Art (Les Laboratoires Servier, France, originals available at: https://smart.servier.com), are free to use for scientific publications under a Creative Commons Attribution 3.0 Unported License (CC BY 3.0, https://creativecommons.org/licenses/by/3.0/legalcode) and have been modified and put into a new context for this purpose.

5 RESULTS

5.1 BA induces IL-10^{+}IgM^{+} plasma cells *ex vivo*

5.1.1 BA induces splenic CD138^{high} plasma cells ex vivo

Since it was previously reported that microbial metabolites from the family of SCFAs increase the antibody response *in vivo*, it has been hypothesized that SCFAs increase the differentiation of plasma cells [156,179].

Thus, selected SCFAs were tested in an *ex vivo* approach for plasma cell-inducing effects. Naïve murine B cells were isolated from spleens of wild-type C57BL/6J-mice using MACS isolation. B cells were then incubated in B cell media under plasma cell-inducing conditions (3 µg/ml LPS, 10 ng/ml IL-6, and 100 nM all-trans Retinoic Acid (atRA), see **4.4**) [156,179,183–185]. On the first day of incubation, the SCFAs PA and/or BA were added in concentrations between 0.1 and 0.5 mM. After 4 days of incubation, cells were harvested and stained with fluorescence-conjugated antibodies before flow cytometry was performed. A simple gating strategy using FSC-A and FSC-H signals was used to select single cells. eBioscience Fixable Viability Dye (Thermo Fisher, USA) was used to distinguish viable from dead cells and CD138-staining was used as a reliable marker of murine plasma cells (**Figure 7A**).

After 4 days of incubation, only the highest concentration of PA induced a slight increase of CD138^{high} plasma cells among single, living cells compared to the control ($p = 0.0215$, **Figure 7A+B**), whereas no significant effect was observed for 0.1 and 0.25 mM PA. BA treatment on the other hand strongly induced the expression of CD138 in a dose-dependent manner (**Figure 7A+B**). At 0.5 mM BA more than doubled the frequency of CD138^{high} plasma cells ($p < 0.0001$, **Figure 7A+B**). Furthermore, when 0.5 mM PA was added to 0.5 mM BA no inhibiting or enhancing effect of PA was observed (**Figure 7A+B**).

Together these data indicate that BA, but not PA is an efficient inducer of CD138^{high} plasma cell differentiation from naïve murine B cells *ex vivo*.

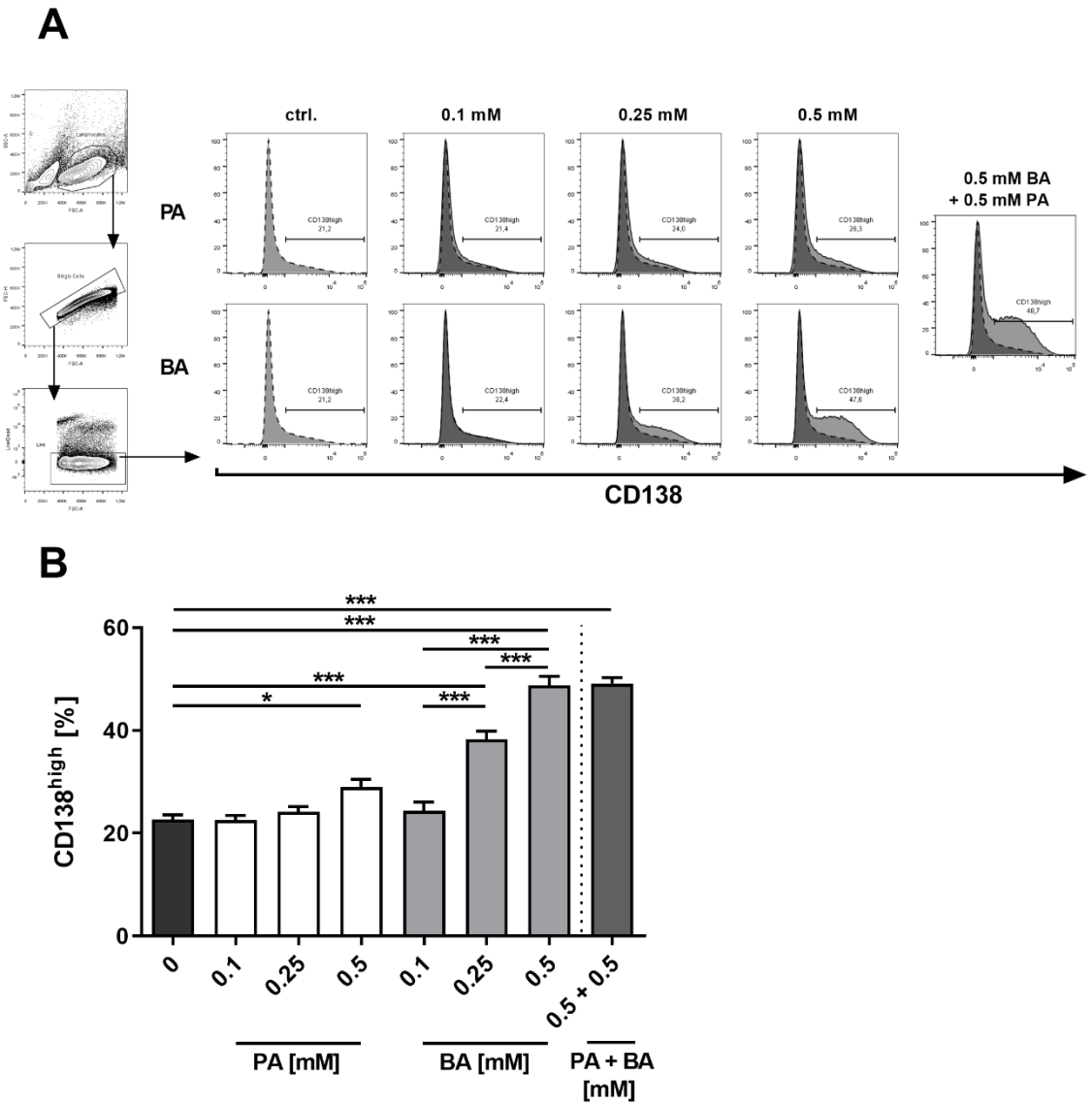

Figure 7: BA induces CD138^{high} plasma cells *ex vivo*. (A) Flow cytometric analyses of isolated, murine B cells treated under plasma cell-inducing conditions with increasing concentrations of PA and/or BA for 4 days. Representative gating plots and histogram plots of CD138 expression are shown. **(B)** Flow cytometric analyses of isolated, murine B cells treated with various concentrations of PA or BA for 4 days. Statistics: mixed-effects model, followed by Tukey's post-hoc test. Data are expressed as mean ± SEM, n = 5. * $p < 0.05$, *** $p < 0.001$. These plots and diagrams are also shown in Föh et al, 2022 [1].

5.1.2 BA alters the expression of several regulators of plasma cell differentiation

Plasma cell differentiation is tightly regulated by several regulators, most of which act as transcription factors [90]. To test whether the observed induction of plasma cells was

linked to altered gene expression of plasma cell-specific regulatory proteins, B cells were harvested after one day of cell culture under plasma cell-inducing conditions in the presence of BA. From these cells, mRNA was isolated, transcribed into cDNA, and subsequently subjected to qPCR analysis using primers specifically designed to target several regulatory factors of plasma cell differentiation.

Gene expression of the master regulator for plasma cell differentiation *Prdm1 (Blimp1)* was upregulated after incubation with BA ($p = 0.0359$, **Figure 8**) [206]. Accordingly, the expression of *Irf4*, which serves as an important checkpoint in initiating plasma cell differentiation in conjunction with *Prdm1* [207], was increased approximately 5-fold ($p = 0.0220$, **Figure 8**). Notably, no expression of *Irf8*, a potent repressor of plasma cell differentiation that acts as a counterpart to *Irf4* in plasma cell differentiation [208], was detectable after BA treatment (**Figure 8**), suggesting repression by BA. No significant changes were detected for *Bcl6* and *Xbp1*, two transcriptional regulators closely linked to inhibition [100] and induction [111] of plasma cell differentiation, respectively. Interestingly, the expression of *Aicda*, which is the master regulator of secondary antibody diversification, particularly class switch recombination, was significantly reduced in BA-treated B cells ($p = 0.0033$, **Figure 8**).

Overall, these results indicate increased transcriptional regulation towards plasma cell differentiation and suggest reduced antibody class switch recombination.

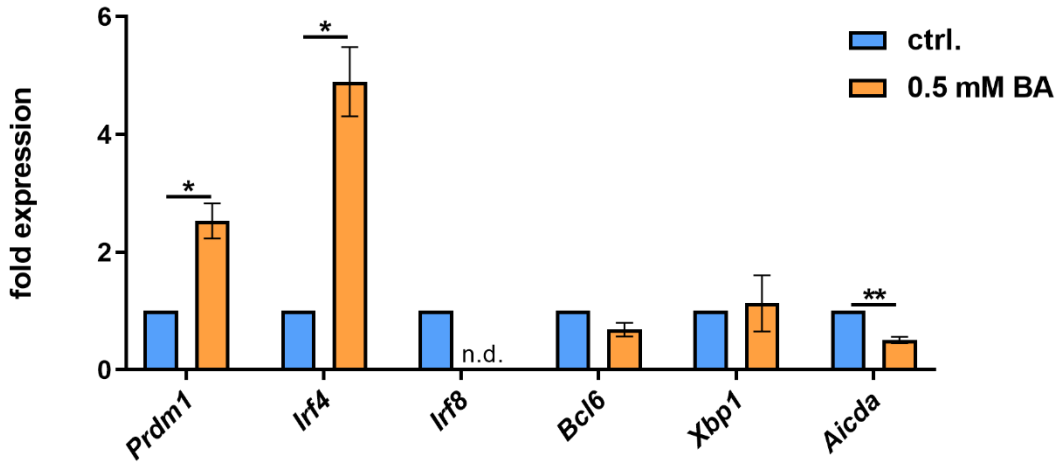

Figure 8: BA skews the expression of several regulatory genes towards plasma cell differentiation. Isolated murine B cells were incubated under plasma cell-inducing conditions with 0.5 mM BA for 1 day. mRNA was isolated and transcribed into cDNA. Subsequently, qPCR analysis for transcriptional regulators of plasma cell differentiation was performed. Statistics: two-tailed, paired student's t-tests. Data are expressed as fold expression and as mean ± SEM, n = 3-4.* $p < 0.05$, ** $p < 0.01$, n.d.: not detected. This graph is also shown in Föh et al, 2022 [1].

5.1.3 BA but not PA induces gene expression of regulatory cytokines *ex vivo*

Recently, plasma cells have been recognized as major contributors to regulatory functions of the B cell family. Breg function has been most widely linked to the expression of IL-10 as the most relevant immunosuppressive cytokine, which also serves as a major identifying feature for Bregs [4]. Additionally, increased TGFβ expression by Bregs has been demonstrated, inhibiting the function of pro-inflammatory $CD4^+$ and $CD8^+$ T cells and thereby taking part in the Breg-mediated immunosuppression [3]. More recently, IL-35 has been reported to contribute to immunosuppressive functions, particularly of regulatory plasma cells [75]. IL-35 is a heterodimeric, immunosuppressive protein consisting of IL-12α and IL-27β chains, that are products of the p35 gene and the Epstein-Barr virus-induced gene 3 (EBI3), respectively [209]. To test whether the induction of plasma cell differentiation by BA is paralleled by increased expression of regulatory cytokines indicative of regulatory function, mRNA was extracted from naïve B cells treated under plasma cell-inducing conditions with BA or PA for 4 days. mRNA was then transcribed into cDNA and

qPCR-analysis was performed using primers designed for targeting the aforementioned regulatory cytokines.

As a result, the incubation of isolated murine B cells with 0.5 mM PA led to changes in neither *Il10*, *Tgfβ1*, *Ebi3*, or *p35* expression on the transcriptional level (**Figure 9A**) paralleling the largely missing effects of PA on CD138 expression. BA treatment on the other hand increased the gene expression of *Il10* (0.5 mM BA: $p = 0.0003$), *Tgfβ1* (major member of the mammalian TGFβ-family [210], 0.5 mM BA: $p = 0.0004$), and *Ebi3* (0.5 mM BA: $p = 0.0003$) in a dose-dependent manner, while *p35* showed a similar tendency that did not reach statistical significance (**Figure 9B**).

Thus, PA did not increase the gene expression of regulatory cytokines that are typically involved in Breg function. BA, however, induced the gene expression of IL-10, TGFβ, and EBI3, indicating the induction of regulatory cytokines in parallel to the observed induction of plasma cells after 4 days.

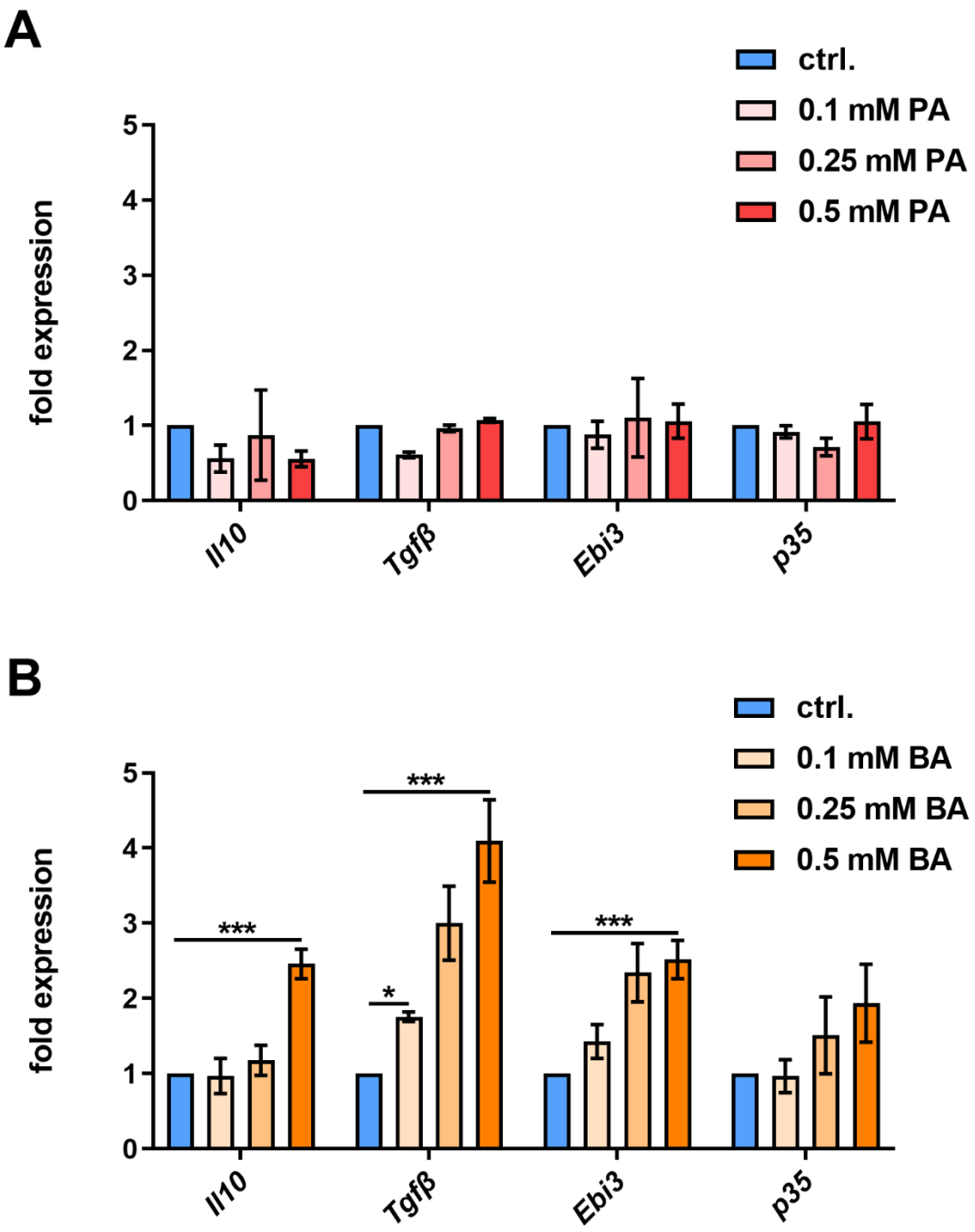

Figure 9: BA but not PA induces the gene expression of regulatory cytokines. (A) Isolated murine B cells were incubated with increasing concentrations of PA for 4 days. mRNA was isolated and transcribed into cDNA. Subsequently, qPCR analysis for the indicated regulatory cytokines was performed. n = 2-5. **(B)** Isolated murine B cells were incubated under plasma cell-inducing conditions with increasing concentrations of BA for 4 days. mRNA was isolated and transcribed into cDNA. Subsequently, qPCR analysis for several regulatory cytokines was performed. n = 3-14. **(A+B)** Statistics: mixed-effects model, followed by Tukey's post-hoc test. Data are expressed as mean ± SEM.* $p < 0.05$, *** $p < 0.001$. Both graphs are also shown in Föh et al, 2022 [1].

5.1.4 BA induces the differentiation of IL-10$^+$ CD138^{high} plasma cells *ex vivo*

Since BA induced the differentiation of CD138^{high} plasma cells and gene expression of important regulatory cytokines associated with regulatory plasma cell function, the expression of IL-10 was next analyzed on the protein level as a functional marker of Bregs. B cells from IL-10 GFP-reporter mice (Vert-X) were isolated from spleens using the same methods as before. B cells were then incubated under plasma cell-inducing conditions in the presence of increasing concentrations of PA and BA for 4 days to analyze the effects of BA and PA on the differentiation of IL-10$^+$ plasma cells.

While the frequency of IL-10$^+$ CD138^{high} plasma cells among all living cells was not significantly affected by increasing concentrations of PA (**Figure 10A+B**), BA treatment increased the frequency in a dose-dependent manner (0.25 mM BA: p = 0.0035, 0.5 mM BA: p = 0.0076, **Figure 10A+B**). When 0.5 mM PA was added to 0.5 mM BA a modest additional effect of PA was observed that did, however, not reach statistical significance (p = 0.2215, **Figure 10A+B**). Additionally, no effect of PA on the frequency of IL-10$^+$ cells among CD138^{high} plasma cells was observed for any of the concentrations applied (**Figure 10C+D**). BA treatment on the other hand led to increased expression of IL-10 in CD138^{high} plasma cells (0.25 mM BA: p = 0.0127, 0.5 mM BA: p = 0.0113, **Figure 10C+D**). The addition of 0.5 mM PA to 0.5 mM BA had no significant additional effect (p = 0.1582, **Figure 10C+D**).

Together these data show that BA induces the differentiation of CD138^{high} plasma cells, their expression of IL-10, and the frequency of IL-10$^+$ CD138^{high} plasma cells *ex vivo*, indicating that BA promotes the differentiation of regulatory plasma cells from isolated B cells.

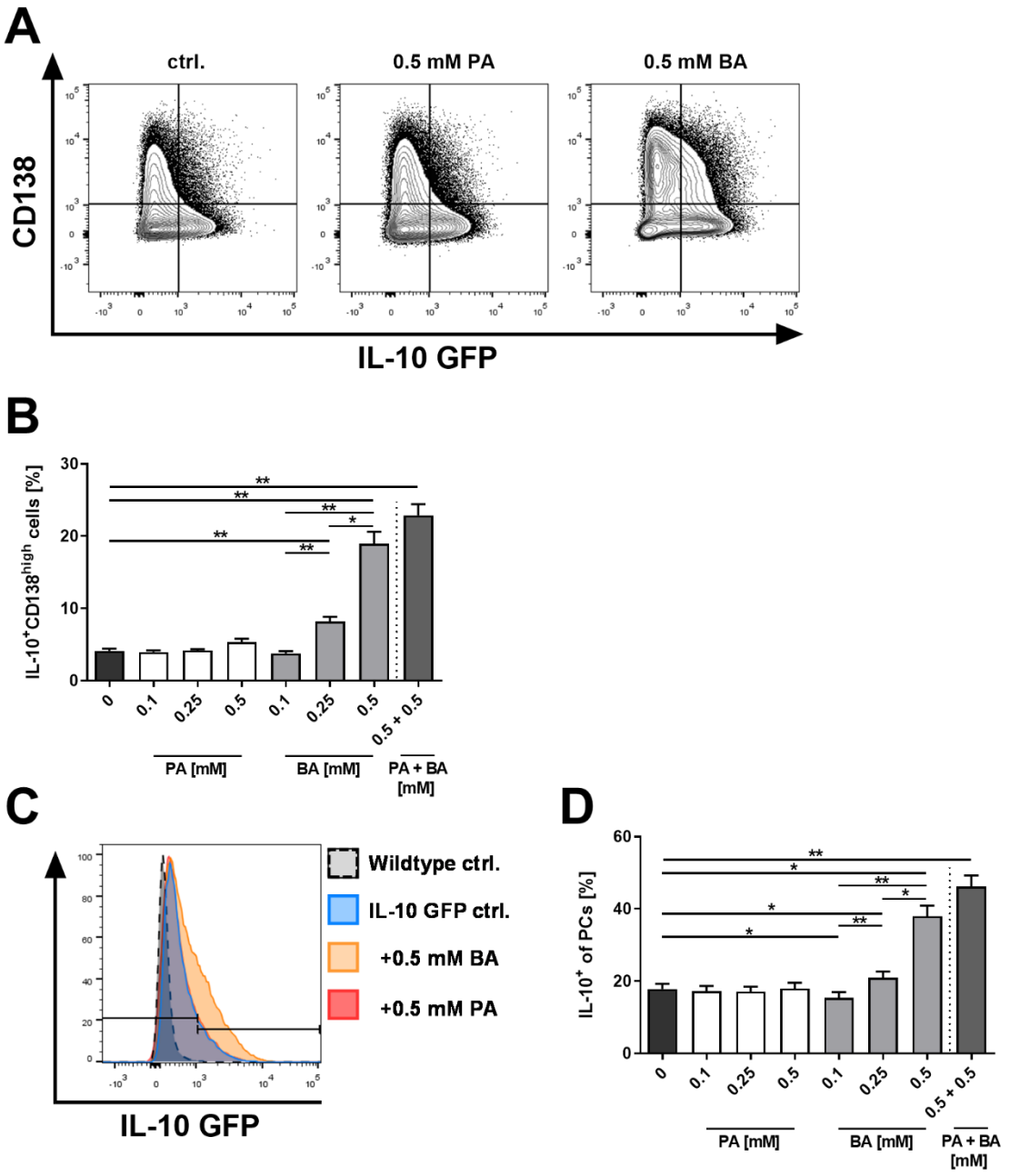

Figure 10: BA induces IL-10^{+} CD138^{high} plasma cells after 4 days of incubation *ex vivo*. Isolated, murine B cells obtained from IL-10 GFP-reporter mice were incubated under plasma cell-inducing conditions with increasing concentrations of BA and PA for 4 days followed by flow cytometry. **(A+B)** Frequencies of IL-10^{+} CD138^{high} plasma cells among all cells are shown in representative contour plots and a column diagram. **(C+D)** Frequencies of IL-10^{+} cells among CD138^{high} plasma cells are shown in a representative histogram plot and column diagram. **(B+D)** Statistics: mixed-effects models, followed by Tukey's post-hoc test. Data are expressed as mean ± SEM. n = 5 from representative experiments. * $p < 0.05$, ** $p < 0.01$, *** $p < 0.001$. All plots and diagrams are also shown in Föh et al, 2022 [1].

5.1.5 IL-10^{+} CD138^{high} plasma cells preferentially express IgM *ex vivo*

Since previous publications showed regulatory plasma cells to express IgM, rather than other immunoglobulin classes [75,211], the IgM expression of IL-10^{+} plasma cells was examined in comparison to IL-10^{-} plasma cells *ex vivo* after four days of basic plasma cell-inducing conditions as described above. Although both populations showed high frequencies of IgM^{+} cells, significantly higher proportions of IgM^{+} cells were observed in IL-10^{+} plasma cells compared to IL-10^{-} plasma cells ($p < 0.0001$, **Figure 11**), indicating that IL-10^{+} CD138^{high} plasma cells preferentially express IgM *ex vivo*.

Together, these results suggest that BA might be able to induce IL-10^{+}IgM^{+} regulatory plasma cells.

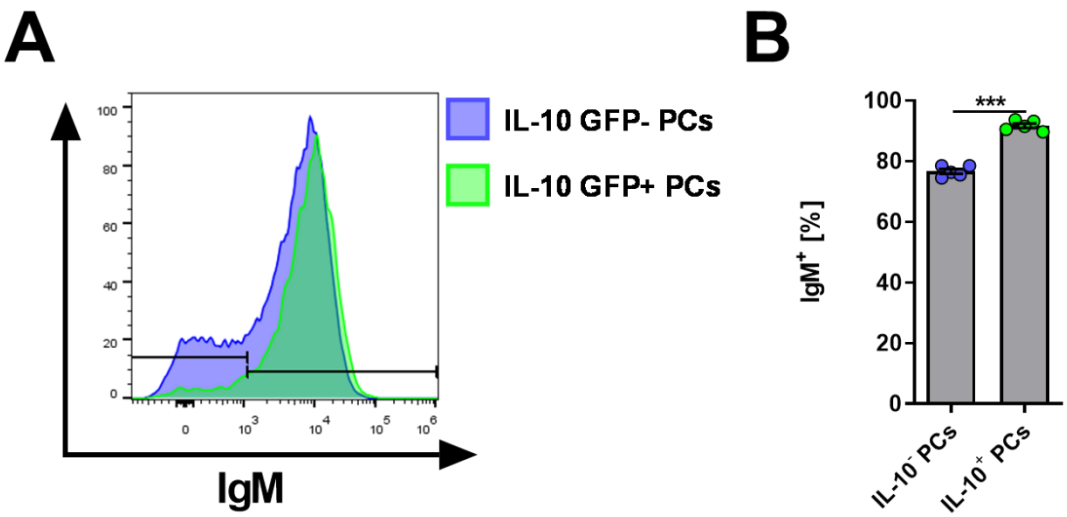

Figure 11: IL-10^{+} plasma cells preferentially express IgM *ex vivo*. Isolated, murine B cells obtained from IL-10 GFP-reporter mice were incubated under plasma cell-inducing conditions for 4 days followed by flow cytometry. **(A)** Representative histogram plot of IgM expression among IL-10-GFP^{+} compared to IL-10-GFP^{-} CD138^{high} plasma cells. **(B)** Frequencies of IgM^{+} cells among IL-10-GFP^{+} compared to IL-10-GFP^{-} CD138^{high} plasma cells. two-tailed, paired student's t-test. n = 5. *** $p < 0.001$. The plot and graph are also shown in Föh et al, 2022 [1].

5.2 BA induces splenic IL-10$^+$IgM$^+$ plasma cells *in vivo*

Because BA but not PA induced the expression of IL-10$^+$ plasma cells *ex vivo*, the effects of BA application *in vivo* were analyzed. Two different application routes of BA to C57BL/6J (wildtype) and IL-10 reporter (Vert-X) mice were utilized. For enteral application, BA was added to drinking water at a concentration of 150 mM compared to a drinking water control group without supplementation (DW). For parenteral application circumventing initial intestinal and hepatic metabolization, BA was applied via intraperitoneal injection (i.p.) in a dosage of 100 mg/kg body weight. PBS was used as the vehicle control in the control group. After seven days of either enteral or parenteral application of BA, mice were immunized with Ova/CFA to activate the immune system and induce an immunological reaction. After another 12 days, murine spleens were harvested. Splenic cells were then stained with fluorophore-conjugated antibodies and subjected to flow cytometry (s. experimental setup in **Figure 3**).

5.2.1 BA induces splenic CD138^{high} plasma cells *in vivo*

To examine the effects of *in vivo* application of BA on plasma cell differentiation, splenic cells were stained using viability dye and fluorophore-conjugated antibodies against B220 and CD138 to identify plasma cells. The gating strategy used for the assessment of splenic plasma cells is depicted in **Figure 12A** for one representative experiment with BA in drinking water.

When mice were treated with 150 mM BA in drinking water, there was a significant increase of the CD138^{high} plasma cell frequency among splenic lymphocytes ($p = 0.0005$, **Figure 12B**, left panel), as well as plasma cell counts ($p = 0.0478$, **Figure 12B**, right panel). Similarly, parenteral application of BA via intraperitoneal injection led to a significantly increased CD138^{high} plasma cell frequency ($p = 0.0461$, **Figure 12C**, left panel) and splenic plasma cell counts ($p = 0.0014$, **Figure 12C**, right panel). These data demonstrate increased plasma cells in the spleens of BA-treated mice regardless of the route of administration and indicate that BA promotes the differentiation of splenic CD138^{high} plasma cells.

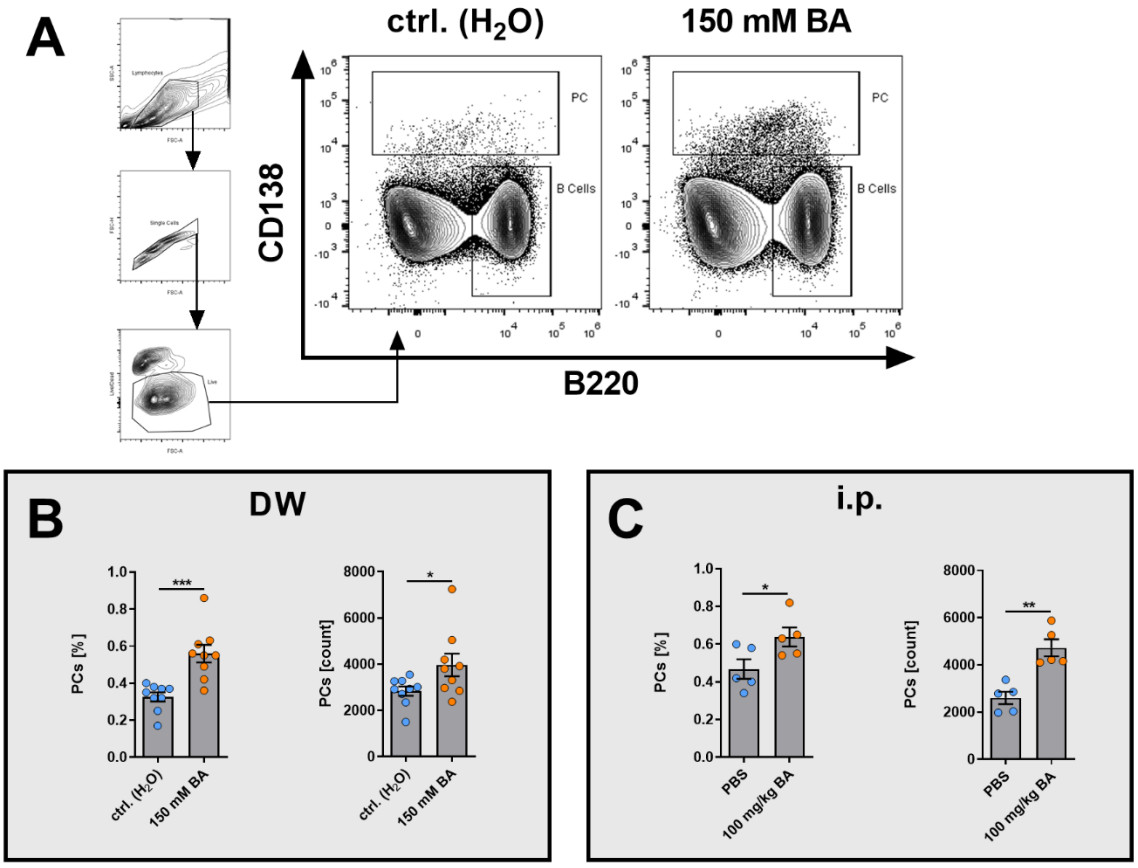

Figure 12: Administration of BA via drinking water or i.p. injection induces splenic plasma cells. Flow cytometric analyses of plasma cells in splenic tissue after administration of BA via different routes and immunization with Ova-CFA (application scheme shown in **Figure 3**). **(A)** Gating strategy and representative contour plots of mice treated with 150 mM BA and drinking water controls. **(B)** Mice were supplied with 150 mM BA or control drinking water. Left panel: Frequency of $CD138^{high}$ plasma cells among total lymphocytes. Right panel: $CD138^{high}$ plasma cell counts. n = 9. **(C)** 100 mg/kg body weight BA was administered via intraperitoneal injection (i.p.) every day. Left panel: Frequency of $CD138^{high}$ plasma cells among total lymphocytes. Right panel: $CD138^{high}$ plasma cell counts. n = 5. **(B+C)** DW = drinking water, i.p. = intraperitoneal injection. Statistics: two-tailed, unpaired student's t-tests, data are expressed as mean ± SEM. * $p < 0.05$, ** $p < 0.01$, *** $p < 0.001$. The plots and diagrams are also shown in Föh et al, 2022 [1].

5.2.2 BA administration induces splenic IL-10^{+} plasma cells *in vivo*

Since regulatory plasma cells have been implicated as a major subset of Bregs [211,212], and since *ex vivo* data showed elevated expression of IL-10 after BA administration, the effects of *in vivo* BA administration on the expression of IL-10 in plasma cells were analyzed using IL-10 GFP-reporter mice 12 days after Ova/CFA-immunization (s. **Figure 3** for application scheme).

The gating strategy from the previous experiment was used for the identification of CD138^{high} plasma cells in splenic lymphocytes. Subsequently, IL-10 GFP signals were analyzed (**Figure 13A**). Notably, BA administration via drinking water increased the frequency of IL-10^{+} cells among CD138^{high} plasma cells (p = 0.0322, **Figure 13B**, left panel) as well as cell counts of IL-10^{+} CD138^{high} plasma cells (p = 0.0138, **Figure 13B**, right panel). Furthermore, parenteral application of BA via i.p. injection led to increased IL-10^{+} CD138^{high} plasma cell counts (p = 0.0014, **Figure 13C**, right panel), whereas no significant increase in IL-10^{+} frequency was observed (**Figure 13C**, left panel). These results indicate that systemic BA administration, particularly in drinking water, induces splenic CD138^{high} plasma cells that express IL-10, recapitulating similar results obtained in cell culture experiments.

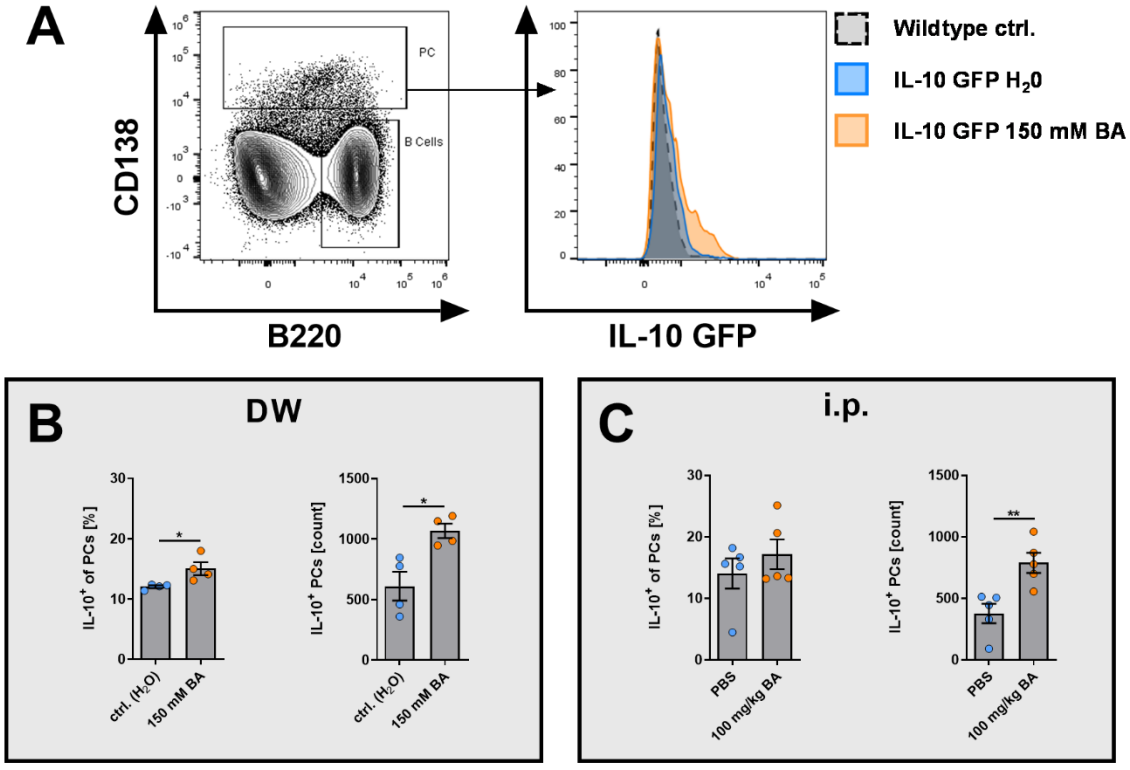

Figure 13: Application of BA via drinking water and i.p. injection increases splenic IL-10^{+} plasma cells. Flow cytometric analyses of plasma cells in splenic tissue of IL-10 reporter-mice after administration of BA via different routes and immunization with Ova/CFA. See **Figure 3** for the application scheme. **(A)** Gating strategy and representative histogram plot of mice treated with 150 mM BA and drinking water controls. **(B)** Mice were supplied with 150 mM BA or control drinking water. Left panel: Frequency of IL-10^{+} cells among CD138^{high} plasma cells. Right panel: IL-10^{+} CD138^{high} plasma cell counts. n = 4. **(C)** Mice were

administered 100 mg/kg body weight BA via intraperitoneal injection (i.p.). Left panel: Frequency of IL-10^{+} cells among CD138^{high} plasma cells. Right panel: IL-10^{+} CD138^{high} plasma cell counts. n = 4. **(B+C)** Statistics: two-tailed, unpaired student's t-tests, data are expressed as mean ± SEM, * $p < 0.05$, ** $p < 0.01$. The plots and diagrams are also shown in Föh et al, 2022 [1].

5.2.3 IL-10^{+} plasma cells preferentially express IgM *in vivo* after BA treatment

Since IL-10^{+} plasma cells showed preferential expression of IgM *ex vivo*, and since previous literature suggested regulatory plasma cells express IgM as well [75], IgM expression of IL-10^{+} plasma cells was investigated *in vivo* by flow cytometry (gating strategy: **Figure 14A**).

As a result, IL-10^{+} CD138^{high} plasma cells overwhelmingly expressed IgM at a frequency of 82.1% after BA treatment via drinking water (**Figure 14B**, left panel) and 90.8% after BA treatment via i.p. injection (**Figure 14C**, left panel). Notably, IgM expression of IL-10^{+} CD138^{high} plasma cells was drastically higher compared to IL-10^{-} CD138^{high} plasma cells as determined via the frequency of IgM^{+} cells among plasma cells ($p < 0.0001$, **Figure 14B**, left panel) and the anti-IgM-PE-cyanine7 MFI ($p < 0.0001$, **Figure 14B**, right panel) after treatment with 150 mM BA in drinking water. Similarly, IgM^{+} frequency ($p < 0.0001$, **Figure 14C**, left panel) and anti-IgM-PE-cyanine7 MFI ($p < 0.0001$, **Figure 14C**, right panel) were elevated in IL-10^{+} CD138^{high} plasma cells compared to IL-10^{-} CD138^{high} plasma cells after administration of 100 mg/kg BA i.p..

These data demonstrate preferential expression of IgM by IL-10^{+} plasma cells *in vivo* compared to IL-10^{-} plasma cells, indicating that the overwhelming majority of IL-10^{+} plasma cells express the IgM isotype of antibodies *in vivo*.

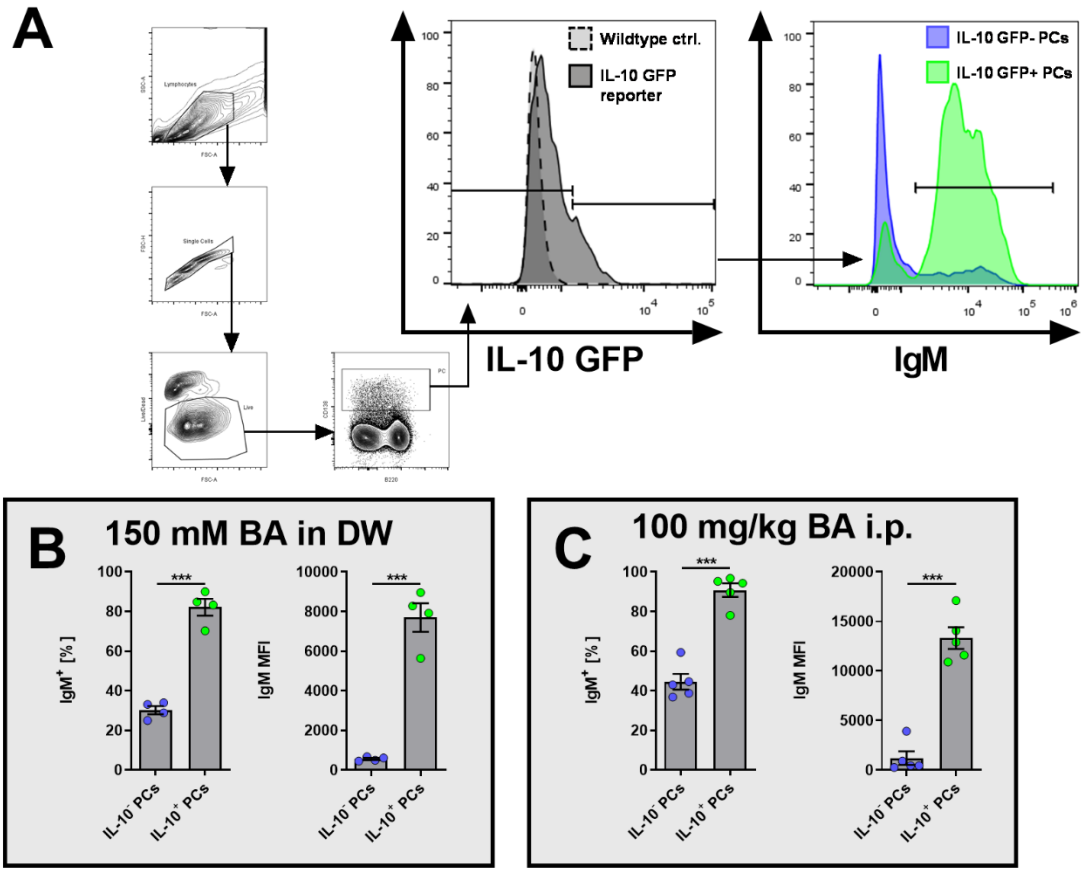

Figure 14: IL-10$^+$ CD138^{high} plasma cells preferentially express IgM *in vivo*. Flow cytometric analyses of IgM-expression in splenic IL-10$^+$ and IL-10$^-$ CD138^{high} plasma cells obtained from IL-10 reporter-mice after administration of BA via different routes and immunization with Ova/CFA (application scheme shown in **Figure 3**). **(A)** Gating strategy and representative histogram plots of IL-10 GFP expression in CD138^{high} plasma cells compared to wildtype control and IgM expression in IL-10 GFP$^-$ and IL-10 GFP$^+$ CD138^{high} plasma cells. **(B)** All mice were supplied with 150 mM BA in drinking water. Left panel: Frequency of IgM$^+$ cells among IL-10$^+$ and IL-10$^-$ CD138^{high} plasma cells. Right panel: PE-cyanine7 (anti-IgM) MFI. n = 4. **(C)** All mice were administered 100 mg/kg body weight BA via intraperitoneal injection (i.p.). Left panel: Frequency of IgM$^+$ cells among IL-10$^+$ and IL-10$^-$ CD138^{high} plasma cells. Right panel: PE-cyanine7 (anti-IgM) MFI. n = 4. **(B+C)** Statistics: two-tailed, unpaired student's t-tests, data are expressed as mean ± SEM. *** $p < 0.001$. The plots and diagrams are also shown in Föh et al, 2022 [1].

5.2.4 IgM$^+$ plasma cells preferentially express IL-10 *in vivo* after BA treatment

The preferential expression of IgM by IL-10$^+$ CD138^{high} plasma cells *in vivo* raised the reciprocal question of whether IL-10 expression is particularly increased in IgM$^+$ plasma cells compared to plasma cells expressing other immunoglobulin classes. Hence, to further

characterize the relation of IL-10 and IgM expression in plasma cells after BA treatment IL-10 expression in IgM^+ and IgM^- plasma cells was compared (gating strategy: **Figure 15A**).

The proportion of IL-10^+ cells among IgM^+ $CD138^{high}$ plasma cells was 33.8% after BA treatment via drinking water (**Figure 15B**, left panel) and 34.5% after BA treatment via i.p. injection (**Figure 15C**, left panel). When compared to IgM^- plasma cells these frequencies were drastically elevated from only 4.1% for enteral ($p < 0.001$, **Figure 15B**, left panel) and 3.2% for parenteral administration of BA ($p < 0.001$, **Figure 15B**, left panel), respectively. Similarly, IL-10 GFP MFIs were significantly increased in IgM^+ compared to IgM^- $CD138^{high}$ plasma cells for both routes of application (both $p < 0.001$, **Figure 15B+C**, right panels).

These results reveal preferential expression of IL-10 in IgM^+ plasma cells *in vivo*. Whereas the expression of IL-10 is observed in low frequencies of plasma cells expressing other antibody isotypes (IgM^- plasma cells), approximately a third of the splenic IgM^+ plasma cells expressed IL-10 after BA treatment.

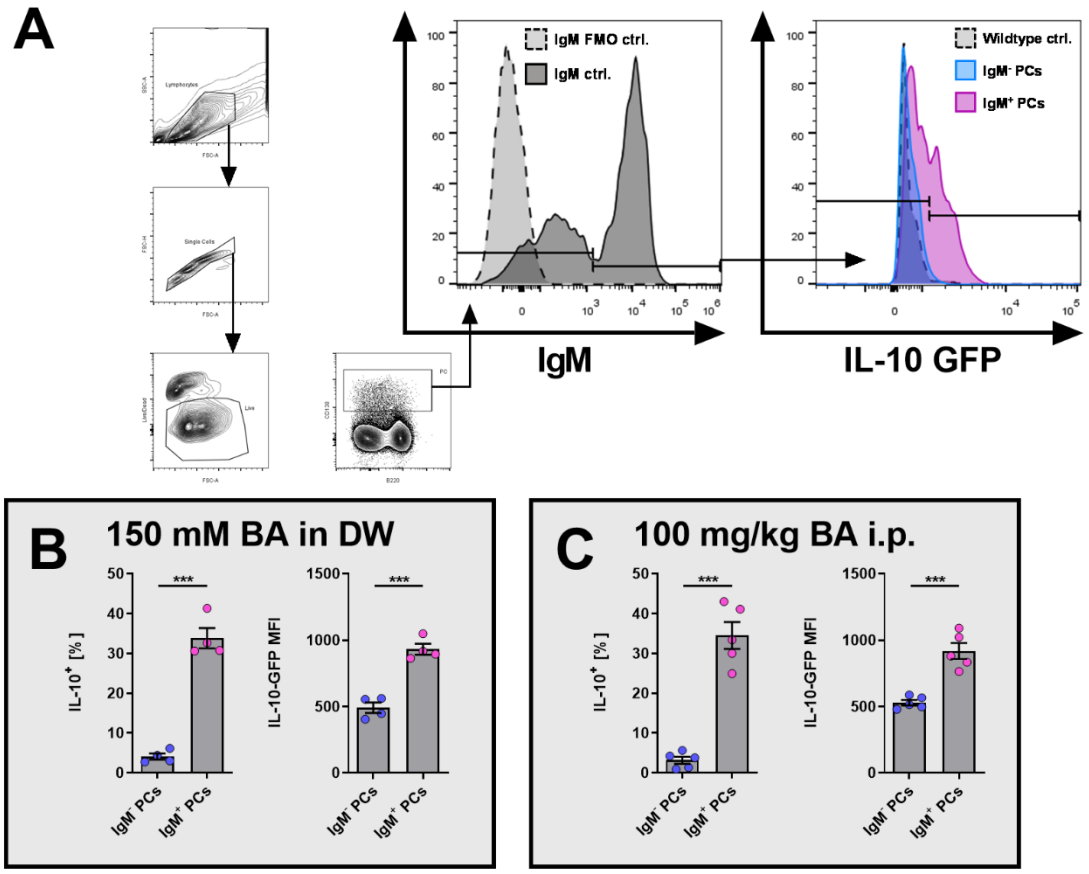

Figure 15: IgM$^+$ CD138^{high} plasma cells preferentially express IL-10 *in vivo*. Flow cytometric analyses of IL-10 expression in IgM$^+$ and IgM$^-$ CD138^{high} plasma cells in splenic tissue of IL-10 reporter-mice after administration of BA via different routes and immunization with Ova/CFA (application scheme shown in **Figure 3**). **(A)** Gating strategy and representative histogram plots of IgM expression in CD138^{high} plasma cells compared to the isotype control and IL-10 GFP expression in IgM$^+$ and IgM$^-$ CD138^{high} plasma cells. **(B)** Mice were supplied with 150 mM BA in drinking water. Left panel: Frequency of IL-10$^+$ cells among IgM$^+$ and IgM$^-$ CD138^{high} plasma cells. Right panel: IL-10 GFP MFI of IgM$^+$ and IgM$^-$ CD138^{high} plasma cells. n = 4. **(C)** Mice were administered 100 mg/kg body weight BA via intraperitoneal injection (i.p.). Left panel: Frequency of IL-10$^+$ cells among IgM$^+$ and IgM$^-$ CD138^{high} plasma cells. Right panel: IL-10 GFP MFI of IgM$^+$ and IgM$^-$ CD138^{high} plasma cells. n = 4. **(B+C)** Statistics: two-tailed, unpaired student's t-tests, data are expressed as mean ± SEM. *** p < 0.001. The plots and diagrams are also shown in Föh et al, 2022 [1].

5.2.5 BA induces IL-10$^+$IgM$^+$ CD138^{high} plasma cells *in vivo*

Considering the high frequency of IL-10-expressing cells among IgM$^+$ plasma cells and vice versa, the effects of BA application on IL-10- and IgM-expression in plasma cells were examined.

Increased splenic cell counts of IL-10^{+}IgM^{+} CD138^{high} plasma cells were observed after BA treatment via drinking water (p = 0.0290, **Figure 16B**, left panel) and i.p. injection (p = 0.0117, **Figure 16C**, left panel). Furthermore, BA increased the expression of IL-10 GFP MFI in IgM^{+} PCs in both modes of application (DW: p = 0.0093; i.p.: p = 0.0497; **Figure 16B+C**, center panels), indicating that BA promotes regulatory IL-10^{+}IgM^{+} plasma cells. To test whether increased IL-10^{+}IgM^{+} plasma cells are reflected by increased IgM antibody secretion, the serum levels of total IgM were determined using ELISA. Serum IgM levels were increased significantly after treatment with 150 mM BA in drinking water (p = 0.0057, **Figure 16B**, right panel), but only slightly without reaching statistical significance after i.p. injection of 100 mg/kg BA (p = 0.1796, **Figure 16C**, right panel).

Taken together, BA induced IL-10^{+}IgM^{+} CD138^{high} plasma cells and IL-10 expression in IgM^{+} plasma cells in spleens of Ova/CFA immunized mice. Furthermore, increased total IgM serum levels were detected after BA treatment in drinking water.

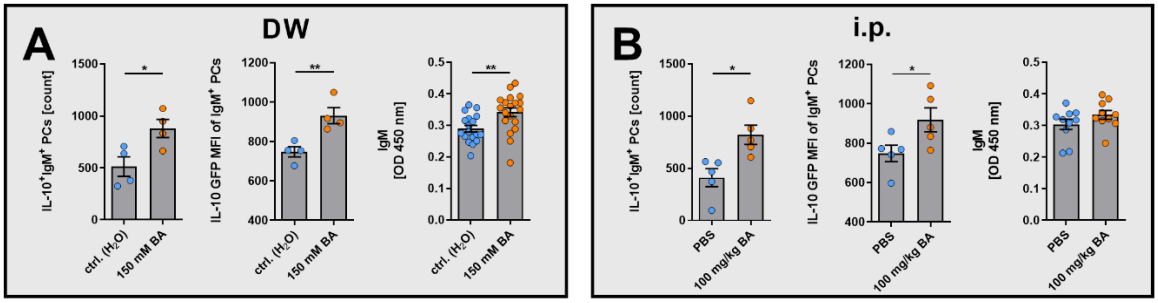

Figure 16: BA increases IL-10^{+}IgM^{+} plasma cells and serum levels of IgM. Flow cytometric analyses of IL-10 and IgM expression in splenic CD138^{high} plasma cells obtained from IL-10 reporter-mice and ELISA analysis of total IgM levels after administration of BA via different routes and immunization with Ova/CFA (application scheme shown in **Figure 3**). **(A)** Mice were supplied with 150 mM BA in drinking water. Left panel: Cell counts of IL-10^{+}IgM^{+} CD138^{high} plasma cell counts, n = 4. Center panel: IL-10 GFP MFI of IgM^{+} CD138^{high} plasma cells, n = 4. Right panel: Serum levels of total IgM determined by ELISA, n = 18-19. **(B)** Mice were administered 100 mg/kg body weight BA via intraperitoneal injection (i.p.). Left panel: IL-10^{+}IgM^{+} CD138^{high} plasma cell counts, n = 5. Center panel: IL-10 GFP MFI of IgM^{+} CD138^{high} plasma cells, n = 5. Right panel: Serum levels of total IgM determined by ELISA, n = 10. **(A+B)** two-tailed, unpaired student's t-tests, data are expressed as mean ± SEM. * $p < 0.05$, ** $p < 0.01$. OD = Optical density. All plots and diagrams are also shown in Föh et al, 2022 [1].

5.2.6 BA promotes antigen-specific plasma cells and IgM *in vivo*

Additionally, the Ova/CFA-immunization model was used to analyze the effects of BA on antigen-specific plasma cells and antigen-specific IgM production, considering a lack of information on the antigen-specificity of regulatory plasma cells in previous literature [211].

Antigen-specific plasma cells were determined using AF647-conjugated Ova in flow cytometry to stain antigen-specific plasma cells (**Figure 17A**). Administration of 150 mM BA in drinking water increased the frequency (p = 0.0139, **Figure 17B**, left panel) and cell counts (p = 0.0139, **Figure 17B**, right panel) of Ova-specific plasma cells among all plasma cells significantly. Similar effects on cell counts of Ova-specific plasma cells were observed after daily i.p. injection of BA (p = 0.0436, **Figure 17C**, right panel), although the frequency of Ova-specific plasma cells remained the same (p = 0.4495, **Figure 17C**, left panel).

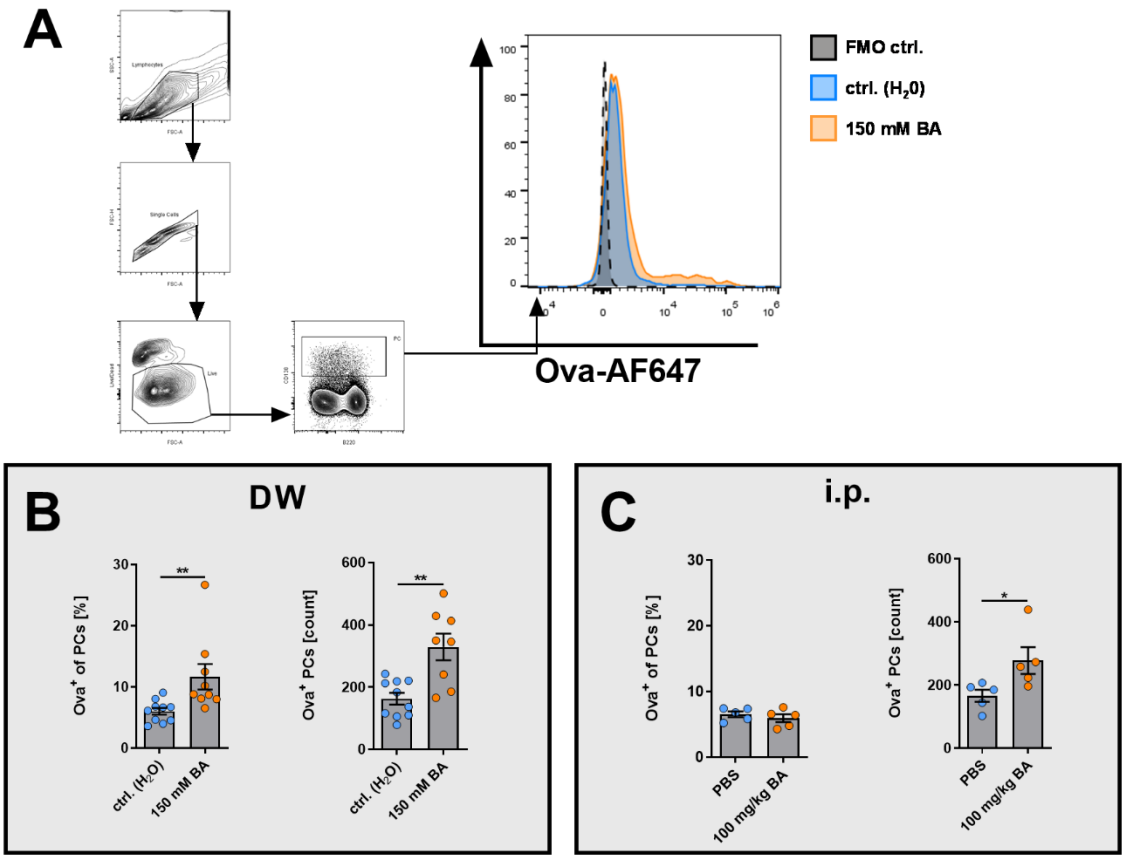

Figure 17: BA in drinking water promotes Ova-specific splenic plasma cells after Ova/CFA-immunization. Flow cytometric analyses of Ova-specific CD138^{high} plasma cells in splenic tissue after administration of BA via different routes and immunization with Ova/CFA

(application scheme shown in **Figure 3**). **(A)** Gating strategy and representative histogram plots of Ova-specific plasma cells after administration of BA via drinking water. **(B)** Mice were supplied with 150 mM BA in drinking water. Left panel: Frequency of Ova-specific (Ova^+) cells among all $CD138^{high}$ plasma cells. Right panel: Cell counts of Ova^+ plasma cells. n = 8-10. **(C)** Mice were administered 100 mg/kg body weight BA via intraperitoneal injection (i.p.). Left panel: Frequency of Ova-specific (Ova^+) cells among all $CD138^{high}$ plasma cells. Right panel: Cell counts of Ova^+ plasma cells. n = 5. **(B+C)** Statistics: two-tailed, unpaired student's t-tests, data are expressed as mean ± SEM. * $p < 0.05$, ** $p < 0.01$. All plots and diagrams are also shown in Föh et al, 2022 [1].

To test whether increased antigen-specificity of plasma cells after BA treatment is reflected by increased secretion of antigen-specific antibodies, serum levels of anti-Ova IgM antibodies were analyzed. As a result, BA in drinking water increased serum levels of anti-Ova IgM significantly ($p = 0.0069$, **Figure 18B**). No significant differences in anti-Ova serum IgM levels were observed after BA administration via i.p. injection (**Figure 18F-J**). Notably, additional anti-Ova serum antibody isotypes (IgA, IgG1, IgG2b, and IgG2c) were analyzed in a separate project by Jana Sophia Buhre of the same working group as part of her project. Her results have been presented in Föh et al, 2022 [1] and will be briefly discussed in the discussion part below.

Together these data indicate increased antigen-specificity of splenic plasma cells and increased serum levels of antigen-specific IgM antibodies after BA administration in drinking water. These results might point to an additional induction of antigen-specific regulatory PCs after enteral BA application. I.p. injection of BA on the other hand hardly recapitulates these results.

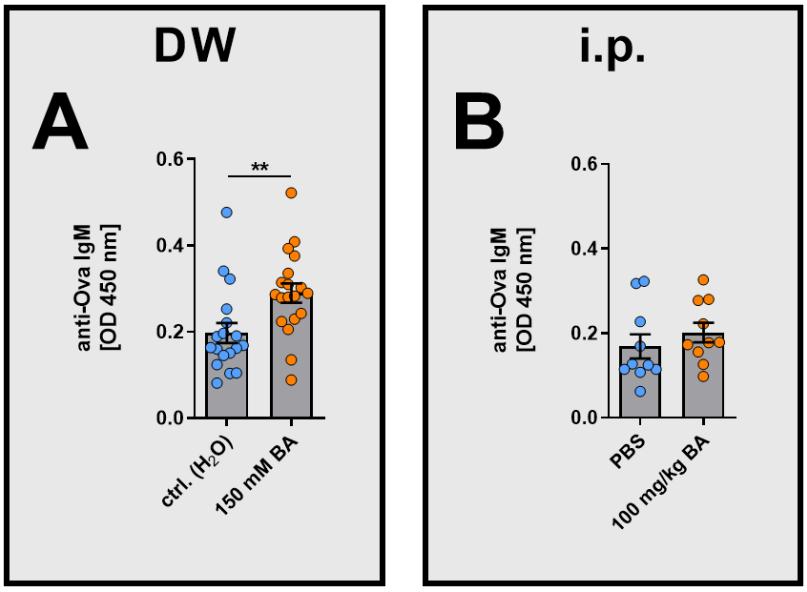

Figure 18: BA in drinking water increases serum levels of anti-Ova serum IgM. Serum levels of anti-Ova IgM were detected using ELISA after administration of BA via different routes and immunization with Ova/CFA (application scheme shown in **Figure 3**). Serum levels of anti-Ova IgM **(A+B)** antibodies of mice treated with either **(A)** control drinking water or BA (150 mM, n = 18-19) or **(B)** PBS vehicle control or BA (100 mg/kg, n = 10) by i.p. injection. Statistics: two-tailed, unpaired student's t-tests, data are expressed as mean ± SEM. * $p < 0.05$, ** $p < 0.01$. OD = optical density. Both graphs are also shown in Föh et al, 2022 [1].

5.3 Sialylation capacity of IL-10$^+$ plasma cells

5.3.1 Splenic IL-10$^+$ plasma cells express increased levels of St6gal1

Regulatory plasma cells have been shown to exert regulatory functions by producing immunoregulatory cytokines, especially IL-10. However, there are additional pathways that might contribute to the anti-inflammatory capacity of plasma cells [211,212]. One of those pathways is the type of Fc glycosylation of antibodies, which is crucial in determining their (anti-)inflammatory properties [121,127]. Terminal sialylation of IgG, IgA, and IgM antibodies has been linked to less or even anti-inflammatory properties [124,126,127,129,130,135,136,198,213,214].

It remains unclear if regulatory IL-10$^+$ plasma cells differ from IL-10$^-$ plasma cells regarding their capacity for antibody glycosylation. Thus, we used flow cytometry to assess the

intracellular expression of St6gal1, which is a reliable marker for the antibody sialylation in plasma cells [126,129,133,198], in IL-10^{+} and IL-10^{-} plasma cells from IL-10 reporter mice.

As a result, the MFI of St6gal1-AF488 was increased 3.1-fold in splenic IL-10^{+} plasma cells compared to IL-10^{-} plasma cells ($p < 0.0001$, **Figure 19**), indicating higher expression of St6gal1 in regulatory IL-10^{+} plasma cells and thus increased capacity for terminal sialylation of antibodies in IL-10^{+} regulatory plasma cells.

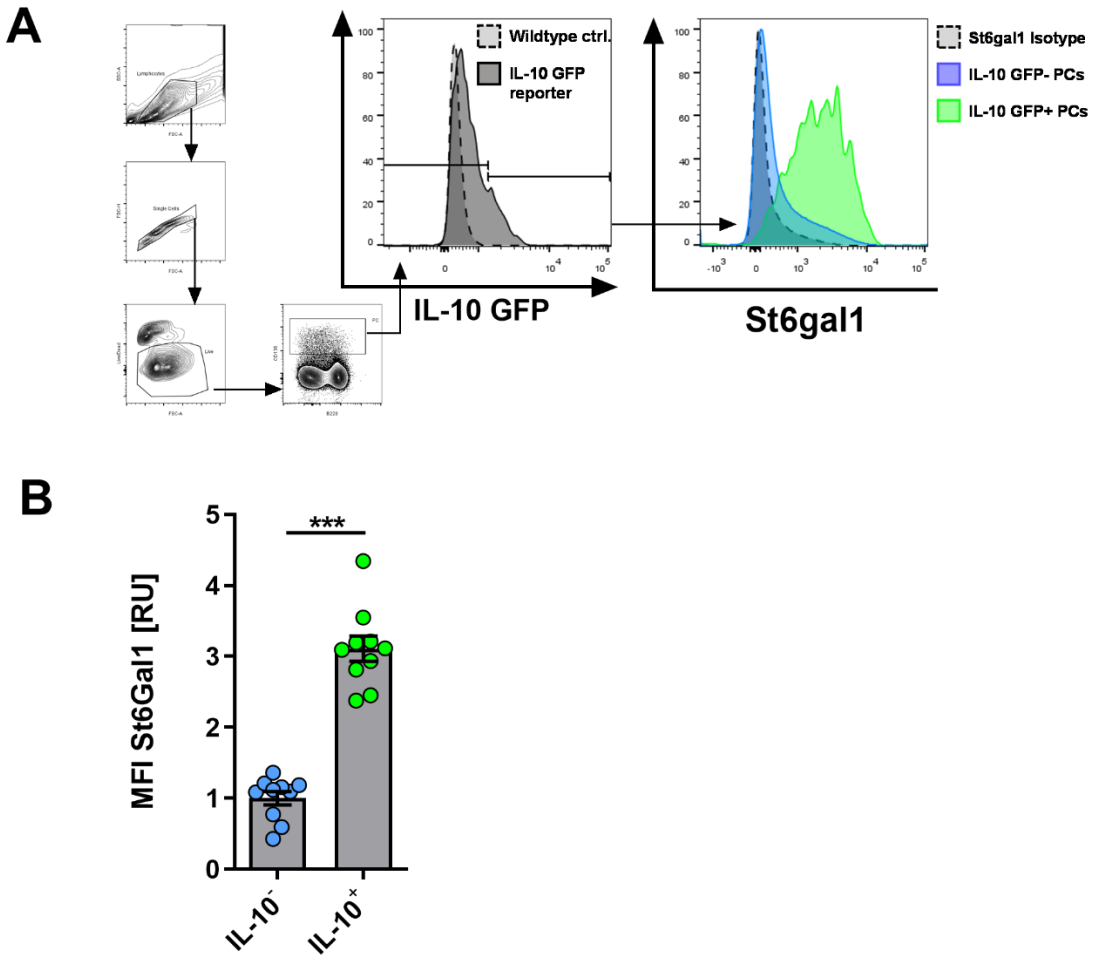

Figure 19: St6gal1 expression is increased in regulatory IL-10^{+} plasma cells. Flow cytometric analyses of St6gal1 expression in IL-10^{+} and IL-10^{-} CD138^{high} plasma cells in splenic tissue after administration of 150 mM BA via drinking water and immunization with Ova/CFA (application scheme shown in Fig. 2). **(A)** Gating strategy and representative histogram plots for splenic IL-10^{+} plasma cells compared to IL-10^{-} plasma cells of Ova/CFA-immunized mice. **(B)** St6gal1-AF488 MFI of regulatory IL-10^{+} plasma cells compared to IL-10^{-} plasma cells. RU = Relative units. (A+B) Mann-Whitney test, data are expressed as mean ± SEM, n = 10 from representative experiments. *** $p < 0.001$.

5.4 Mechanisms of IL-10 plasma cell induction by BA

Since BA effectively induced regulatory IL-10^{+} plasma cells in cell culture and *in vivo*, possible underlying mechanisms were examined next using isolated, murine B cells *ex vivo*. Previously, three main modes of action have been described for BA effects on immune cells and were thus investigated:

1. Direct activation of GPCRs by BA [148]
2. Intracellular inhibition of HDACs [148]
3. Regulation of mitochondrial metabolism [30,171,215]

5.4.1 GPR43 ligands do not induce plasma cells *ex vivo*

BA is a ligand for three major GPRs: GPR41, GPR43, and GPR109A [148]. Under physiological circumstances, neither of those receptors is expressed at relevant levels in inactivated B cells [162,179,216]. In contrast to GPR41 and GPR109A however, GPR43 is expressed at significant levels in activated murine B cells [156]. Thus, GPR43 activation by BA was considered a possible underlying pathway for the induction of plasma cells.

To test whether GPR43 was expressed in murine B cells in the experimental setting utilized here, qPCR was used. When isolated splenic B cells were incubated under plasma cell-inducing conditions, GPR43 gene expression was detected and further drastically increased under BA treatment ($p < 0.0001$, **Figure 20A**).

To test whether activation of GPR43 is sufficient to induce similar frequencies of plasma cells as BA, we used an allosteric GPR43-agonist in the same *ex vivo* setup and analyzed the expression of CD138^{high} plasma cells after 4 days of incubation. As a result, no increase in CD138^{high} plasma cells was observed for the allosteric GPR43 agonist ($p= 0.5997$, **Figure 20B+C**) even when used in a concentration of 1 µM exceeding the reported IC50 value (IC50 = 0.7 µM [217]), but for BA ($p < 0.0001$, **Figure 20B+C**). Notably, PA is another potent activator of GPR43 [148] and, as shown in **Figure 7**, did not induce plasma cells from naïve B cells as well.

These results indicate that GPR43 activation is not sufficient to induce CD138 expression in naïve B cells. Thus, it is unlikely that BA-induced plasma cell differentiation is mediated by GPR43 activation.

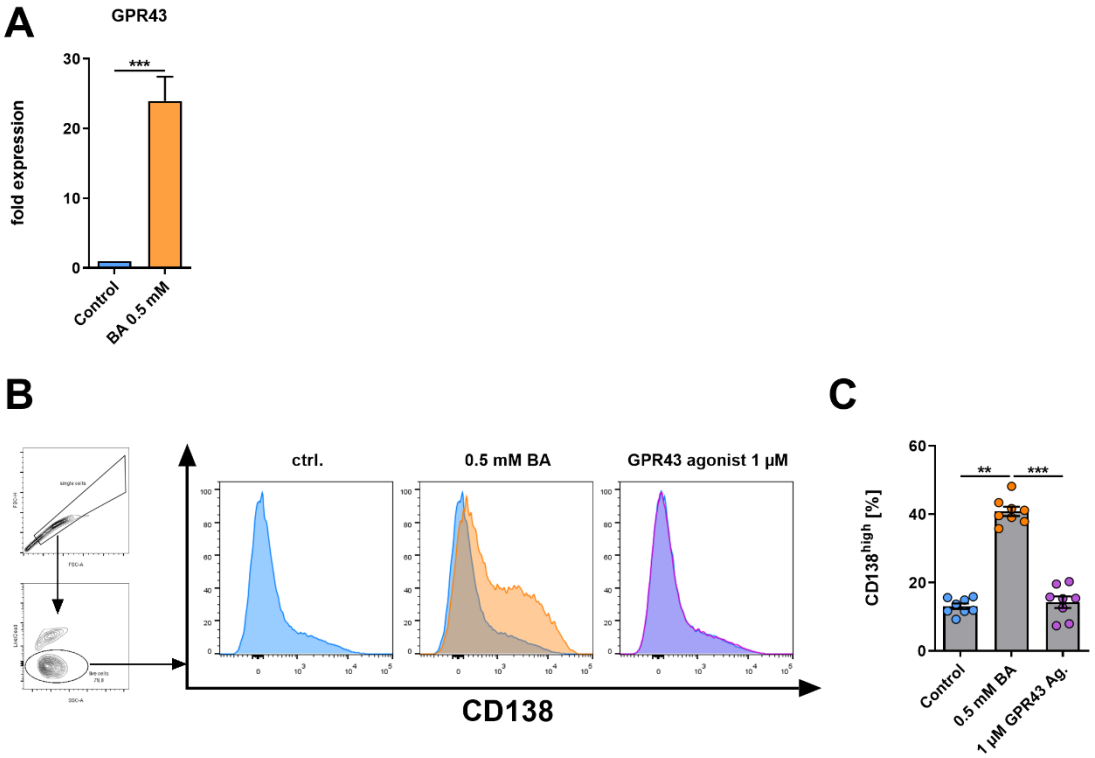

Figure 20: GPR43 agonist does not induce CD138^{high} plasma cells *ex vivo*. (A) Naïve B cells were incubated under plasma cell-inducing conditions with 0.5 mM BA for 4 days. mRNA was isolated and transcribed into cDNA. Subsequently, qPCR analysis for GPR43 was performed. n = 14. Statistics: two-tailed, paired student's t-test. **(B)** Naïve B cells were incubated under plasma cell-inducing conditions with 0.5 mM BA or 1 µM GPR43 agonist for 4 days. Gating strategy and representative histogram plots for flow cytometric analyses of CD138 expression are shown. **(C)** Naïve B cells were incubated under plasma cell-inducing conditions with 0.5 mM BA or 1 µM GPR43 agonist for 4 days. Frequencies of CD138^{high} plasma cells are shown in column diagrams. n = 8. Statistics: mixed-effects model followed by Tukey's post-hoc test. **(B+C)** Data are expressed as mean ± SEM. ** $p < 0.01$, *** $p < 0.001$. The plots and graphs in B and C are also shown in the supplementary data of Föh et al, 2022 [1].

5.4.2 BA but not PA increases H3K27 acetylation in B cells *ex vivo*

Several immunomodulatory functions of BA are mediated by inhibition of histone deacetylase (HDAC) activity [148,167,218]. Therefore, HDAC inhibition was considered a possible mode of action for BA-induced differentiation of regulatory IL-10$^+$ plasma cells. To test whether PA or BA have HDAC-inhibitory capacity on B cells, the acetylation of the lysine residue at the N-terminal position 27 of histone H3 (H3K27ac) was determined in B cell cultures via flow cytometry with an antibody recognizing acetylated K27 of histone H3 (H3K27ac) as a readout for HDAC activity.

No significant changes in H3K27 acetylation were observed for any concentration of PA (**Figure 21**). In contrast, BA increased the frequency of H3K27ac$^+$ cells significantly from approximately 4% to 22% ($p = 0.0274$, **Figure 21**). Additionally, the specific HDAC3 inhibitor RGFP966 was included since the previous literature suggests that inhibition of HDAC3 is a specific feature of BA compared to PA [169] and that HDAC3 inhibition plays a crucial role in BA-mediated immunoregulation [171]. Indeed, RGFP966 and BA increased the frequency of H3K27ac$^+$ cells in a similar manner suggesting HDAC(3)-inhibitory properties of BA in murine B cells.

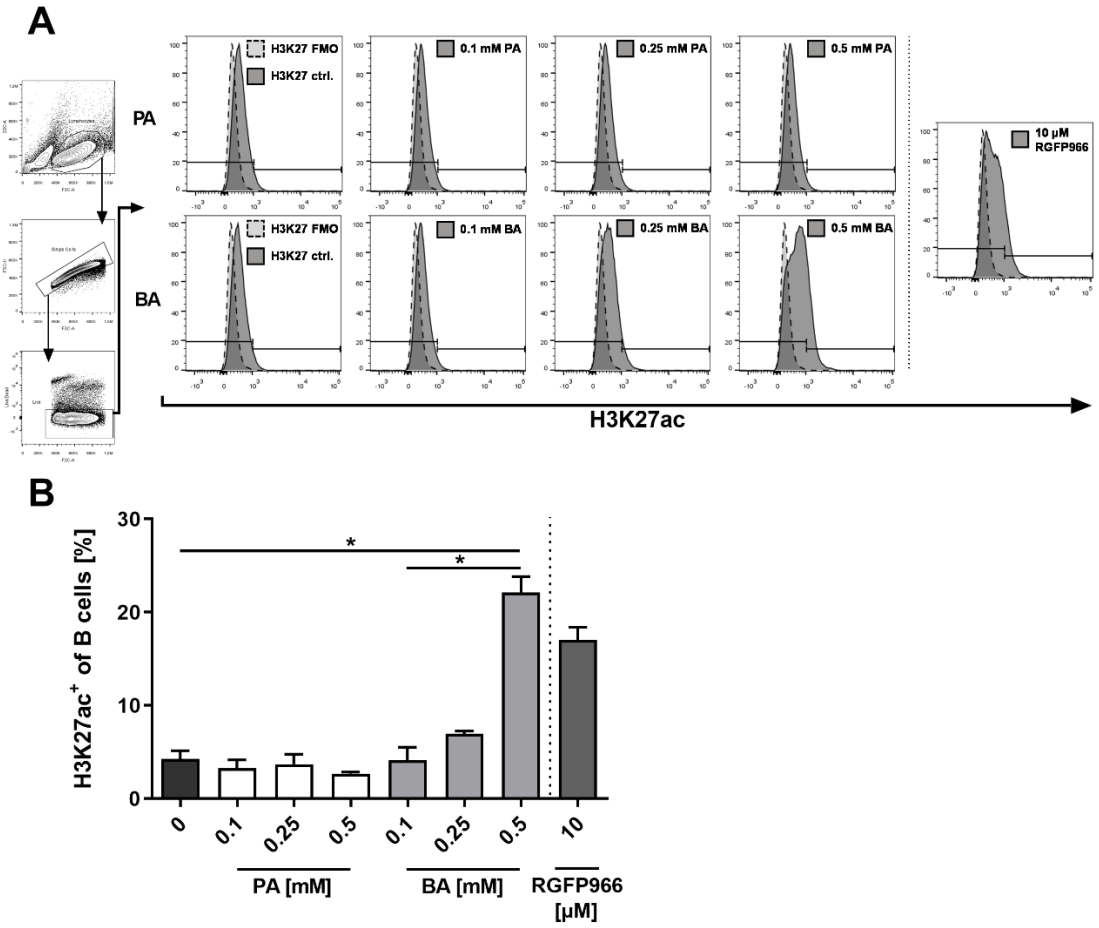

Figure 21: BA treatment induces H3K27 acetylation in isolated murine B cells. (A) Flow cytometric gating strategy and representative histograms for H3K27 acetylation in isolated murine B cells after three days of incubation under plasma cell-inducing conditions with increasing concentrations of PA or BA. AF488-Fluorochrome-conjugated antibody against murine H3K27ac was used for intracellular staining of H3K27ac. HDAC3 inhibitor RGFP966 was included as a positive control. **(B)** Column diagram of the frequencies of H3K27ac$^+$ B cells. n = 3. Statistics: mixed-effects model followed by Tukey's post-hoc test. Data are expressed as mean ± SEM. * $p < 0.05$. A modified version of this figure is also shown in Föh et al, 2022 [1].

5.4.3 HDAC3 inhibition is sufficient to induce plasma cells *ex vivo*

Since BA, but not PA enhanced H3K27 acetylation similar to the HDAC3 inhibitor RGFP966, these data indicate that HDAC3 inhibition might also be involved in the effects of BA on plasma cell differentiation. Isolated murine B cells were incubated in the same *ex vivo* setup as before with the HDAC3 inhibitor RGFP966 and the effect on CD138^{high} plasma cell frequency was analyzed via flow cytometry. In addition, trichostatin A (TSA) was selected as an unspecific HDAC inhibitor.

As a result, CD138^{high} plasma cells were significantly increased after TSA treatment compared to the DMSO vehicle control (p = 0.0007, **Figure 22**). Furthermore, RGFP966 treatment induced similar changes (p = 0.0013, **Figure 22**), although not to the same extent as TSA (p = 0.0040, **Figure 22**). Together these results demonstrate HDAC3 inhibition to be sufficient for the induction of CD138^{high} plasma cells *ex vivo*.

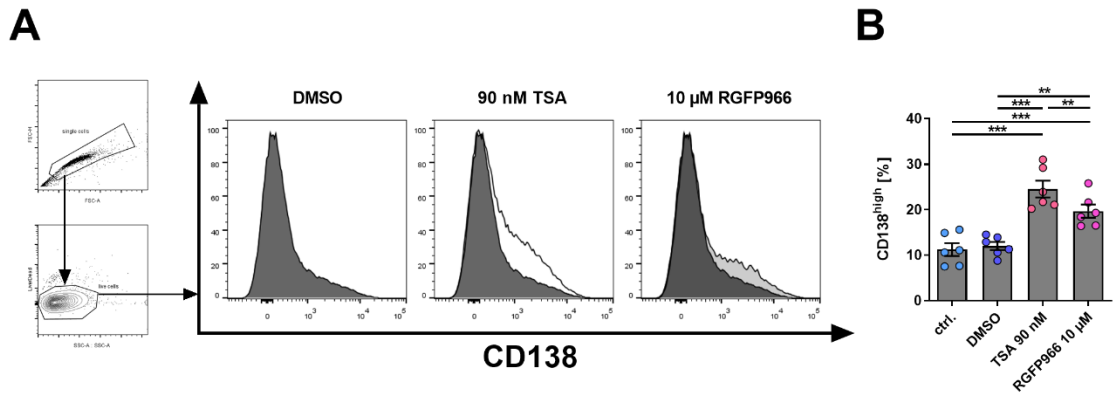

Figure 22: HDAC inhibitors increase CD138 expression in murine B cells. Naïve B cells were incubated with 90 nM trichostatin A (TSA) or 10 µM of HDAC3 inhibitor RGFP966 under plasma cell-inducing conditions for 4 days, followed by flow cytometric analyses of CD138 expression. **(A)** Gating strategy and representative histogram plots for CD138 expression. **(B)** Frequencies of CD138^{high} plasma cells among all living cells after 4 days of incubation of murine B cells with either TSA or RGFP966, n = 6, Statistics: mixed-effects model followed by Tukey's post-hoc test. Data are expressed as mean ± SEM. ** p < 0.01, *** p < 0.001. (B) is also shown in Föh et al, 2022 [1].

5.4.4 HDAC3 inhibition is sufficient to induce regulatory cytokines *ex vivo*

Since specific HDAC3 inhibition by RGFP966 was sufficient to induce CD138^{high} plasma cells similarly to BA, its effects on the expression of regulatory cytokines in B cells and plasma cells were tested next.

Gene expression of the regulatory cytokines IL-10, TGFβ, and IL-35 was investigated in B cell cultures by qPCR after 4 days of incubation with RGFP966. Strikingly, RGFP966 increased these cytokines similarly to the observed effects of BA. Compared to the DMSO control, *Il10* and *Tgfβ1* mRNA levels were increased 3.8-fold (p = 0.0284) and 8-fold (p = 0.0055), respectively. Furthermore, *Ebi3* gene expression was increased 7-fold (p = 0.0087),

whereas a similar tendency but no significant difference was found for *p35* (p = 0.2505, **Figure 23A**) recapitulating the results for BA (s. **Figure 9**).

Next, IL-10 expression was examined on the protein level by using isolated B cells from IL-10 GFP reporter (Vert-X) mice in the same *ex vivo* setup. The frequency of IL-10^{+} cells among all B cells was significantly increased after incubation with 10 µM RGFP966 (p = 0.0007, **Figure 23B**). Furthermore, RGFP966 enhanced the frequency of IL-10^{+} CD138^{high} plasma cells approximately 3-fold compared to the DMSO control group (p < 0.0001, **Figure 23C**).

HDAC3 inhibitor RGFP966 recapitulated the effects of BA on the differentiation of CD138^{high} plasma cells, on gene expression of several regulatory cytokines, and IL-10 expression in plasma cells on the protein level. Taken together, these data indicate HDAC3 inhibition to be sufficient for the induction of regulatory plasma cells *ex vivo* similar to BA.

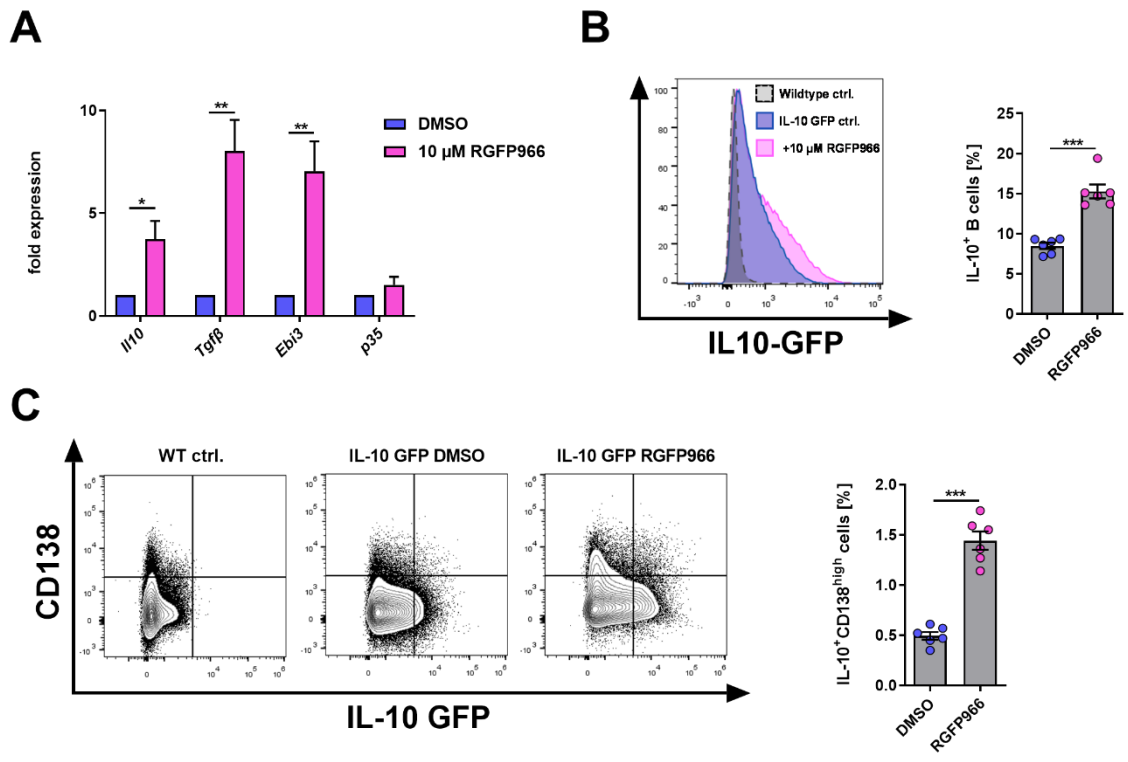

Figure 23: HDAC3 inhibitor RGFP966 induces the expression of regulatory cytokines in B cells. Naïve B cells obtained from IL-10 reporter mice were incubated with 10 µM of HDAC3 inhibitor RGFP966 under plasma cell-inducing conditions for 4 days. **(A)** mRNA was isolated and transcribed into cDNA. Subsequently, qPCR analysis for the indicated cytokines was performed. **(B)** Frequencies of IL-10^{+} B cells among all living B cells, as determined by flow cytometry. **(C)** Frequencies of CD138^{high}IL-10^{+} cells as determined by flow cytometry. Data are shown as representative contour plots and column diagrams. **(A-C)** Statistics: two-

tailed, paired student's t-tests, n = 6, data are expressed as mean ± SEM. * $p < 0.05$, ** $p < 0.01$, *** $p < 0.001$. A modified version of this figure is also shown in Föh et al, 2022 [1].

5.4.5 Short-term BA treatment increases mitochondrial respiration in isolated murine B cells

The differentiation of B cells towards plasma cells is linked to a BLIMP-1-mediated reduction of the mitochondrial mass leading to reduced levels of mitochondrial reactive oxygen species (ROS) [96]. Notably, BA is deeply involved in regulating mitochondrial metabolism by serving as an energy substrate for fatty acid oxidation in mitochondria, thereby fueling oxidative phosphorylation (OXPHOS) [179,219]. Moreover, HDAC3 has been recently shown to increase mitochondrial ROS production, thereby linking BA-mediated HDAC(3) inhibition of plasma cell differentiation to reduced mitochondrial ROS production [220]. To test whether BA might change mitochondrial function in B cells by acting as an energy substrate or by HDAC(3) inhibition, extracellular flux analysis (Seahorse, Agilent, USA) was used. Acute and delayed effects of BA on the mitochondrial metabolism of B cells were tested by applying BA via acute injection to the assay (**Figure 24**) and by incubating B cells for one day in the presence or absence of 0.5 mM BA before performing the assay (**Figure 25**), respectively.

Acute injection of 0.5 mM BA to an extracellular flux assay overall increased oxidative phosphorylation as measured by the oxygen consumption rate of B cells (**Figure 24A**). Before injection of BA into the assay, basal respiration did not differ between the experimental groups ($p = 0.7943$, **Figure 24B**). After the injection of 0.5 mM BA mitochondrial respiration increased rapidly ($p = 0.0056$, **Figure 24C**, $p = 0.0001$, **Figure 24D**), indicating the utilization of BA as an energy substrate rather than underlying HDAC-related epigenetic effects that would not take effect immediately. ATP production increased ($p = 0.0018$, **Figure 24E**) and spare respiratory capacity decreased ($p = 0.0057$, **Figure 24G**), while maximal respiration did not change significantly in the presence of BA ($p = 0.1001$, **Figure 24F**), supporting the role of BA as fuel for OXPHOS. Furthermore, mitochondrial coupling efficiency was slightly but significantly increased after BA injection ($p = 0.0258$, **Figure 24H**), indicating increased respiratory efficiency after BA treatment.

Thus, these results indicate that BA primarily acts as a source of energy during short-term application.

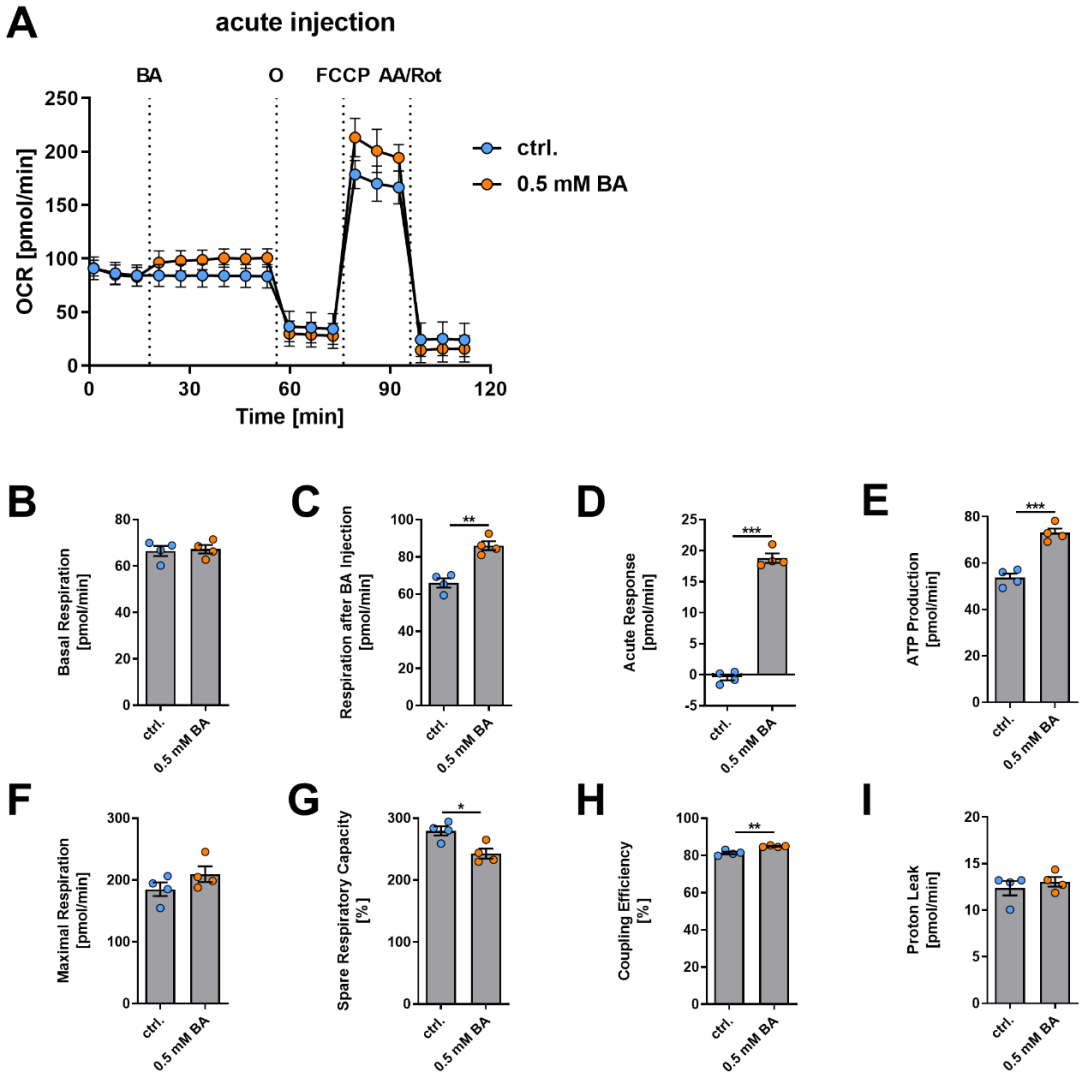

Figure 24: Acute injection of 0.5 mM BA to B cells increases mitochondrial metabolism. Oxygen consumption rates were measured in an extracellular flux assay before and after 0.5 mM of BA was added. Chemical modulators of the OXPHOS chain were used to assess various parameters of mitochondrial respiration. **(A)** Overview of OCR measurements during the assay and after injection of modulators of mitochondrial functions. **(B)** Basal respiration of B cells before BA injection. **(C)** Basal respiration after BA injection. **(D)** Acute response of mitochondrial respiration to BA injection; gap between basal OCR after and before BA injection. **(E)** ATP production after BA injection; gap between OCR after BA injection and OCR after inhibition of ATP-synthase by oligomycin. **(F)** Maximal respiration; OCR after uncoupling of the respiratory chain from ATP production by FCCP. **(G)** Spare respiratory capacity; maximal respiration divided by basal respiration after BA injection x

100. **(H)** Coupling efficiency; ATP production rate divided by basal respiration after BA injection x 100. **(I)** Proton leak; Respiration after inhibition of ATP-synthase by oligomycin minus respiration after complete inhibition of mitochondrial respiration by antimycin A/ rotenone. **(B-I)** For detailed information on the calculation of parameters of mitochondrial respiration please refer to chapter **4.10.4**. Statistics: two-tailed, paired student's t-tests, n = 4, data are expressed as mean ± SEM. * $p < 0.05$, ** $p < 0.01$, *** $p < 0.001$. BA = Butyrate injection, O = Oligomycin injection, FCCP = FCCP injection, AA/Rot = Antimycin A and rotenone injection.

5.4.6 BA treatment for 24 hours suppresses mitochondrial respiration in B cells

According to its known role as a substrate for fatty acid oxidation [179,219], acute injection of BA increased mitochondrial respiration in B cells (**Figure 24**). However, these acute effects of BA might be accompanied by delayed effects of BA on mitochondrial metabolism. In particular, transcriptional changes after HDAC inhibition, as observed for BA, would not take effect immediately after BA addition. Thus, B cells were incubated for 24 hours under plasma cell-inducing conditions in the presence of 0.5 mM BA. Afterward, BA was removed and the extracellular flux assay was performed to assess mitochondrial respiration after the prolonged exposition of B cells to BA.

After 24 hours of cultivation in the presence of 0.5 mM BA, mitochondrial respiration overall was reduced (**Figure 25A**). The basal oxygen consumption rate of B cells decreased after 24 hours of BA treatment from 113.4 to 63.3 pmol/min ($p = 0.0170$, **Figure 25B**). Similarly, ATP production was significantly reduced ($p = 0.0105$, **Figure 25C**). While spare respiratory capacity ($p = 0.6608$, **Figure 25E**) and coupling efficiency ($p = 0.9188$, **Figure 25F**) remained unchanged by BA treatment, maximal respiration decreased significantly ($p = 0.0235$, **Figure 25D**). Proton leak decreased after BA treatment, but the difference did not reach statistical significance ($p = 0.0762$, **Figure 25G**).

Together, these results indicate two separate roles for BA in regulating mitochondrial respiration in B cells. Acutely, BA increases the oxygen consumption rates, indicating increased OXPHOS (**Figure 24**). In concordance with previous literature [179,219], these data suggest, that BA acts as a substrate for fatty acid oxidation and OXPHOS, thereby rapidly increasing mitochondrial respiration. After one day of cell culture, however, BA reduced the mitochondrial respiration of B cells indicating a second, slower mechanism of

BA effects on mitochondrial function, possibly related to the HDAC-inhibitory capacity of BA (**Figure 25**).

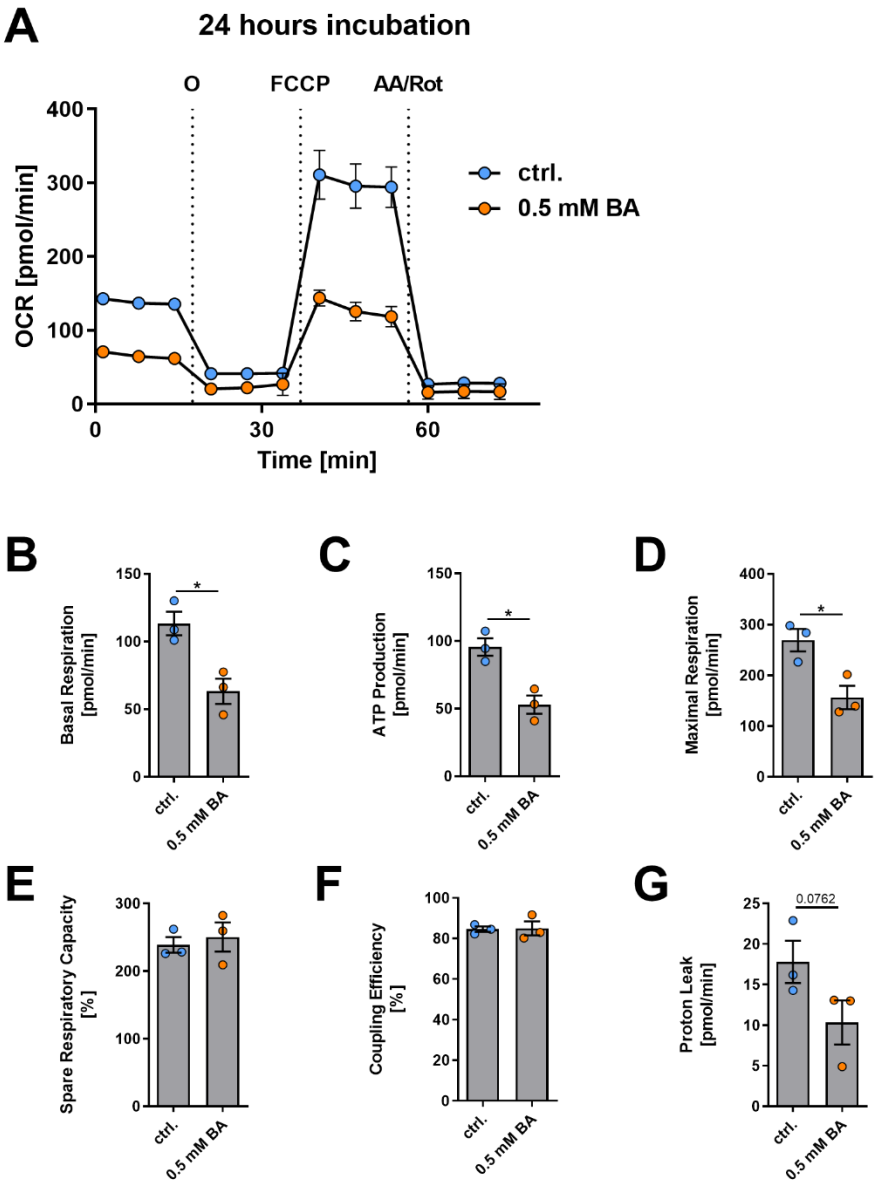

Figure 25: 24 hours of cultivation in the presence of 0.5 mM BA decreases mitochondrial respiration in B cells. Oxygen consumption rates were measured in an extracellular flux assay after treatment with 0.5 mM of BA for 24 hours under plasma cell-inducing conditions. Chemical modulators of the OXPHOS chain were used to assess various parameters of mitochondrial respiration. **(A)** Overview of OCR measurements during the assay and after injection of modulators of mitochondrial functions. **(B)** Basal respiration of B cells after 24 hours of BA treatment and respective controls. **(C)** ATP production after BA treatment; gap between basal OCR and OCR after inhibition of ATP-synthase by oligomycin. **(D)** Maximal respiration; OCR after uncoupling of the respiratory chain from ATP production by FCCP. **(E)** Spare respiratory capacity; maximal respiration divided by basal respiration after BA injection x 100. **(F)** Coupling efficiency; ATP production rate divided by

basal respiration after BA treatment x 100. **(G)** Proton leak; Respiration after inhibition of ATP-synthase by oligomycin minus respiration after complete inhibition of mitochondrial respiration by antimycin A/ rotenone. **(B-G)** For detailed information on the calculation of parameters of mitochondrial respiration please refer to chapter **4.10.4**. Statistics: two-tailed, paired student's t-tests, N = 3, data are expressed as mean ± SEM. * $p < 0.05$. BA = Butyrate, O = Oligomycin injection, FCCP = FCCP injection, AA/Rot = Antimycin A and Rotenone injection. A modified version of this figure is shown in Föh et al, 2022 [1].

5.4.7 BA reduces mitochondrial mass and ROS after 24 hours of incubation

Because slight changes in mtROS levels are instructive to the regulation of plasma cell differentiation [96], the effects of BA on mitochondrial mass, membrane potential, and mtROS levels were examined next. B cells were incubated again with 0.5 mM BA for 24 hours and then subjected to staining with MitoTracker Green FM (mitochondrial mass), TMRE (mitochondrial activity/membrane potential), and/or MitoSOX Red (mtROS/superoxid) (see **4.5.7**). Subsequently, flow cytometric analyses of fluorescence intensities of the three dyes were performed.

First, MT Green/TMRE co-staining was used to examine mitochondrial activity/membrane potential per mass after 24 hours of BA treatment. BA induced a shift from B cells with high mitochondrial mass and membrane potential as indicated by high intensity of MT Green and TMRE (population P1) towards B cells with low mitochondrial mass and membrane potential (population P2, **Figure 26A**). The frequency of P1 cells was decreased from 40.9 to 35.4% ($p = 0.0497$, **Figure 26B**), while P2 cells accordingly increased from 20.1 to 26.5% ($p = 0.0232$, **Figure 26C**). Notably, features of the P2 population, which were increased after BA treatment, are instructive for plasma cell differentiation [96]. Furthermore, the TMRE/MT Green-ratio was reduced ($p = 0.0147$, **Figure 26D**), indicating reduced mitochondrial activity per mass, underlining the results from the extracellular flux assay.

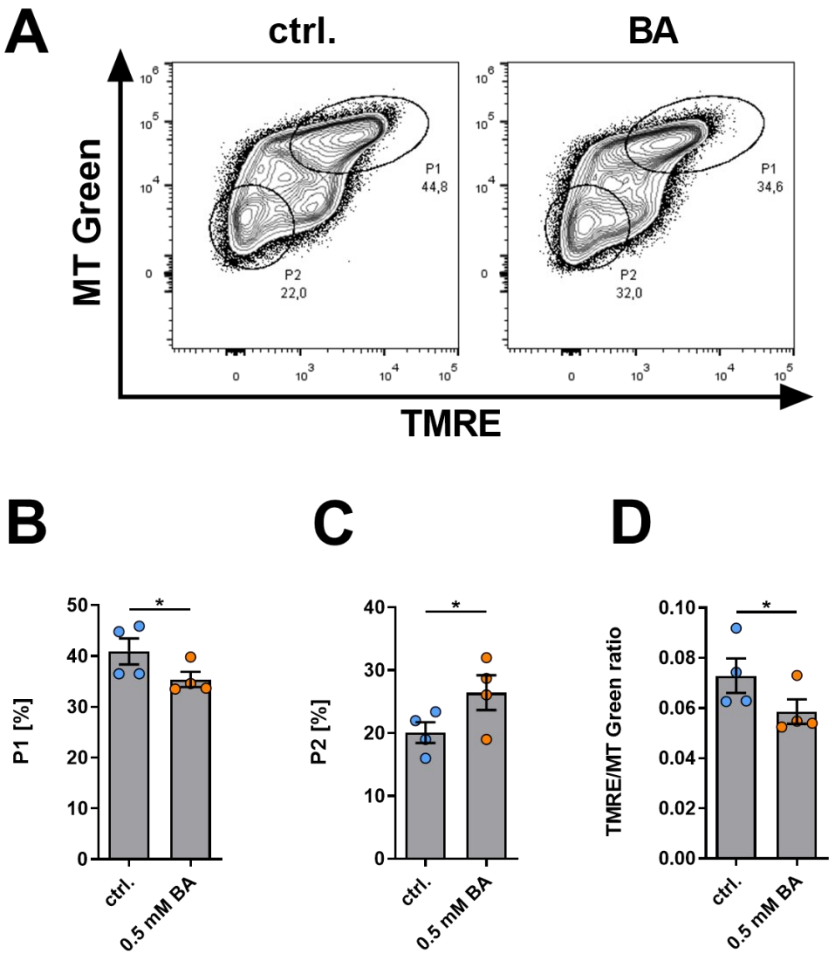

Figure 26: BA decreases mitochondrial mass and membrane potential in B cells. Naïve B cells were incubated under plasma cell-inducing conditions with 0.5 mM BA for 24 hours and subsequently stained with B220, Live/Dead staining, MT Green and TMRE, followed by flow cytometry. **(A)** Representative contour plots of B cells after 24 hours of incubation in the presence or absence of 0.5 mM BA. P1 and P2 represent cell populations with high and low mitochondrial mass and membrane potential, respectively. **(B)** Frequencies of cells belonging to the P1 population gate within viable $B220^+$ B cells after 24 hours of treatment with BA. **(C)** Frequencies of cells belonging to the P2 population gate within viable $B220^+$ B cells after 24 hours of treatment with BA. **(D)** MFI ratio of TMRE to MT Green signals within viable $B220^+$ B cells after 24 hours of treatment with BA. **(B-D)** Statistics: two-tailed, paired student's t-tests, N = 3, data are expressed as mean ± SEM. * $p < 0.05$. All plots and diagrams are also shown in Föh et al, 2022 [1].

Next, the effects of BA on mitochondrial superoxide levels were examined. After 24 hours of incubation, BA decreased mitochondrial superoxide as determined by MitoSOX Red flow cytometric assay. MFI of MitoSOX Red was decreased significantly compared to matched,

biological controls ($p < 0.0001$, **Figure 27A**). Similarly, MitoSOX signals in B cells were decreased after specific inhibition of HDAC3 by RGFP966 ($p = 0.0110$, **Figure 27B**).

These data demonstrate that both BA and HDAC3 inhibitor RGFP966 effectively reduced mitochondrial superoxide levels in isolated murine B cells after one day of cell culture.

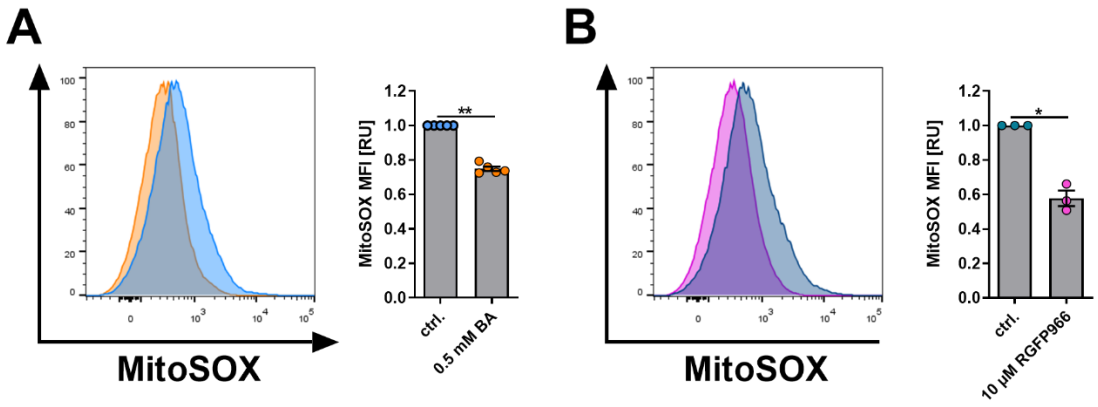

Figure 27: BA and RGFP966 reduce mtROS levels after 24 hours of incubation. (A) Naïve B cells were incubated under plasma cell-inducing conditions with 0.5 mM BA for 24 hours and subsequently stained with MitoSOX. MFI of MitoSOX was determined within viable $B220^+$ B cells using flow cytometry, N = 5. **(B)** Naïve B cells were incubated with 10 µM RGFP966 for 24 hours and subsequently stained with MitoSOX. MFI of MitoSOX was determined within viable $B220^+$ B cells using flow cytometry, N = 3. **(A+B)** RU = relative units. Representative histogram plots and column diagrams are shown. Statistics: two-tailed, paired student's t-tests, data are expressed as mean ± SEM. * $p < 0.05$, ** $p < 0.01$. All plots and diagrams are also shown in Föh et al, 2022 [1].

To test whether reduced, mitochondrial ROS levels are linked to BA-induced plasma cell differentiation as well as expression of IL-10, B cells were additionally incubated with BA and/or PMA, which is a known inducer specifically of mitochondrial superoxide [221–223]. B-cells from IL-10 GFP-reporter mice were used to assess IL-10 expression. Strikingly, the addition of PMA together with BA to isolated B cells completely abrogated the induction of $CD138^{high}$ plasma cells (BA vs. BA+PMA: $p = 0.0004$, **Figure 28A+B**). However, the addition of PMA to BA did not decrease the expression of IL-10 in overall B cells compared to BA alone (BA vs. BA+PMA: $p = 0.2134$, **Figure 28A+C**).

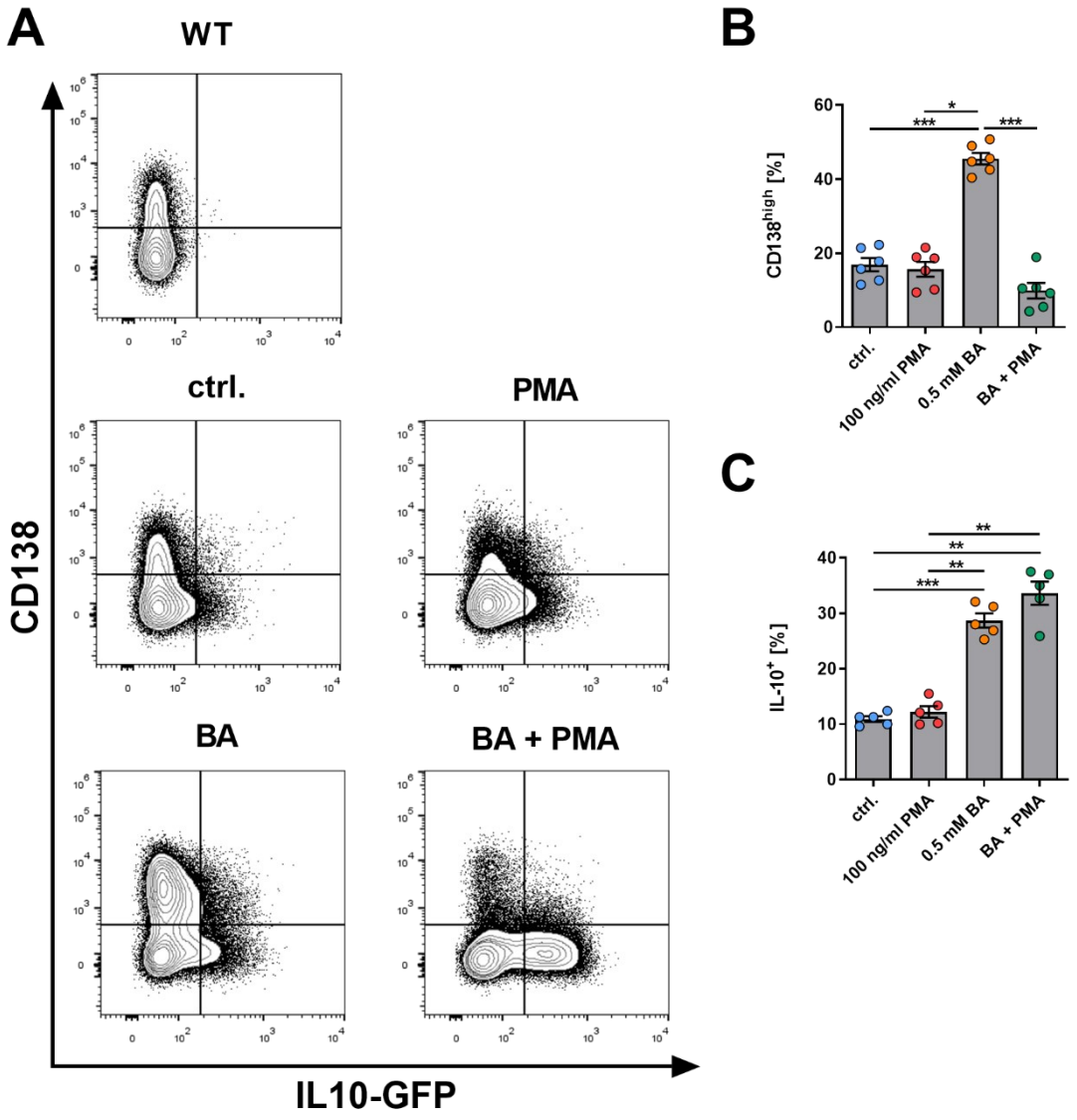

Figure 28: Mitochondrial superoxide-inducer PMA abrogates the induction of plasma cells, but not IL-10 by BA. Naïve B cells obtained from IL-10 GFP-reporter mice were incubated under plasma cell-inducing conditions with 0.5 mM BA, and/or 100 ng/ml PMA for 4 days. Cell viability and the expression of B220, CD138, and IL-10 GFP were determined by flow cytometry. **(A)** Representative contour plots. **(B)** Frequencies of $CD138^{high}$ plasma cells depicted in column diagrams, N = 6. **(C)** Frequencies of $IL\text{-}10^{+}$ B cells depicted in column diagrams, N = 5. **(B-C)** Statistics: mixed-effects models, data are expressed as mean ± SEM. * $p < 0.05$, ** $p < 0.01$, *** $p < 0.001$. All plots and diagrams are also shown in Föh et al, 2022 [1].

To further support these results another known inducer of mitochondrial ROS, 2DG [96], was used in a second set of experiments under the same conditions. Similarly, the addition of 2DG abrogated the induction of $CD138^{high}$ plasma cells almost completely (BA vs.

BA+2DG: p = 0.0001, **Figure 29A+B**), reflecting the results from the previous experiment. Furthermore, 2DG in addition to BA did not decrease, but in this case even increased the expression of IL-10 in overall B cells compared to BA alone (BA vs. BA+2DG: p = 0.0014, **Figure 29A+C**).

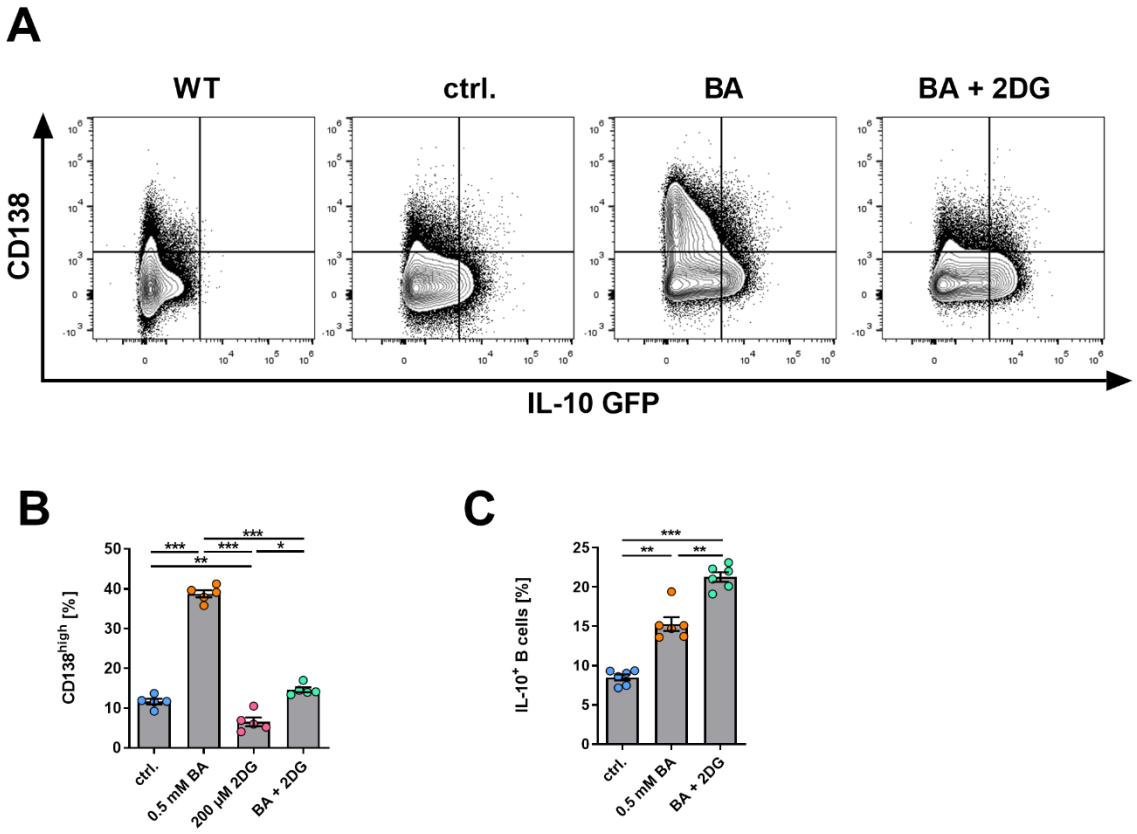

Figure 29: Mitochondrial superoxide-inducer 2DG abrogates the induction of plasma cells, but not IL-10 by BA. Naïve B cells obtained from IL-10 GFP-reporter mice were incubated under plasma cell-inducing conditions with 0.5 mM BA, and/or 200 µM 2DG for 4 days. Cell viability and the expression of B220, CD138, and IL-10-GFP were determined by flow cytometry. **(A)** Representative contour plots. **(B)** Frequencies of $CD138^{high}$ plasma cells depicted in column diagrams, N = 6. **(C)** Frequencies of $IL\text{-}10^{+}$ B cells depicted in column diagrams, N = 6. **(B-C)** Statistics: mixed-effects models, data are expressed as mean ± SEM. * $p < 0.05$, ** $p < 0.01$, *** $p < 0.001$. All plots and diagrams are also shown in Föh et al, 2022 [1].

Finally, in a third set of experiments, the effects of ROS-inducer 2DG in addition to the HDAC3 inhibitor RGFP966 on plasma cell differentiation with isolated B cells from wild-type mice were tested. Recapitulating the results from previous experiments with BA, the addition of 2DG abrogated the induction of $CD138^{high}$ plasma cells by RGFP966, even

decreasing plasma cell differentiation (RGFP966 vs. RGFP966+2DG: p = 0.0002, **Figure 30A+B**).

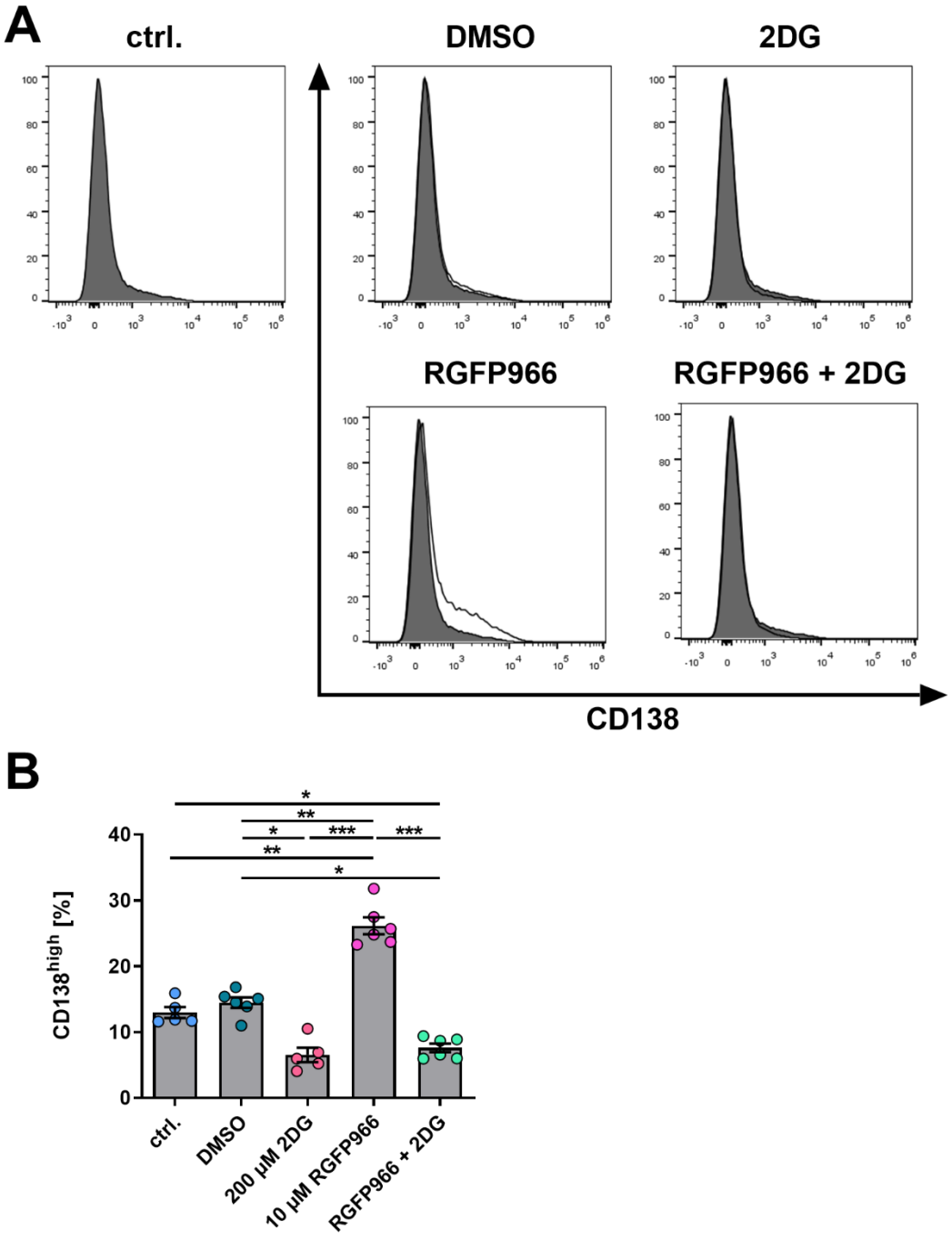

Figure 30: Mitochondrial superoxide-inducer 2DG abrogates the induction of plasma cells by HDAC3 inhibitor RGFP966. Naïve B cells obtained from wild-type mice were incubated under plasma cell-inducing conditions with 0.5 mM BA, and/or 200 µM 2DG for 4 days. Cell viability and the expression of B220, CD138, and IL-10 GFP were determined by flow cytometry. **(A)** Representative contour plots. **(B)** Frequencies of $CD138^{high}$ plasma cells depicted in column diagrams, N = 6. Statistics: Mixed-effects model, data are expressed as

mean ± SEM. * $p < 0.05$, ** $p < 0.01$, *** $p < 0.001$. All plots and diagrams are also shown in the supplementary data of Föh et al, 2022 [1].

Together, these results indicate that reduction of mitochondrial superoxide levels by BA or HDAC3 inhibitor RGFP966 is linked to the induction of plasma cells, but not IL-10 expression. Therefore, increased IL-10 expression after BA treatment is possibly occurring rather in parallel than as a consequence of plasma cell induction.

6 DISCUSSION

6.1 Overview

B cells are major contributors to the adaptive immune system [224]. Activation of B cells through T cell-dependent and -independent mechanisms induces the differentiation towards plasma cells, whose main function is the production and secretion of antibodies [224]. The antibody response is crucial for effective protection against pathogens on the one hand, while the production of antibodies directed against auto-antigens can lead to autoimmune diseases [224]. In recent years, subsets of B cells have been recognized for their immunosuppressive functions, therefore being termed regulatory B cells [3]. A common feature of regulatory B cells is the expression of the anti-inflammatory cytokine IL-10 [3] and a predisposition to developing into antibody-secreting cells [211]. Accordingly, IL-10^{+} regulatory plasma cells have been proposed to be the main source of B cell-derived immunosuppressive effects *in vivo* [211,212]. Because of their distinct anti-inflammatory capacities, IL-10-producing regulatory plasma cells are considered a valuable target for therapeutic strategies against autoinflammation [211]. However, the exact mechanisms and external factors leading to the induction of regulatory plasma cells remain elusive [3]. Thus, inducers of regulatory plasma cell phenotypes have the potential to be valuable assets for the prevention or treatment of autoimmune conditions.

In this thesis, the effects of the immunomodulatory SCFA butyrate (BA) on the differentiation of plasma cells with immunoregulatory properties and possible underlying mechanisms were investigated. As a result, stimulation of plasma cell differentiation in the presence of BA was found to increase the frequencies of plasma cells *ex vivo* and *in vivo*. Furthermore, BA led to increased frequencies of immunoregulatory IL-10^{+}IgM^{+} CD138^{high} plasma cells. Importantly, after BA application via drinking water serum levels of the total as well as antigen-specific IgM were elevated (see graphical overview in **Figure 31**).

Mechanistically, BA increased histone H3k27 acetylation most likely via its HDAC3 inhibitory function. Accordingly, specific HDAC3 inhibition was sufficient for the induction of plasma cell differentiation and the expression of IL-10 in isolated B cells. Moreover, BA reduced mitochondrial metabolism and superoxide levels in B cells after one day of cell

culture, and these reduced mitochondrial superoxide levels were necessary for BA-induced plasma cell differentiation. However, reduced superoxide levels were expendable for induction of IL-10 by BA, indicating that these outcomes might both be dependent on HDAC3-inhibition, but only plasma cell differentiation is regulated by mitochondrial ROS levels.

This study, therefore, demonstrates the induction of regulatory IL-10^{+}IgM^{+} CD138^{high} plasma cells by BA and provides possible underlying mechanisms. The following chapter provides an interpretation and discussion of the results and the corresponding literature.

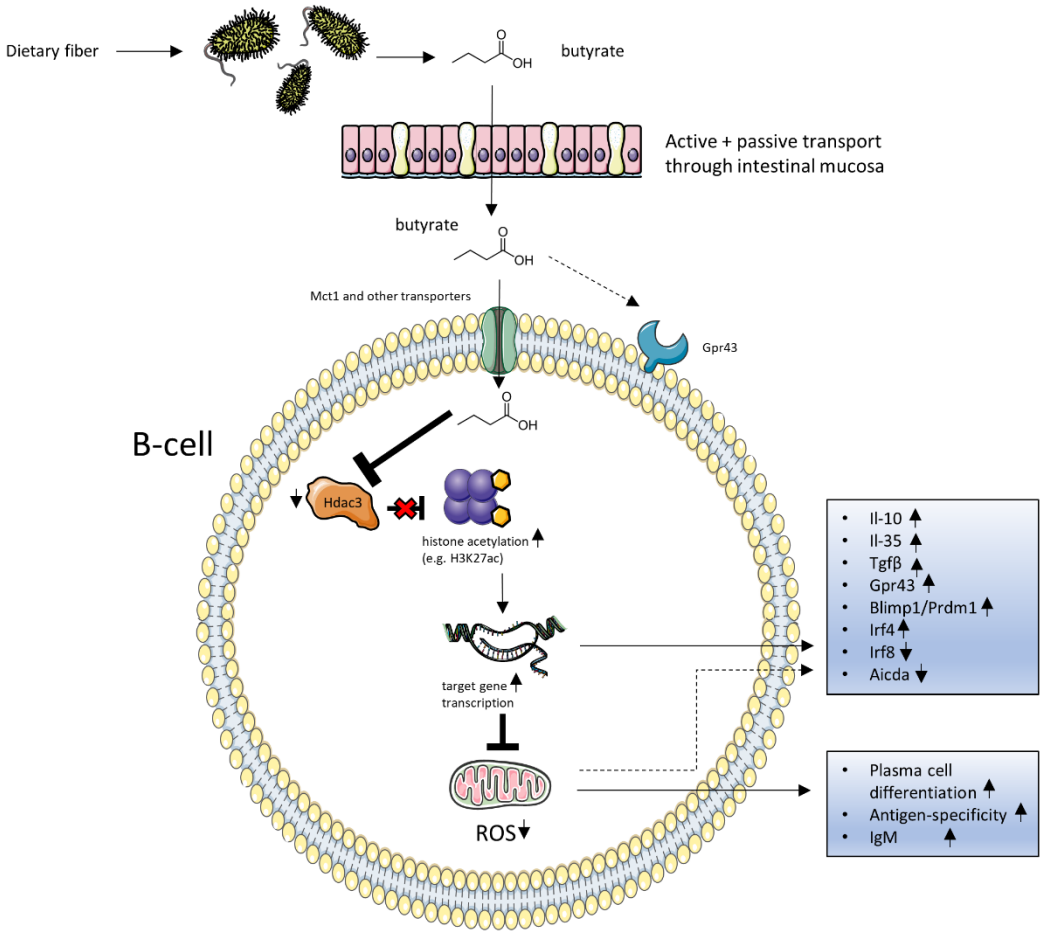

Figure 31: Simplified graphical summary of the effects of BA on B cells and proposed underlying mechanisms. Under physiological conditions, BA is provided to the host after fermentation of dietary fiber by commensal bacteria. It is subsequently absorbed by active and passive transport through the intestinal mucosa. BA is then taken up into B cells in the intestinal mucosa or immunological effector organs, where it accumulates. In the B cell, BA exerts its HDAC3-inhibitory effects leading to increased acetylation of histones, particularly

H3K27. Increased histone acetylation mediates transcription of target genes, including anti-inflammatory cytokines and regulators of plasma cell differentiation. Furthermore, reduced mitochondrial ROS levels are necessary for the induction of plasma cell differentiation.

6.2 BA induces plasma cell differentiation

One major result of this study is the induction of regulatory plasma cell differentiation by BA. While this section focuses on discussing plasma cell induction in the context of previous literature, later sections will discuss their regulatory features, including IL-10 expression.

Plasma cells are effector cells of adaptive immunity [90,224] and the induction of plasma cells by the microbial metabolite BA shows a pathway, by which the gut microbiome directly affects the host's adaptive immune system. In *ex vivo* experiments murine B cells were isolated from spleens using MACS technology. Cell culture conditions were chosen to provide an environment, in which plasma cells can differentiate from MACS-isolated B cells including LPS, IL-6, and atRA. Additional stimulation of the isolated B cells with BA in physiological concentrations observed in splenic and lymphoid tissues [156] consistently and dose-dependently led to increased frequencies of plasma cells, identified by high expression levels of CD138, which is a reliable marker of murine plasma cells [225–227].

Notably, we did not observe the same effects when B cells were stimulated with PA. In fact, the frequencies of $CD138^{high}$ plasma cells remained largely unchanged regardless of the dose of PA that was used. Considering the overlapping properties of the SCFAs BA and PA these results might come as a surprise. For example, both BA and PA are produced by microbiota in the large intestine via fermentation of dietary fiber reaching local concentrations of up to 130 mM [228]. Furthermore, both SCFAs are ligands for the G-protein coupled receptors GPR43 and GPR41 and are known as potent inhibitors of HDACs [148], exerting several immunomodulatory functions via these mechanisms, including the inhibition of TNFα production and NF-κB activity in peripheral mononuclear blood cells (PBMC) [174], and the induction of Tregs [229,230]. However, there are known differences in HDAC-specificity between PA and BA [169], indicating a possible mechanism for the observed BA-induced plasma cell differentiation, which will be discussed in detail further below.

One strength of this study is the inclusion of two different routes of BA administration *in vivo*. The application of BA to Ova/CFA-immunized mice both via drinking water and i.p. injection recapitulated increased frequencies of $CD138^{high}$ plasma cells observed in cell culture. Importantly, a short-term BA application of only seven days prior to Ova/CFA immunization and an additional twelve days after immunization was sufficient to induce significant effects, indicating that short-term treatment with BA specifically is sufficient to enhance the differentiation of splenic plasma cells in mice.

The main canonical function of plasma cells is the production and secretion of antibodies that are crucially involved in mediating immune function and host defense against pathogens [90]. Thus, the induction of plasma cells by BA is supported by a previous study by *Kim et al.*, which showed increased antibody production in mice after a high-fiber diet or the administration of a mixture of low-dosed SCFAs containing BA in drinking water for at least eight weeks [179]. In this study, enteral SCFA administration was shown to increase antibody production locally in mesenteric lymph nodes, Peyer's patches, and splenic B cells [179]. Increased antibody production after SCFA administration under baseline conditions and infection with *C. rodentium* suggested increased plasma cell differentiation, although CD138 expression was not investigated as a marker for murine plasma cells [179].

Sanchez et al. provided further evidence by showing increased Blimp-1/Prdm1 expression, IgG^+ B cells, $CD138^+$ plasma cells, antigen-binding, and circulating IgG2b and IgG3 after a combination of a comparably low-dosed mixture of BA (20 mM) and PA (30 mM) in drinking water for seven to eight weeks [156]. However, the results differed when *Sanchez et al.* applied a high-dosed SCFA mixture as drinking water. After seven to eight weeks of treatment with this dose, the plasma cell differentiation, and the production of IgG2b and IgG3 were significantly reduced [156]. However, the methods that were used differed significantly from the present study. Most importantly, the high-dosed SCFA mixture used by *Sanchez et al.* contained 150 mM PA, 150 mM BA as well as its prodrug tributyrin in a concentration of 20 mg/ml, amounting to an effective dose equivalent of almost 340 mM BA after tributyrin conversion [156]. Thus, the dose used by *Sanchez et al.* is likely supraphysiological and does not reflect physiological processes.

Additionally, in the aforementioned studies, the SCFA treatments were continued for a considerably longer time of at least *seven to eight weeks* during the experiments [156,179], whereas we here only used a short-term treatment of *under three* weeks (19 days). Therefore, our results using a moderate dose of 150 mM BA in short term are reflected by the results from long-term SCFA application including BA in low doses in both of these studies. Together these data indicate that differentiation of plasma cells is efficiently induced when low doses are applied continuously, or moderate doses are applied in the short term, whereas supraphysiological SCFA doses might lead to detrimental effects on plasma cell differentiation. In terms of applicability in humans, this might be an important factor to consider, since small dietary adjustments or nutritional supplementations over longer periods might be better suitable in terms of side effects and patient compliance than the acute application of high doses of BA, considering also the repelling smell and taste of BA in solution.

Considering the parenteral application of BA, i.p. injection has been reported to alleviate autoinflammation in the gut and the central nervous system [231,232]. To the best knowledge, there is, however, no previous data on its effect on plasma cell differentiation. Here, we report that direct systemic application of BA via intraperitoneal injection is as effective in inducing plasma cell differentiation as the enteral application via drinking water. It might not surprise that the circumvention of the gastrointestinal tract, which is not only the main producer (via its microbiota) but also one of the main consumers of BA (via its colonocytes) [153], might be an effective way of delivering BA to the systemic circulation. Additionally, i.p. injection circumvents the initial hepatic metabolization of BA [149]. On the other hand, the increased splenic plasma cells after i.p. injection of BA demonstrates that the priming of B cells for plasma cell differentiation is not dependent on enteral delivery. Thus, we can largely rule out, that increased splenic plasma cell frequencies after i.p. injection are caused by recirculating plasma cells from the gut. For the application in drinking water, however, this mechanism might still take place, since recirculation of IL-10^{+} regulatory plasma cells from the intestines has been described as an underlying mechanism in ameliorating neuroinflammation in EAE [80].

6.3 BA induces transcription of plasma cell-specific genes

To test whether plasma cell induction by BA was linked to the expression of transcriptional regulators of plasma cell differentiation the expression of several plasma cell-specific genes was determined in isolated murine B cells after treatment with BA. The gene expression of *Prdm1* (*Blimp1*), which serves as the master transcriptional node of plasma cell differentiation [101,233], was significantly upregulated in isolated B cells after BA stimulation. Prdm1 directly represses Aicda and thereby inhibits B cell-specific genes and processes including class switch recombination and antigen presentation [101]. Accordingly, Aicda expression was reduced following BA treatment as would be expected during the differentiation of B cells towards plasma cells. Irf4 and Irf8 are additional regulatory factors during B cell maturation that act in a kind of "tug-of-war" for B cell fate: Irf4 is known to directly induce Prdm1 [101] while acting in a concentration-dependent competition with Irf8, which is a negative regulator of plasma cell differentiation and represses Prdm1 [208]. Here, BA treatment reduced *Irf8* gene expression to a non-detectable level while increasing *Irf4*, indicating increased plasma cell differentiation. No significant differences were found for *Bcl6* and *Xbp1*.

Previous studies on this topic have come to inconsistent conclusions [156,179]. Whereas *Kim et al.* reported increased gene expression of *Aicda*, *Irf4*, and *Prdm1* in isolated murine B cells after three days of BA treatment (0.1 mM BA) [179], *Sanchez et al.* observed decreased expression of both *Aicda* and *Prdm1* after four days of treatment with BA (0.5 mM) [156]. Additionally, *Sanchez et al.* were able to corroborate their results with data from *in vivo* studies. However, these results were again obtained after seven to eight weeks of administration of unphysiologically high-dosed SCFA mixtures via drinking water [156]. Although the genes are regulated conversely between these studies, BA leads to a unidirectional change of *Aicda* and *Prdm1* within each study. Notably, Prdm1 directly suppresses Aicda in plasma cells [101], according to the fact that potential class switching occurs before plasma cell differentiation [234]. Thus, it is surprising that BA would regulate both genes in the same direction. Here, we report the upregulation of *Prdm1*, while *Aicda* is simultaneously downregulated, indicating increased plasma cell differentiation and reduced class switch recombination.

The differences between all three studies can be attributed to methodical differences. For example, while all three studies used physiological concentrations of BA (0.1 – 0.5 mM), the results were obtained at different time points after BA stimulation. In the present study gene expression analysis was performed after one day of BA treatment, while the other studies started at three or four days [156,179]. After three to four days of cell culture without any stimulation, B cells already lose viability by a considerable amount [235]. Thus, all three studies used additional, but different stimulating factors to increase viability, proliferation, and/or plasma cell differentiation. In the present study, LPS, IL-6, and atRA were chosen for their known capability to support the differentiation of plasma cells, especially in the gut [236], where the highest levels of BA are found. In contrast, the aforementioned studies used a variety of different cytokine compositions, mostly not including IL-6 and atRA [156,179]. The differences in *Aicda* and *Prdm1* expression that were found between the studies might thus be attributed to varying cell culture conditions.

The observed changes in the expression of plasma-cell-specific genes support the induction of plasma cell differentiation by BA. Because there is both opposing and supporting evidence from previous reports, future studies should compare the different conditions, in which the results were obtained and possibly try to obtain real-life data in human subjects after BA supplementation.

6.4 BA induces IL-10 expression in B cells and plasma cells *ex vivo*

Although antibody production and antigen presentation are recognized as the main function of B cells, a more complex role has been shown in recent years [224]. B cells can positively and negatively regulate other parts of the immune system by cytokine production and secretion. B cell-derived cytokines regulate the development of lymphatic tissues, promote T cell responses, and take part in tissue regeneration [237]. Furthermore, subsets of B cells have been described to exert immunosuppressive functions by the provision of the anti-inflammatory cytokines IL-10, IL-35, and TGFβ [3]. Although multiple regulatory subsets of B cells expressing IL-10 have been described in mice [3], $CD138^{high}$ plasma cells are the main source of B cell-derived IL-10 and IL-35 as shown in SLE [137], EAE

[75,76], and *Salmonella typhimurium* infection [74,75]. Since BA induced CD138^{high} plasma cells, its effects on the expression of regulatory cytokines were investigated.

Gene expression of *Il10* and *Tgfβ* was significantly increased after BA treatment of isolated murine B cells in a dose-dependent manner. IL-35 is composed of two subunits encoded by *Ebi3* and *p35*, respectively. The expression of both genes was increased as well, although not reaching statistical significance for *p35*. The expression of these genes was not upregulated when isolated B cells were treated with PA in the same manner. These results show that BA but not PA increases gene expression of immunosuppressive cytokines characteristic for regulatory plasma cells in isolated murine B cells, reflecting the lacking effects of PA on plasma cell differentiation *ex vivo*. Notably, Blimp1/Prdm1 has been demonstrated to directly induce IL-10 expression providing a mechanistic link between the induction of plasma cells and IL-10 [101].

IL-10 GFP-reporter mice were used to investigate the expression of IL-10 on the protein level. BA induced increased expression of IL-10 in plasma cells as well as non-plasma cells at least *ex vivo* (s. **Figure 28** and **Figure 29**). Together with the notion that not all plasma cells express IL-10, although they express Blimp1/Prmd1, an additional effect of BA might be responsible for IL-10 induction. Supporting evidence stems from a recent publication by *Luu et al.*, that reported increased expression of IL-10 in B cells after treatment with BA and other SCFAs. The authors, however, did not show data on CD138 expression or antibody secretion in these cells, leaving the question, of whether IL-10^{+} plasma cells were induced unanswered [30]. In the present study, BA induced IL-10^{+} B cells (non-plasma cells) including IL-10^{+} CD138^{+} plasma cells, which are the main source for B cell-derived IL-10 in vivo [75,76], indicating that BA supports both IL-10 expression as well as plasma cell differentiation, which led to the development of regulatory IL-10^{+} plasma cells *ex vivo*.

6.5 BA induces IL-10 expression in plasma cells *in vivo*

To investigate whether BA induces regulatory plasma cells *in vivo*, IL-10 GFP-reporter mice were treated with BA via two different routes of BA application and immune activation was induced by Ova/CFA-immunization. Direct administration of BA via drinking water or i.p. injection led to increased frequencies and cell counts of splenic IL-10^{+} CD138^{high} plasma

cells recapitulating the effects observed *ex vivo*. To the best knowledge, BA-dependent induction of regulatory plasma cells *in vivo* has not been reported as of yet. However, it was shown that BA was able to induce protective IL-10^{+} Bregs in models of Sjögren's Syndrome [180], inflammatory bowel disease, and rheumatoid arthritis [181]. Nothing was reported on whether these cells might be CD138^{high} plasma cells, but the results underline the potential of BA to induce regulatory cells of the B cell lineage that might be a valuable therapeutic target.

Furthermore, regulatory B cells have been induced *ex vivo* by the SCFA pentanoate and have been shown to ameliorate the development of EAE *in vivo* [30]. Again, it remains elusive, whether regulatory plasma cells might have been induced because the corresponding data, e.g. on antibody secretion or CD138 expression was not reported [30]. It can therefore only be speculated if pentanoate similarly to BA might be able to induce regulatory plasma cells. However, SCFAs other than PA may promote a regulatory phenotype of B cells similar to BA.

Together, *ex* and *in vivo* data show that BA induces the differentiation of IL-10^{+} CD138^{high} plasma cells, which have been previously described for their regulatory properties [211,212]. The results are supported by recent data on BA-induced IL-10^{+} B cells, although it is unclear whether those were plasma cells. Increasing the systemic frequencies of regulatory IL-10^{+} CD138^{high} plasma cells by the provision of BA, or possibly pentanoate might be of great use in ameliorating autoimmune or allergic disorders.

Furthermore, the data imply that BA-induced plasma cell differentiation and expression of regulatory cytokines (e.g. IL-10) in B cells including plasma cells are two separate pathways that, however, likely depend on HDAC inhibition.

6.6 IL-10^{+} plasma cells preferentially express IgM

The phenotype of IL-10^{+} CD138^{high} plasma cells was further characterized by determining their prevailing immunoglobulin isotype. *Ex vivo* experiments revealed that more than 90% of IL-10^{+} and only around 77% of IL-10^{-} plasma cells expressed IgM as their immunoglobulin isotype in the here used experimental setup. Since IgM is expressed by naïve B cells before

class switch recombination [92], preferential expression of IgM by regulatory plasma cells might indicate that they are derived from rather naïve B cells, prior to any class switch recombination, and might belong to the innate-like B1 or marginal zone B cells. In fact, these cells have been suggested as possible precursors of regulatory plasma cells, due to their similar phenotype and their propensity to directly differentiate into antibody-secreting plasma cells [238].

It needs to be emphasized that the antibody isotype expressed by B cells and plasma cells is inherently dependent on the surrounding immunological milieu. Most importantly, cytokines produced by the surrounding tissues play a crucial role in determining immunoglobulin class switching [92]. In the present study LPS, IL-6 and atRA were mainly used for induction of plasma cell differentiation, not distinctively inducing class switch recombination. Thus, it might be worthwhile to test whether preferential expression of IgM by IL-10^{+} plasma cells can be confirmed in cell culture conditions containing additional class switch-inducing agents, e.g. IL-4 (induces murine IgG1 and IgE), or TGFβ (induces IgA) [239]. Furthermore, different B cell subpopulations (marginal zone B cells, B-1a and B-1b cells, and B2 cells) should be tested in order to identify a possible precursor of regulatory plasma cells.

Notably, the preferential expression of IgM by IL-10^{+} plasma cells was not only shown *ex vivo* but also *in vivo* 12 days after Ova/CFA immunization. Approximately 90% of splenic IL-10^{+} plasma cells expressed IgM, drastically exceeding the 44% of IL-10^{-} plasma cells expressing IgM (i.p. experiments, **Figure 14C**). Supporting evidence stems from previous literature. Regulatory B cell subsets have been reported to express IgM as their antibody class [211]. Most importantly, regulatory plasma cells that are the main source of IL-10 and IL-35 in models of autoimmunity and infection express remarkably high levels of IgM and are found in murine spleens [75,78]. Accordingly, IgM^{+} plasma cells expressed significantly higher levels of IL-10 *in vivo* as determined by the fluorescence intensity of IL-10 GFP.

Since BA induced IL-10^{+} plasma cells that preferentially express IgM *ex vivo*, the effects of BA on IL-10^{+}IgM^{+} CD138^{high} plasma cell generation were analyzed *in vivo*. As a result, BA application via drinking water or i.p. injection not only increased IL-10^{+}IgM^{+} CD138^{high} plasma cell frequencies but also the expression of IL-10 in splenic IgM^{+} plasma cells of

Ova/CFA-immunized mice, indicating that BA induces IgM^+ plasma cells of regulatory capacity *in vivo*. Elevated IgM serum levels were found after BA administration via drinking water but not i.p. injection, although further differences might be hidden due to saturation of the assay. Further dilutions of the sera could be useful to distinguish here and will be performed in the future. Increased levels of total IgM might be a possible consequence of increased $IL\text{-}10^+IgM^+$ plasma cell frequencies.

Ova/CFA-immunization furthermore allowed for the analysis of antigen-specific plasma cells and antibodies, distinguishing the present work from the earlier study that showed increased antibody levels after SCFA administration by *Kim et al.* [179]. Interestingly, BA administration via drinking water but not i.p. injection increased the frequency of Ova^+ cells among total plasma cells, indicating increased antigen-specificity. Thus, the serum levels of antigen-specific anti-Ova antibodies were determined. After BA administration via drinking water anti-Ova IgM levels were significantly increased reflecting the increased total IgM serum levels, as well as increased antigen-specific plasma cell frequencies. These findings raised the question of whether BA might also favor the induction of Ova-specific regulatory B cells.

In an independent study that will only be briefly mentioned here, Jana Sophia Buhre from the same laboratory at the Institute of Nutritional Medicine identified that indeed the strongly activating (inflammatory) IgG subclasses, IgG2b, and IgG2c, were reduced after enteral BA treatment (Föh et al, 2022 [1]). Future studies have to show whether the induction of anti-Ova IgM antibodies and the reduction of anti-Ova IgG2b and IgG2c antibodies were coupled and BA-dependent, or whether the reduced anti-Ova IgG2b and IgG2c levels were for instance a consequence of the increased IgM levels or the IL-10-producing cells. Alternatively, the reduced *Aicda* expression after BA treatment *ex vivo* might be mechanistically involved and indicate the observed effects to be a consequence of reduced class switch recombination prior to plasma cell differentiation.

6.7 Increased St6gal1 expression in $IL\text{-}10^+$ plasma cells

Since terminal sialylation of IgG, IgA, and IgM antibodies has been linked to anti-inflammatory effects [124,126,127,129,135,136,198,214], the expression of the

responsible enzyme St6gal1 in splenic IL-10$^+$ plasma cells was assessed after enteral BA treatment. Notably, St6gal1 expression was significantly increased in IL-10$^+$ compared to IL-10$^-$ plasma cells, indicating an increased capacity of regulatory plasma cells to sialylate glycan chains particularly of IgM, thus opening new pathways for anti-inflammatory functions of IL-10$^+$ plasma cells. Future studies have to investigate total as well as anti-Ova IgM glycosylation patterns to verify this assumption. Such a finding would establish for the first time that IL-10$^+$ regulatory plasma cells and plasma cells generating IgM antibodies with “high” sialylation levels could be the same plasma cells with two immunosuppressive functions.

6.8 HDAC3 inhibition is a possible underlying pathway

Considering the effects of BA on plasma cell differentiation and IL-10 expression in cell culture and animal experiments, possible underlying mechanisms were investigated. Previous literature has suggested three main mechanistic pathways for immunoregulatory functions of SCFAs: (I) the direct activation of G-protein coupled receptors leading to downstream signaling cascades [148], (II) the inhibition of HDACs changing the expression of target genes [148], and (III) regulation of mitochondrial metabolism [30,171,215]. Since plasma cell differentiation and IL-10 expression were only induced after BA but not PA treatment of isolated murine B cells, previously reported functional differences between these molecules were evaluated as underlying mechanisms. Although PA and BA share many similarities in structure and function, there are significant differences regarding the specificity of BA towards both GPRs and HDACs:

For GPRs, both PA and BA activate GPR41 and GPR43, but only GPR109a is activated by BA [228]. Hence, the possibility of GPR109a activation as an underlying mechanism was considered. However, the major SCFA receptors (GPR41, Gpr109a) are not expressed on murine B cells except for GPR43 [156]. It is therefore highly unlikely for GPR41 or GPR109a activation on B cells to be the underlying mechanism of plasma cell differentiation by BA, leaving only GPR43. The effects of an allosteric GPR43 agonist on plasma cell differentiation in the same cell culture setup as utilized for BA were thus tested. No induction of plasma cells was observed under effective concentrations of the GPR43 agonist, largely ruling out

the possibility of GPR43-activation on B cells to be decisively involved in the induction of B cells by BA. Previous literature supports this conclusion by demonstrating that neither a GPR43 agonist nor an antagonist interfered with plasma cell differentiation from B cells [156]. To ultimately rule out the possibility of a role of GPRs *in vivo*, conditional knockouts for these receptors in B cells would be a suitable model.

Similar to receptor-specificity, HDAC inhibitory activity varies between BA and PA. Whereas BA inhibits the activity of most Class I and Class II HDACs, including HDAC3 [167], PA has been shown to inhibit the HDAC isotypes 2 and 8, but specifically not HDAC3 [169] (s. **Table 2** for known HDAC classes and isotypes), which has been implicated in mediating the immunoregulatory effects of BA on macrophages [171]. We speculated that HDAC3 inhibition might also be involved in the underlying pathway(s), by which BA induces plasma cell differentiation and possibly IL-10 expression in B cells. HDAC inhibition, in general, has been frequently implicated as the leading mechanism behind the immunoregulatory functions of SCFAs [148], including the differentiation of $Foxp3^+$ Tregs from $CD4^+$ T-cell precursors [240–242] and the downregulation of proinflammatory cytokines [176]. Importantly these effects were reported to be independent of the expression or activation of G-protein coupled SCFA receptors.

In B cells, HDAC inhibition was implicated in the observed induction of plasma cells by *Kim et al.* [179]. Furthermore, *Sanchez et al.* replicated the HDAC inhibitory function of BA in B cells and additionally determined that the property of BA as a possible substrate for cell respiration did not affect plasma cell differentiation [156]. HDAC inhibition increased acetylation of the *Blimp1/Prdm1* and *Aicda* promoter regions [156], which opens up the chromatin structure, leading to increased accessibility for transcription factors and enhanced gene expression [243]. Accordingly, histone hyperacetylation in the *Prdm1* promoter region has been shown to effectively enhance the transcription of *Prdm1* [244], corresponding to the results for *Prdm1* expression and plasma cell differentiation observed here.

Taken together, both studies implicated HDAC inhibition to be the crucial function of BA in regulating plasma cell differentiation, although in different directions. Furthermore, they did not include investigations, in which HDAC was specifically responsible for the observed

effects. Here, it was shown that BA increased H3K27 acetylation similar to the effects of the specific HDAC3 inhibitor RGFP966, whereas no such effects were observed for PA. By showing that TSA (a specific class I and II HDAC inhibitor) and especially RGFP966 induce plasma cell differentiation and IL-10 expression similar to BA under the same cell culture conditions, significant evidence is provided to suggest that HDAC3 inhibition is the driving factor underlying both observed effects.

Notably, HDAC3 knockout in murine T cells leads to increased H3K27 acetylation and *Prdm1* transcription [245] corroborating the results of the present study. Moreover, H3K27 acetylation is associated with CD138 expression during PC differentiation [246] providing a direct link between the observed effects on H3K27 acetylation and plasma cell differentiation of BA. More insights into the effects of HDAC3 on B cell differentiation could be obtained using a conditional knockout of HDAC3 in B cells. Notably, similar studies were already conducted by *Stengel et al.* knocking out HDAC3 in B cells. As a result, early pre-mature B cell progenitors depend on HDAC3 expression for normal B cell development, resulting in an absence of mature B cells [247]. Thus, a knockout of HDAC3 in mature B cells was conducted leading to increased expression of *Prdm1* and *Irf4*, further supporting the results of the present study [248]. However, the expression of CD138 was downregulated, possibly indicating that a basic level of HDAC3 activity is still needed for successful plasma cell differentiation, even though Prdm1 is upregulated [248]. A possible explanation for this phenomenon is that Prdm1-dependent repression of B cell genes is, in fact, mediated by HDAC3 [249]. A future direction to elegantly prove the significance of HDAC3 activity in regulating plasma cell differentiation might therefore be a conditional knockdown of HDAC3 in mature B cells as opposed to a complete knockout.

Further studies also have to prove whether BA-induced plasma cell differentiation and expression of regulatory cytokines (e.g. IL-10) in B cells including plasma cells are two separate pathways that, however, both depend on HDAC inhibition.

6.9 Decreased mitochondrial ROS production after HDAC3 inhibition mediates plasma cell differentiation

Since low mitochondrial ROS levels, especially superoxide, have been established to play a pivotal role in promoting plasma cell differentiation [96], and since HDAC3 has been shown to induce mitochondrial ROS production [220,250], the effects of BA and HDAC3 inhibitor RGFP966 on mitochondrial respiration and superoxide production were analyzed. As a result, acute injection of BA to a B cell culture increased respiration slightly in a short-term manner. These results indicate that BA might be used as an energy substrate in B cell culture after acute injection similar to its function as the main energy substrate for colonocytes [154] via fatty acid oxidation and introduction into the Krebs cycle [153]. After one day, however, when HDAC inhibition and downstream signaling were allowed to occur, mitochondrial respiration and superoxide levels decreased significantly. Notably, mitochondrial superoxide levels were decreased in a similar manner, when B cells were instead incubated with the specific HDAC3 inhibitor RGFP966, supporting the hypothesis that reduced mitochondrial superoxide levels were induced downstream of HDAC3 inhibition by BA.

Mitochondrial superoxide inducers PMA and 2DG [96,221–223] were used to test whether plasma cell induction and IL-10 expression depend on reduced mitochondrial ROS levels. As a result, plasma cell differentiation was completely abrogated by the addition of PMA or 2DG, indicating that increased plasma cell differentiation after BA treatment relies on reduced mitochondrial ROS levels. Interestingly, PMA and 2DG did not abrogate the expression of IL-10 in B cells similarly to PC differentiation. Thus, reduced mitochondrial superoxide levels seem to be necessary for the induction of PCs by BA, whereas IL-10 expression is likely induced independently from mitochondrial superoxide levels. Notably, 2DG abrogated the induction of plasma cells by HDAC3 inhibitor RGFP966 as well, indicating that mitochondrial ROS levels are most likely a downstream target of HDAC3 inhibition.

Thus, BA-induced plasma cell differentiation most likely depends on HDAC inhibition with a resulting reduction of mitochondrial superoxide levels. BA-induced induction of regulatory (IL-10^{+}) B cells including plasma cells was also dependent on HDAC inhibition, but not reduced superoxide levels.

6.10 Additional limitations and outlook

A limitation of the present study is that underlying mechanisms of regulatory plasma cell induction have mainly been investigated in *ex vivo* experiments. While these experiments allow for the observation of B cell-specific effects of BA and HDAC3 inhibitors, they do not reflect the complex reality of a biological organism. Hence, further studies need to address this issue and test the conclusions that have been drawn here in *in vivo* models. The inclusion of B cell-specific knockdowns of HDAC3 and mitochondrial ROS production should allow for B cell-specific validation of the here proposed underlying mechanisms in an *in vivo* model.

Future studies should also include additional analyses of the phenotype of BA-induced regulatory plasma cells. The expression of additional surface markers of Bregs and functional characteristics are of particular relevance. Especially, PD-L1 expression should be examined, since it is not only expressed by some Breg subtypes but is moreover deeply involved in exerting immunoregulatory functions including suppression of antibody production and T cell activation [14]. Accordingly, PD-L1^{high} B cells have been shown to protect against EAE [14]. Additionally, the lymphocyte-activation gene 3 (LAG-3) is a surface antigen that has recently emerged as a potential surface marker identifying regulatory PCs [78] and should therefore be included in future analyses.

Further limitations of the study include that the observed *in vivo* effects are based on a model of Ova/CFA-immunized, but healthy mice. Additional studies have to determine whether BA treatment and the observed induction of IL-10^{+}IgM^{+} CD138^{high}plasma cells with proposed regulatory functions lead to a possible amelioration of inflammatory processes. Therefore, the application of BA, or possibly pharmaceutical inhibitors of HDAC3, preferentially in the context of B cell-dependent inflammation [251], e.g. models of rheumatoid arthritis [252], systemic lupus erythematosus [252], or multiple sclerosis [253] is needed to evaluate for potential therapeutic uses of BA or specific inhibitors of HDAC3 for their induction of regulatory plasma cells, that may be implemented into clinical use eventually. Since BA is an approved nutritional supplement without any known significant side effects [254], its use as a therapeutic agent would be effective and easily available, while implementation of HDAC3 inhibitors would need considerably more effort for clinical approval. Finally, a shift of the intestinal microbiome to BA-generating microbes by using

pro- or prebiotics might be a suitable way to increase the endogenous production of BA for the treatment of inflammatory diseases.

7 REFERENCES

1. Föh B, Buhre JS, Lunding HB, Moreno-Fernandez ME, König P, Sina C, et al. Microbial metabolite butyrate promotes induction of IL-10+IgM+ plasma cells. PLoS One. 2022 Mar 25;17(3):e0266071. Available from: https://pubmed.ncbi.nlm.nih.gov/35333906/
2. Mauri C, Menon M. The expanding family of regulatory B cells. Int Immunol. 2015 Oct;27(10):479–86. Available from: http://www.ncbi.nlm.nih.gov/pubmed/26071023
3. Rosser EC, Mauri C. Regulatory B Cells: Origin, Phenotype, and Function. Immunity. 2015;42(4):607–12. Available from: http://dx.doi.org/10.1016/j.immuni.2015.04.005
4. Mauri C, Bosma A. Immune regulatory function of B cells. Annual Review of Immunology. Annual Reviews; 2012. p. 221–41. Available from: http://www.annualreviews.org/doi/10.1146/annurev-immunol-020711-074934
5. Ouyang W, Rutz S, Crellin NK, Valdez PA, Hymowitz SG. Regulation and Functions of the IL-10 Family of Cytokines in Inflammation and Disease. Annu Rev Immunol. 2011 Apr 23;29(1):71–109. Available from: http://www.annualreviews.org/doi/10.1146/annurev-immunol-031210-101312
6. Ouyang W, O'Garra A. IL-10 Family Cytokines IL-10 and IL-22: from Basic Science to Clinical Translation. Immunity. 2019;50(4):871–91. Available from: https://doi.org/10.1016/j.immuni.2019.03.020
7. Medzhitov R. Origin and physiological roles of inflammation. Nature. 2008;454(7203):428–35.
8. Nathan C, Ding A. Nonresolving Inflammation. Cell. 2010;140(6):871–82. Available from: http://dx.doi.org/10.1016/j.cell.2010.02.029
9. Couper KN, Blount DG, Riley EM. IL-10: The Master Regulator of Immunity to Infection. J Immunol. 2008 May 1;180(9):5771–7.
10. Amu S, Saunders SP, Kronenberg M, Mangan NE, Atzberger A, Fallon PG. Regulatory B cells prevent and reverse allergic airway inflammation via FoxP3-positive T regulatory cells in a murine model. J Allergy Clin Immunol. 2010;125(5).
11. Carter NA, Vasconcellos R, Rosser EC, Tulone C, Muñoz-Suano A, Kamanaka M, et al. Mice Lacking Endogenous IL-10–Producing Regulatory B Cells Develop Exacerbated Disease and Present with an Increased Frequency of Th1/Th17 but a Decrease in Regulatory T Cells. J Immunol. 2011 May 15;186(10):5569–79.
12. Blair PA, Noreña LY, Flores-Borja F, Rawlings DJ, Isenberg DA, Ehrenstein MR, et al. CD19+CD24hiCD38hi B Cells Exhibit Regulatory Capacity in Healthy Individuals but Are Functionally Impaired in Systemic Lupus Erythematosus Patients. Immunity. 2010 Jan 29;32(1):129–40.
13. Flores-Borja F, Bosma A, Ng D, Reddy V, Ehrenstein MR, Isenberg DA, et al. CD19+CD24hiCD38hi B cells maintain regulatory T cells while limiting TH1 and TH17

differentiation. Sci Transl Med. 2013 Feb 20;5(173).

14. Khan AR, Hams E, Floudas A, Sparwasser T, Weaver CT, Fallon PG. PD-L1hi B cells are critical regulators of humoral immunity. Nat Commun. 2015 Jan 22;6(1):1–16.

15. Mauri C, Menon M. Human regulatory B cells in health and disease: Therapeutic potential. Vol. 127, Journal of Clinical Investigation. American Society for Clinical Investigation; 2017. p. 772–9.

16. Neta R, Salvin SB. Specific suppression of delayed hypersensitivity: the possible presence of a suppressor B cell in the regulation of delayed hypersensitivity. J Immunol. 1974 Dec 1;113(6):1716–25. Available from: http://www.ncbi.nlm.nih.gov/pubmed/4279260

17. Katz, Parker D, Turk JL. B-cell suppression of delayed hypersensitivity reactions. Nature. 1974;251(5475):550–1.

18. Wolf SD, Dittel BN, Hardardottir F, Janeway CA. Experimental autoimmune encephalomyelitis induction in genetically B cell-deficient mice. J Exp Med. 1996;184(6):2271–8.

19. Mizoguchi A, Mizoguchi E, Smith RN, Preffer FI, Bhan AK. Suppressive role of B cells in chronic colitis of T cell receptor α mutant mice. J Exp Med. 1997 Nov 17;186(10):1749–56.

20. Fillatreau S, Sweenie CH, McGeachy MJ, Gray D, Anderton SM. B cells regulate autoimmunity by provision of IL-10. Nat Immunol. 2002;3(10):944–50.

21. Mizoguchi A, Mizoguchi E, Takedatsu H, Blumberg RS, Bhan AK. Chronic intestinal inflammatory condition generates IL-10-producing regulatory B cell subset characterized by CD1d upregulation. Immunity. 2002;16(2):219–30.

22. Mauri C, Gray D, Mushtaq N, Londei M. Prevention of arthritis by interleukin 10-producing B cells. J Exp Med. 2003 Feb 17;197(4):489–501.

23. Mangan NE, Fallon RE, Smith P, van Rooijen N, McKenzie AN, Fallon PG. Helminth Infection Protects Mice from Anaphylaxis via IL-10-Producing B Cells. J Immunol. 2004 Nov 15;173(10):6346–56.

24. Mishima Y, Ishihara S, Aziz MM, Oka A, Kusunoki R, Otani A, et al. Decreased production of interleukin-10 and transforming growth factor-β in Toll-like receptor-activated intestinal B cells in SAMP1/Yit mice. Immunology. 2010 Dec;131(4):473–87.

25. Yanaba K, Yoshizaki A, Asano Y, Kadono T, Tedder TF, Sato S. IL-10-producing regulatory B10 cells inhibit intestinal injury in a mouse model. Am J Pathol. 2011;178(2):735–43.

26. Maseda D, Candando KM, Smith SH, Kalampokis I, Weaver CT, Plevy SE, et al. Peritoneal cavity regulatory B cells (B10 cells) modulate IFN-γ+CD4+ T cell numbers during colitis development in mice. J Immunol. 2013 Sep 1;191(5):2780–95. Available from: http://www.ncbi.nlm.nih.gov/pubmed/23918988

27. Schmidt EGW, Larsen HL, Kristensen NN, Poulsen SS, Claesson MH, Pedersen AE. B cells exposed to enterobacterial components suppress development of experimental colitis. Inflamm Bowel Dis. 2012 Feb;18(2):284–93.

28. Sattler S, Ling GS, Xu D, Hussaarts L, Romaine A, Zhao H, et al. IL-10-producing regulatory B cells induced by IL-33 (BregIL-33) effectively attenuate mucosal inflammatory responses in the gut. J Autoimmun. 2014;50(100):107–22.

29. Oka A, Ishihara S, Mishima Y, Tada Y, Kusunoki R, Fukuba N, et al. Role of Regulatory B Cells in Chronic Intestinal Inflammation. Inflamm Bowel Dis. 2014 Feb 1;20(2):315–28. Available from: https://academic.oup.com/ibdjournal/article/20/2/315-328/4578968

30. Luu M, Pautz S, Kohl V, Singh R, Romero R, Lucas S, et al. The short-chain fatty acid pentanoate suppresses autoimmunity by modulating the metabolic-epigenetic crosstalk in lymphocytes. Nat Commun. 2019;10(1):760. Available from: http://www.ncbi.nlm.nih.gov/pubmed/30770822

31. Li R, Patterson KR, Bar-Or A. Reassessing B cell contributions in multiple sclerosis. Nat Immunol. 2018;19(7):696–707. Available from: http://dx.doi.org/10.1038/s41590-018-0135-x

32. Duddy M, Niino M, Adatia F, Hebert S, Freedman M, Atkins H, et al. Distinct Effector Cytokine Profiles of Memory and Naive Human B Cell Subsets and Implication in Multiple Sclerosis. J Immunol. 2007 May 15;178(10):6092–9.

33. Knippenberg S, Peelen E, Smolders J, Thewissen M, Menheere P, Cohen Tervaert JW, et al. Reduction in IL-10 producing B cells (Breg) in multiple sclerosis is accompanied by a reduced naïve/memory Breg ratio during a relapse but not in remission. J Neuroimmunol. 2011 Oct 28;239(1–2):80–6.

34. Michel L, Degauque N, Garcia A, Salou M, Ngono AE, Soulillou J-P, et al. Loss of IL-10 secretion by regulatory B lymphocytes in multiple sclerosis patients. J Transl Med. 2011 Dec;9(S2):P25.

35. Correale J, Farez M, Razzitte G. Helminth infections associated with multiple sclerosis induce regulatory B cells. Ann Neurol. 2008 Aug;64(2):187–99.

36. Thompson SAJ, Jones JL, Cox AL, Compston DAS, Coles AJ. B-Cell reconstitution and BAFF after alemtuzumab (Campath-1H) treatment of multiple sclerosis. J Clin Immunol. 2010 Jan;30(1):99–105.

37. Heidt S, Hester J, Shankar S, Friend PJ, Wood KJ. B cell repopulation after alemtuzumab induction - Transient increase in transitional B cells and long-term dominance of naïve B cells. Am J Transplant. 2012 Jul;12(7):1784–92.

38. Grützke B, Hucke S, Gross CC, Herold MVB, Posevitz-Fejfar A, Wildemann BT, et al. Fingolimod treatment promotes regulatory phenotype and function of B cells. Ann Clin Transl Neurol. 2015 Feb 1;2(2):119–30.

39. Schubert RD, Hu Y, Kumar G, Szeto S, Abraham P, Winderl J, et al. IFN-β Treatment Requires B Cells for Efficacy in Neuroautoimmunity. J Immunol. 2015 Mar 1;194(5):2110–6.

40. Piancone F, Saresella M, Marventano I, La Rosa F, Zoppis M, Agostini S, et al. B lymphocytes in multiple sclerosis: Bregs and BTLA/CD272 expressing-CD19+ lymphocytes modulate disease severity. Sci Rep. 2016 Jul 14;6.

41. Lundy SK, Wu Q, Wang Q, Dowling CA, Taitano SH, Mao G, et al. Dimethyl fumarate

treatment of relapsing-remitting multiple sclerosis influences B-cell subsets. Neurol Neuroimmunol NeuroInflammation. 2016;3(2).

42. Kim Y, Kim G, Shin HJ, Hyun JW, Kim SH, Lee E, et al. Restoration of regulatory B cell deficiency following alemtuzumab therapy in patients with relapsing multiple sclerosis. J Neuroinflammation. 2018 Oct 30;15(1).

43. Wu Q, Mills EA, Wang Q, Dowling CA, Fisher C, Kirch B, et al. Siponimod enriches regulatory T and B lymphocytes in secondary progressive multiple sclerosis. JCI Insight. 2020 Feb 13;5(3).

44. Amel Kashipazl MR, Huggins ML, Lanyon P, Robins A, Powell RJ, Todd I. Assessment of Be1 and Be2 cells in systemic lupus erythematosus indicates elevated interleukin-10 producing CD5+ B cells. Lupus. 2003;12(5):356–63.

45. Iwata Y, Matsushita T, Horikawa M, DiLillo DJ, Yanaba K, Venturi GM, et al. Characterization of a rare IL-10-competent B-cell subset in humans that parallels mouse regulatory B10 cells. Blood. 2011 Jan 13;117(2):530–41.

46. Yang X, Yang J, Chu Y, Xue Y, Xuan D, Zheng S, et al. T follicular helper cells and regulatory B cells dynamics in systemic lupus erythematosus. PLoS One. 2014 Feb 14;9(2).

47. Gao N, Dresel J, Eckstein V, Gellert R, Störch H, Venigalla RKC, et al. Impaired suppressive capacity of activation-induced regulatory B cells in systemic lupus erythematosus. Arthritis Rheumatol. 2014 Oct 1;66(10):2849–61.

48. Heinemann K, Wilde B, Hoerning A, Tebbe B, Kribben A, Witzke O, et al. Decreased IL-10+ regulatory B cells (Bregs) in lupus nephritis patients. Scand J Rheumatol. 2016 Jul 3;45(4):312–6.

49. Menon M, Blair PA, Isenberg DA, Mauri C. A Regulatory Feedback between Plasmacytoid Dendritic Cells and Regulatory B Cells Is Aberrant in Systemic Lupus Erythematosus. Immunity. 2016 Mar 15;44(3):683–97.

50. Anolik JH, Barnard J, Owen T, Zheng B, Kemshetti S, Looney RJ, et al. Delayed memory B cell recovery in peripheral blood and lymphoid tissue in systemic lupus erythematosus after B cell depletion therapy. Arthritis Rheum. 2007 Sep 1;56(9):3044–56.

51. Bosma A, Abdel-Gadir A, Isenberg DA, Jury EC, Mauri C. Lipid-Antigen Presentation by CD1d + B Cells Is Essential for the Maintenance of Invariant Natural Killer T Cells. Immunity. 2012 Mar 23;36(3):477–90.

52. Daien CI, Gailhac S, Mura T, Audo R, Combe B, Hahne M, et al. Regulatory B10 cells are decreased in patients with rheumatoid arthritis and are inversely correlated with disease activity. Arthritis Rheumatol. 2014;66(8):2037–46.

53. Ma L, Liu B, Jiang Z, Jiang Y. Reduced numbers of regulatory B cells are negatively correlated with disease activity in patients with new-onset rheumatoid arthritis. Clin Rheumatol. 2014 Feb;33(2):187–95.

54. Cui D, Zhang L, Chen J, Zhu M, Hou L, Chen B, et al. Changes in regulatory B cells and their relationship with rheumatoid arthritis disease activity. Clin Exp Med. 2015 Aug 3;15(3):285–92.

55. Zacca ER, Onofrio LI, Acosta CDV, Ferrero P V., Alonso SM, Ramello MC, et al. PD-L1+ Regulatory B cells are significantly decreased in rheumatoid arthritis patients and increase after successful treatment. Front Immunol. 2018 Oct 1;9(OCT).

56. Wang X, Zhu Y, Zhang M, Wang H, Jiang Y, Gao P. Ulcerative colitis is characterized by a decrease in regulatory B cells. J Crohn's Colitis. 2016;10(10):1212–23.

57. Fonseca-Camarillo G, Furuzawa-Carballeda J, Yamamoto-Furusho JK. Interleukin 35 (IL-35) and IL-37: Intestinal and peripheral expression by T and B regulatory cells in patients with Inflammatory Bowel Disease. Cytokine. 2015 Oct 1;75(2):389–402.

58. Evans JG, Chavez-Rueda KA, Eddaoudi A, Meyer-Bahlburg A, Rawlings DJ, Ehrenstein MR, et al. Novel Suppressive Function of Transitional 2 B Cells in Experimental Arthritis. J Immunol. 2007 Jun 15;178(12):7868–78.

59. Blair PA, Chavez-Rueda KA, Evans JG, Shlomchik MJ, Eddaoudi A, Isenberg DA, et al. Selective Targeting of B Cells with Agonistic Anti-CD40 Is an Efficacious Strategy for the Generation of Induced Regulatory T2-Like B Cells and for the Suppression of Lupus in MRL/ lpr Mice . J Immunol. 2009 Mar 15;182(6):3492–502.

60. Said SS, Barut GT, Mansur N, Korkmaz A, Sayi-Yazgan A. Bacterially activated B-cells drive T cell differentiation towards Tr1 through PD-1/PD-L1 expression. Mol Immunol. 2018 Apr 1;96:48–60.

61. Gray M, Miles K, Salter D, Gray D, Savill J. Apoptotic cells protect mice from autoimmune inflammation by the induction of regulatory B cells. Proc Natl Acad Sci U S A. 2007 Aug 28;104(35):14080–5.

62. Bankoti R, Gupta K, Levchenko A, Stäger S. Marginal Zone B Cells Regulate Antigen-Specific T Cell Responses during Infection. J Immunol. 2012 Apr 15;188(8):3961–71.

63. Miles K, Heaney J, Sibinska Z, Salter D, Savill J, Gray D, et al. A tolerogenic role for Toll-like receptor 9 is revealed by B-cell interaction with DNA complexes expressed on apoptotic cells. Proc Natl Acad Sci U S A. 2012 Jan 17;109(3):887–92.

64. Chagnon-Choquet J, Fontaine J, Poudrier J, Roger M. IL-10 and lymphotoxin-α expression profiles within marginal zone-like B-cell populations are associated with control of HIV-1 disease progression. PLoS One. 2014 Jul 8;9(7).

65. Huber K, Sármay G, Kövesdi D. MZ B cells migrate in a T-bet dependent manner and might contribute to the remission of collagen-induced arthritis by the secretion of IL-10. Eur J Immunol. 2016 Sep 1;46(9):2239–46.

66. Appelgren D, Eriksson P, Ernerudh J, Segelmark M. Marginal-Zone B-Cells are main producers of IgM in humans, and are reduced in patients with autoimmune vasculitis. Front Immunol. 2018 Oct 2;9(OCT).

67. Yanaba K, Bouaziz J-D, Matsushita T, Tsubata T, Tedder TF. The Development and Function of Regulatory B Cells Expressing IL-10 (B10 Cells) Requires Antigen Receptor Diversity and TLR Signals. J Immunol. 2009 Jun 15;182(12):7459–72.

68. Matsushita T, Horikawa M, Iwata Y, Tedder TF. Regulatory B Cells (B10 Cells) and Regulatory T Cells Have Independent Roles in Controlling Experimental Autoimmune Encephalomyelitis Initiation and Late-Phase Immunopathogenesis. J Immunol. 2010 Aug 15;185(4):2240–52.

69. Horikawa M, Weimer ET, DiLillo DJ, Venturi GM, Spolski R, Leonard WJ, et al. Regulatory B Cell (B10 Cell) Expansion during Listeria Infection Governs Innate and Cellular Immune Responses in Mice . J Immunol. 2013 Feb 1;190(3):1158–68.

70. Hasan MM, Thompson-Snipes L, Klintmalm G, Demetris AJ, O'Leary J, Oh S, et al. CD24 hi CD38 hi and CD24 hi CD27 + Human Regulatory B Cells Display Common and Distinct Functional Characteristics. J Immunol. 2019 Oct 15;203(8):2110–20.

71. Zheng Y, Ge W, Ma Y, Xie G, Wang W, Han L, et al. miR-155 regulates IL-10-producing CD24hiCD27+ B cells and impairs their function in patients with Crohn's disease. Front Immunol. 2017 Aug 3;8(AUG).

72. Shi L, Hu F, Zhu L, Xu C, Zhu H, Li Y, et al. CD70-mediated CD27 expression downregulation contributed to the regulatory B10 cell impairment in rheumatoid arthritis. Mol Immunol. 2020 Mar 1;119:92–100.

73. Rafei M, Hsieh J, Zehntner S, Li M, Forner K, Birman E, et al. A granulocyte-macrophage colony-stimulating factor and interleukin-15 fusokine induces a regulatory B cell population with immune suppressive properties. Nat Med. 2009 Sep;15(9):1038–45.

74. Neves P, Lampropoulou V, Calderon-Gomez E, Roch T, Stervbo U, Shen P, et al. Signaling via the MyD88 Adaptor Protein in B Cells Suppresses Protective Immunity during Salmonella typhimurium Infection. Immunity. 2010 Nov 24;33(5):777–90. Available from: http://www.ncbi.nlm.nih.gov/pubmed/21093317

75. Shen P, Roch T, Lampropoulou V, O'Connor RA, Stervbo U, Hilgenberg E, et al. IL-35-producing B cells are critical regulators of immunity during autoimmune and infectious diseases. Nature. 2014;507(7492):366–70.

76. Matsumoto M, Baba A, Yokota T, Nishikawa H, Ohkawa Y, Kayama H, et al. Interleukin-10-Producing Plasmablasts Exert Regulatory Function in Autoimmune Inflammation. Immunity. 2014 Dec 18;41(6):1040–51. Available from: https://www.sciencedirect.com/science/article/pii/S1074761314003926?via%3Dihub

77. Shalapour S, Font-Burgada J, Di Caro G, Zhong Z, Sanchez-Lopez E, Dhar D, et al. Immunosuppressive plasma cells impede T-cell-dependent immunogenic chemotherapy. Nature. 2015 May 7;521(7550):94–8.

78. Lino AC, Dang VD, Lampropoulou V, Welle A, Joedicke J, Pohar J, et al. LAG-3 Inhibitory Receptor Expression Identifies Immunosuppressive Natural Regulatory Plasma Cells. Immunity. 2018 Jul 17;49(1):120-133.e9.

79. Machado-Santos J, Saji E, Tröscher AR, Paunovic M, Liblau R, Gabriely G, et al. The compartmentalized inflammatory response in the multiple sclerosis brain is composed of tissue-resident CD8+ T lymphocytes and B cells. Brain. 2018;141(7):2066–82.

80. Rojas OL, Pröbstel AK, Porfilio EA, Wang AA, Charabati M, Sun T, et al. Recirculating Intestinal IgA-Producing Cells Regulate Neuroinflammation via IL-10. Cell. 2019;176(3):610-624.e18.

81. Ding Q, Yeung M, Camirand G, Zeng Q, Akiba H, Yagita H, et al. Regulatory B cells are identified by expression of TIM-1 and can be induced through TIM-1 ligation to

promote tolerance in mice. J Clin Invest. 2011 Sep;121(9):3645–56. Available from: http://www.ncbi.nlm.nih.gov/pubmed/21821911

82. Xiao S, Brooks CR, Zhu C, Wu C, Sweere JM, Petecka S, et al. Defect in regulatory B-cell function and development of systemic autoimmunity in T-cell Ig mucin 1 (Tim-1) mucin domain-mutant mice. Proc Natl Acad Sci U S A. 2012 Jul 24;109(30):12105–10.

83. Xiao S, Brooks CR, Sobel RA, Kuchroo VK. Tim-1 Is Essential for Induction and Maintenance of IL-10 in Regulatory B Cells and Their Regulation of Tissue Inflammation. J Immunol. 2015 Feb 15;194(4):1602–8.

84. Aravena O, Ferrier A, Menon M, Mauri C, Aguillón JC, Soto L, et al. TIM-1 defines a human regulatory B cell population that is altered in frequency and function in systemic sclerosis patients. Arthritis Res Ther. 2017 Jan 19;19(1):8. Available from: http://www.ncbi.nlm.nih.gov/pubmed/28103916

85. Das A, Ellis G, Pallant C, Lopes AR, Khanna P, Peppa D, et al. IL-10–Producing Regulatory B Cells in the Pathogenesis of Chronic Hepatitis B Virus Infection. J Immunol. 2012 Oct 15;189(8):3925–35.

86. Wang Y, Qin Y, Wang X, Zhang L, Wang J, Xu X, et al. Decrease in the proportion of CD24hiCD38hi B cells and impairment of their regulatory capacity in type 1 diabetes patients. Clin Exp Immunol. 2020 Apr 1;200(1):22–32.

87. Lee SJ, Noh G, Lee JH. In vitro induction of allergen-specific interleukin-10-producing regulatory B cell responses by interferon-γ in non- immunoglobulin E-mediated milk allergy. Allergy, Asthma Immunol Res. 2013 Jan;5(1):48–54.

88. van de Veen W, Stanic B, Wirz OF, Jansen K, Globinska A, Akdis M. Role of regulatory B cells in immune tolerance to allergens and beyond. J Allergy Clin Immunol. 2016 Sep;138(3):654–65. Available from: http://www.ncbi.nlm.nih.gov/pubmed/27596706

89. Allen HC, Sharma P. Histology, Plasma Cells [Internet]. StatPearls. StatPearls Publishing; 2020. Available from: http://www.ncbi.nlm.nih.gov/pubmed/32310542

90. Nutt SL, Hodgkin PD, Tarlinton DM, Corcoran LM. The generation of antibody-secreting plasma cells. Nat Rev Immunol. 2015;15(3):160–71. Available from: http://dx.doi.org/10.1038/nri3795

91. Ise W, Kurosaki T. Plasma cell differentiation during the germinal center reaction. Immunol Rev. 2019 Mar 15;288(1):64–74. Available from: https://onlinelibrary.wiley.com/doi/abs/10.1111/imr.12751

92. Stavnezer J, Guikema JEJ, Schrader CE. Mechanism and regulation of class switch recombination. Annu Rev Immunol. 2008;26:261–92.

93. Stavnezer J, Schrader CE. IgH Chain Class Switch Recombination: Mechanism and Regulation. J Immunol. 2014 Dec 1;193(11):5370–8. Available from: https://www.jimmunol.org/content/193/11/5370

94. Gatto D, Brink R. The germinal center reaction. Vol. 126, Journal of Allergy and Clinical Immunology. J Allergy Clin Immunol; 2010. p. 898–907.

95. Ise W, Fujii K, Shiroguchi K, Ito A, Kometani K, Takeda K, et al. T Follicular Helper Cell-

Germinal Center B Cell Interaction Strength Regulates Entry into Plasma Cell or Recycling Germinal Center Cell Fate. Immunity. 2018 Apr 17;48(4):702-715.e4.

96. Jang K-J, Mano H, Aoki K, Hayashi T, Muto A, Nambu Y, et al. Mitochondrial function provides instructive signals for activation-induced B-cell fates. Nat Commun. 2015 Dec 10;6(1):6750. Available from: http://www.nature.com/articles/ncomms7750

97. Nutt SL, Taubenheim N, Hasbold J, Corcoran LM, Hodgkin PD. The genetic network controlling plasma cell differentiation. Semin Immunol. 2011 Oct;23(5):341–9. Available from: https://pubmed.ncbi.nlm.nih.gov/21924923/

98. Turner CA, Mack DH, Davis MM. Blimp-1, a novel zinc finger-containing protein that can drive the maturation of B lymphocytes into immunoglobulin-secreting cells. Cell. 1994 Apr 22;77(2):297–306.

99. Sciammas R, Davis MM. Modular Nature of Blimp-1 in the Regulation of Gene Expression during B Cell Maturation. J Immunol. 2004 May 1;172(9):5427–40.

100. Shaffer AL, Lin KI, Kuo TC, Yu X, Hurt EM, Rosenwald A, et al. Blimp-1 orchestrates plasma cell differentiation by extinguishing the mature B cell gene expression program. Immunity. 2002 Jul 1;17(1):51–62. Available from: http://www.ncbi.nlm.nih.gov/pubmed/12150891

101. Minnich M, Tagoh H, Bönelt P, Axelsson E, Fischer M, Cebolla B, et al. Multifunctional role of the transcription factor Blimp-1 in coordinating plasma cell differentiation. Nat Immunol. 2016 Feb 16;17(3):331–43.

102. Shaffer AL, Shapiro-Shelef M, Iwakoshi NN, Lee AH, Qian SB, Zhao H, et al. XBP1, downstream of Blimp-1, expands the secretory apparatus and other organelles, and increases protein synthesis in plasma cell differentiation. Immunity. 2004 Jul;21(1):81–93. Available from: https://pubmed.ncbi.nlm.nih.gov/15345222/

103. Sanderson RD, Børset M. Syndecan-1 in B lymphoid malignancies. Ann Hematol. 2002;81(3):125–35.

104. Bataille R, Jego G, Robillard N, Barille-Nion S, Harousseau J, Moreau P, et al. The phenotype of normal, reactive and malignant plasma cells. Identification of “many and multiple myelomas” and of new targets for myeloma therapy. Haematologica. 2006 Jan 1;91(9):1234–40.

105. De Vos J, Hose D, Rème T, Tarte K, Moreaux J, Mahtouk K, et al. Microarray-based understanding of normal and malignant plasma cells. Vol. 210, Immunological Reviews. Inserm; 2006. p. 86–104.

106. Costes V, Magen V, Legouffe E, Durand L, Baldet P, Rossi JF, et al. The Mi15 monoclonal antibody (anti-syndecan-1) is a reliable marker for quantifying plasma cells in paraffin-embedded bone marrow biopsy specimens. Hum Pathol. 1999;30(12):1405–11.

107. Caraux A, Klein B, Paiva B, Bret C, Schmitz A, Fuhler GM, et al. Circulating human B and plasma cells. Age-associated changes in counts and detailed characterization of circulating normal CD138− and CD138+ plasma cells. Haematologica. 2010 Jun 1;95(6):1016–20. Available from: https://haematologica.org/article/view/5607

108. Brynjolfsson SF, Berg LP, Ekerhult TO, Rimkute I, Wick MJ, Martensson IL, et al. Long-

lived plasma cells in mice and men. Front Immunol. 2018 Nov 16;9(NOV):2673.

109. Rickert R, Jellusova J. TNF and TNFR Family Members and B Cell Activation. In: Encyclopedia of Immunobiology. Elsevier Inc.; 2016. p. 259–68.

110. Boi M, Zucca E, Inghirami G, Bertoni F. PRDM1/BLIMP1: A tumor suppressor gene in B and T cell lymphomas. Leuk Lymphoma. 2015;56(5):1223–8.

111. Iwakoshi NN, Lee AH, Vallabhajosyula P, Otipoby KL, Rajewsky K, Glimcher LH. Plasma cell differentiation and the unfolded protein response intersect at the transcription factor XBP-I. Nat Immunol. 2003 Apr 1;4(4):321–9.

112. Klein U, Casola S, Cattoretti G, Shen Q, Lia M, Mo T, et al. Transcription factor IRF4 controls plasma cell differentiation and class-switch recombination. Nat Immunol. 2006 Jul;7(7):773–82.

113. Gualco G, Weiss LM, Bacchi CE. Mum1/Irf4. Appl Immunohistochem Mol Morphol. 2010;18(4):301–10.

114. Chiu ML, Goulet DR, Teplyakov A, Gilliland GL. Antibody Structure and Function: The Basis for Engineering Therapeutics. Antibodies 2019, Vol 8, Page 55. 2019 Dec 3;8(4):55. Available from: https://www.mdpi.com/2073-4468/8/4/55/htm

115. Lilienthal GM, Rahmöller J, Petry J, Bartsch YC, Leliavski A, Ehlers M. Potential of murine IgG1 and Human IgG4 to inhibit the classical complement and Fcγ receptor activation pathways. Front Immunol. 2018;9(MAY).

116. Nimmerjahn F, Ravetch J V. Fcγ receptors as regulators of immune responses. Vol. 8, Nature Reviews Immunology. Nature Publishing Group; 2008. p. 34–47.

117. Tiller T, Kofer J, Kreschel C, Busse CE, Riebel S, Wickert S, et al. Development of self-reactive germinal center B cells and plasma cells in autoimmune FcγRIIB-deficient mice. J Exp Med. 2010 Nov 22;207(12):2767–78. Available from: www.jem.org/cgi/doi/10.1084/jem.20100171

118. Wang TT, Maamary J, Tan GS, Bournazos S, Davis CW, Krammer F, et al. Anti-HA glycoforms drive B cell affinity selection and determine influenza vaccine efficacy. Cell. 2015 Jul 7;162(1):160. Available from: /pmc/articles/PMC4594835/

119. Xiang Z, Cutler AJ, Brownlie RJ, Fairfax K, Lawlor KE, Severinson E, et al. FcγRIIb controls bone marrow plasma cell persistence and apoptosis. Nat Immunol 2007 84. 2007 Feb 18;8(4):419–29. Available from: https://www.nature.com/articles/ni1440

120. Nimmerjahn F, Ravetch J V. Divergent immunoglobulin G subclass activity through selective Fc receptor binding. Science (80-). 2005 Dec 2;310(5753):1510–2.

121. Jennewein MF, Alter G. The Immunoregulatory Roles of Antibody Glycosylation. Trends Immunol. 2017;35(5):358–72. Available from: http://dx.doi.org/10.1016/j.it.2017.02.004

122. Nimmerjahn F, Bruhns P, Horiuchi K, Ravetch J V. FcγRIV: A novel FcR with distinct IgG subclass specificity. Immunity. 2005 Jul;23(1):41–51.

123. Nimmerjahn F, Ravetch J V. Fcγ receptors: Old friends and new family members. Immunity. 2006;24(1):19–28.

124. Bartsch YC, Rahmöller J, Mertes MMM, Eiglmeier S, Lorenz FKM, Stoehr AD, et al.

Sialylated autoantigen-reactive IgG antibodies attenuate disease development in autoimmune mouse models of Lupus nephritis and rheumatoid arthritis. Front Immunol. 2018 Jun 6;9(JUN).

125. Irvine EB, Alter G. Understanding the role of antibody glycosylation through the lens of severe viral and bacterial diseases. Glycobiology. 2020 Mar 20;30(4):241–53.

126. Collin M, Ehlers M. The carbohydrate switch between pathogenic and immunosuppressive antigen-specific antibodies. Vol. 22, Experimental Dermatology. Exp Dermatol; 2013. p. 511–4.

127. Epp A, Sullivan KC, Herr AB, Strait RT. Immunoglobulin Glycosylation Effects in Allergy and Immunity. Curr Allergy Asthma Rep. 2016;16(11). Available from: http://dx.doi.org/10.1007/s11882-016-0658-x

128. Gudelj I, Lauc G, Pezer M. Immunoglobulin G glycosylation in aging and diseases. Cell Immunol. 2018 Nov 1;333:65–79.

129. Kaneko Y, Nimmerjahn F, Ravetch J V. Anti-inflammatory activity of immunoglobulin G resulting from Fc sialylation. Science (80-). 2006 Aug 4;313(5787):670–3.

130. Anthony RM, Wermeling F, Karlsson MCI, Ravetch J V. Identification of a receptor required for the anti-inflammatory activity of IVIG. Proc Natl Acad Sci U S A. 2008 Dec 16;105(50):19571–8.

131. Anthony RM, Kobayashi T, Wermeling F, Ravetch J V. Intravenous gammaglobulin suppresses inflammation through a novel T H 2 pathway. Nature. 2011 Jul 7;475(7354):110–4.

132. Oefner CM, Winkler A, Hess C, Lorenz AK, Holecska V, Huxdorf M, et al. Tolerance induction with T cell–dependent protein antigens induces regulatory sialylated IgGs. J Allergy Clin Immunol. 2012 Jun;129(6):1647-1655.e13. Available from: http://www.ncbi.nlm.nih.gov/pubmed/22502800

133. Ohmi Y, Ise W, Harazono A, Takakura D, Fukuyama H, Baba Y, et al. Sialylation converts arthritogenic IgG into inhibitors of collagen-induced arthritis. Nat Commun. 2016 Apr 5;7(1):1–12.

134. Hess C, Winkler A, Lorenz AK, Holecska V, Blanchard V, Eiglmeier S, et al. T cell-independent B cell activation induces immunosuppressive sialylated IgG antibodies. J Clin Invest. 2013 Sep;123(9):3788–96. Available from: http://www.ncbi.nlm.nih.gov/pubmed/23979161

135. Colucci M, Stöckmann H, Butera A, Masotti A, Baldassarre A, Giorda E, et al. Sialylation of N-linked glycans influences the immunomodulatory effects of IgM on T cells. J Immunol. 2015 Jan 1;194(1):151–7. Available from: https://pubmed.ncbi.nlm.nih.gov/25422509/

136. Steffen U, Koeleman CA, Sokolova M V., Bang H, Kleyer A, Rech J, et al. IgA subclasses have different effector functions associated with distinct glycosylation profiles. Nat Commun 2020 111. 2020 Jan 8;11(1):1–12. Available from: https://www.nature.com/articles/s41467-019-13992-8

137. Scapini P, Lamagna C, Hu Y, Lee K, Tang Q, DeFranco AL, et al. B cell-derived IL-10 suppresses inflammatory disease in Lyn-deficient mice. Proc Natl Acad Sci U S A.

2011 Oct 11;108(41):E823.

138. Ries S, Hilgenberg E, Lampropoulou V, Shen P, Dang VD, Wilantri S, et al. B-type suppression: A role played by “regulatory B cells” or “regulatory plasma cells”? Vol. 44, European Journal of Immunology. Wiley-VCH Verlag; 2014. p. 1251–7.

139. Sun X, Zhang T, Li M, Yin L, Xue J. Immunosuppressive B cells expressing PD-1/PD-L1 in solid tumors: A mini review. QJM An Int J Med. 2019 Jun 26; Available from: https://academic.oup.com/qjmed/advance-article/doi/10.1093/qjmed/hcz162/5523862

140. Shalapour S, Lin XJ, Bastian IN, Brain J, Burt AD, Aksenov AA, et al. Inflammation-induced IgA+ cells dismantle anti-liver cancer immunity. Nature. 2017 Nov 16;551(7680):340–5.

141. Liu J, Hamrouni A, Wolowiec D, Coiteux V, Kuliczkowski K, Hetuin D, et al. Plasma cells from multiple myeloma patients express B7-H1 (PD-L1) and increase expression after stimulation with IFN-γ and TLR ligands via a MyD88-, TRAF6-, and MEK-dependent pathway. Blood. 2007 Jul 1;110(1):296–304.

142. Mussetti A, Pellegrinelli A, Cieri N, Garzone G, Dominoni F, Cabras A, et al. PD-L1, LAG3, and HLA-DR are increasingly expressed during smoldering myeloma progression. Ann Hematol. 2019 Jul 1;98(7):1713–20.

143. Lee BH, Park Y, Kim JH, Kang KW, Lee SJ, Kim SJ, et al. PD-L1 expression in bone marrow plasma cells as a biomarker to predict multiple myeloma prognosis: developing a nomogram-based prognostic model. Sci Rep. 2020 Dec 1;10(1):1–12.

144. Li J, Wang J, Jia H, Cai X, Zhong H, Feng Q, et al. An integrated catalog of reference genes in the human gut microbiome. Nat Biotechnol. 2014;32(8):834–41.

145. Almeida A, Nayfach S, Boland M, Strozzi F, Beracochea M, Shi ZJ, et al. A unified catalog of 204,938 reference genomes from the human gut microbiome. Nat Biotechnol. 2021 Jan 1;39(1):105–14.

146. Craig Venter J, Adams MD, Myers EW, Li PW, Mural RJ, Sutton GG, et al. The sequence of the human genome. Science (80-). 2001 Feb 16;291(5507):1304–51.

147. Kim CH. Immune regulation by microbiome metabolites. Immunology. 2018;154(2):220–9. Available from: http://www.ncbi.nlm.nih.gov/pubmed/29569377

148. Koh A, De Vadder F, Kovatcheva-Datchary P, Bäckhed F. From Dietary Fiber to Host Physiology: Short-Chain Fatty Acids as Key Bacterial Metabolites. Cell. 2016 Jun 2;165(6):1332–45. Available from: http://www.ncbi.nlm.nih.gov/pubmed/27259147

149. Cummings JH, Pomare EW, Branch HWJ, Naylor CPE, MacFarlane GT. Short chain fatty acids in human large intestine, portal, hepatic and venous blood. Gut. 1987 Oct;28(10):1221–7. Available from: http://www.ncbi.nlm.nih.gov/pubmed/3678950

150. Duncan SH, Barcenilla A, Stewart CS, Pryde SE, Flint HJ. Acetate utilization and butyryl coenzyme A (CoA): Acetate-CoA transferase in butyrate-producing bacteria from the human large intestine. Appl Environ Microbiol. 2002;68(10):5186–90.

151. Venegas DP, De La Fuente MK, Landskron G, González MJ, Quera R, Dijkstra G, et al. Short chain fatty acids (SCFAs)mediated gut epithelial and immune regulation and its relevance for inflammatory bowel diseases. Vol. 10, Frontiers in Immunology. Frontiers Media S.A.; 2019. p. 277.

152. Roediger WEW. Role of anaerobic bacteria in the metabolic welfare of the colonic mucosa in man. Gut. 1980;21(9):793–8.

153. Donohoe DR, Garge N, Zhang X, Sun W, O'Connell TM, Bunger MK, et al. The microbiome and butyrate regulate energy metabolism and autophagy in the mammalian colon. Cell Metab. 2011 May 4;13(5):517–26.

154. Roediger WEW. The colonic epithelium in ulcerative colitis: an energy-deficiency disease? Lancet. 1980 Oct 4;316(8197):712–5.

155. Chen J, Vitetta L. Butyrate in Inflammatory Bowel Disease Therapy. Vol. 158, Gastroenterology. W.B. Saunders; 2020. p. 1511.

156. Sanchez HN, Moroney JB, Gan H, Shen T, Im JL, Li T, et al. B cell-intrinsic epigenetic modulation of antibody responses by dietary fiber-derived short-chain fatty acids. Nat Commun. 2020;11(1). Available from: http://dx.doi.org/10.1038/s41467-019-13603-6

157. Tolhurst G, Heffron H, Lam YS, Parker HE, Habib AM, Diakogiannaki E, et al. Short-chain fatty acids stimulate glucagon-like peptide-1 secretion via the G-protein-coupled receptor FFAR2. Diabetes. 2012;61(2):364–71.

158. Singh N, Thangaraju M, Prasad PD, Martin PM, Lambert NA, Boettger T, et al. Blockade of dendritic cell development by bacterial fermentation products butyrate and propionate through a transporter (Slc5a8)-dependent inhibition of histone deacetylases. J Biol Chem. 2010 Sep 3;285(36):27601–8.

159. Sina C, Gavrilova O, Forster M, Till A, Derer S, Hildebrand F, et al. G Protein-Coupled Receptor 43 Is Essential for Neutrophil Recruitment during Intestinal Inflammation. J Immunol. 2009;183(11):7514–22. Available from: http://www.jimmunol.org/cgi/doi/10.4049/jimmunol.0900063

160. Maslowski KM, Vieira AT, Ng A, Kranich J, Sierro F, Di Yu D, et al. Regulation of inflammatory responses by gut microbiota and chemoattractant receptor GPR43. Nature. 2009 Oct 29;461(7268):1282–6. Available from: http://www.ncbi.nlm.nih.gov/pubmed/19865172

161. Zaiss MM, Rapin A, Lebon L, Dubey LK, Mosconi I, Sarter K, et al. The Intestinal Microbiota Contributes to the Ability of Helminths to Modulate Allergic Inflammation. Immunity. 2015 Nov 17;43(5):998–1010.

162. Singh N, Gurav A, Sivaprakasam S, Brady E, Padia R, Shi H, et al. Activation of Gpr109a, receptor for niacin and the commensal metabolite butyrate, suppresses colonic inflammation and carcinogenesis. Immunity. 2014;40(1):128–39. Available from: http://dx.doi.org/10.1016/j.immuni.2013.12.007

163. Macia L, Tan J, Vieira AT, Leach K, Stanley D, Luong S, et al. Metabolite-sensing receptors GPR43 and GPR109A facilitate dietary fibre-induced gut homeostasis through regulation of the inflammasome. Nat Commun. 2015 Apr 1;6(1):1–15.

164. Struhl K. Histone acetylation and transcriptional regulatory mechanisms. Genes Dev. 1998 Mar 1;12(5):599–606. Available from: https://pubmed.ncbi.nlm.nih.gov/9499396/

165. Park SY, Kim JS. A short guide to histone deacetylases including recent progress on class II enzymes. Exp Mol Med 2020 522. 2020 Feb 19;52(2):204–12. Available from: https://www.nature.com/articles/s12276-020-0382-4

166. Riggs MG, Whittaker RG, Neumann JR, Ingram VM. n-Butyrate causes histone modification in HeLa and Friend erythroleukaemia cells. Nature. 1977;268(5619):462–4.

167. Davie JR. Inhibition of Histone Deacetylase Activity by Butyrate. J Nutr. 2003 Jul 1;133(7):2485S-2493S. Available from: http://www.ncbi.nlm.nih.gov/pubmed/12840228

168. Waldecker M, Kautenburger T, Daumann H, Busch C, Schrenk D. Inhibition of histone-deacetylase activity by short-chain fatty acids and some polyphenol metabolites formed in the colon. J Nutr Biochem. 2008;19(9):587–93.

169. Silva LG, Ferguson BS, Avila AS, Faciola AP. Sodium propionate and sodium butyrate effects on histone deacetylase (HDAC) activity, histone acetylation, and inflammatory gene expression in bovine mammary epithelial cells. J Anim Sci. 2018 Sep 25;96(12):5244–52. Available from: http://www.ncbi.nlm.nih.gov/pubmed/30252114

170. Alenghat T, Osborne LC, Saenz SA, Kobuley D, Ziegler CGK, Mullican SE, et al. Histone deacetylase 3 coordinates commensal-bacteria-dependent intestinal homeostasis. Nature. 2013;504(7478):153–7.

171. Schulthess J, Pandey S, Capitani M, Rue-Albrecht KC, Arnold I, Franchini F, et al. The Short Chain Fatty Acid Butyrate Imprints an Antimicrobial Program in Macrophages. Immunity. 2019 Feb 19;50(2):432-445.e7. Available from: http://www.ncbi.nlm.nih.gov/pubmed/30683619

172. Smith PM, Howitt MR, Panikov N, Michaud M, Gallini CA, Bohlooly-Y M, et al. The microbial metabolites, short-chain fatty acids, regulate colonic T reg cell homeostasis. Science (80-). 2013;341(6145):569–73.

173. Maslowski KM, Vieira AT, Ng A, Kranich J, Sierro F, Di Yu, et al. Regulation of inflammatory responses by gut microbiota and chemoattractant receptor GPR43. Nature. 2009;461(7268):1282–6.

174. Usami M, Kishimoto K, Ohata A, Miyoshi M, Aoyama M, Fueda Y, et al. Butyrate and trichostatin A attenuate nuclear factor κB activation and tumor necrosis factor α secretion and increase prostaglandin E2 secretion in human peripheral blood mononuclear cells. Nutr Res. 2008 May;28(5):321–8.

175. Vinolo MAR, Rodrigues HG, Hatanaka E, Sato FT, Sampaio SC, Curi R. Suppressive effect of short-chain fatty acids on production of proinflammatory mediators by neutrophils. J Nutr Biochem. 2011 Sep;22(9):849–55. Available from: http://www.ncbi.nlm.nih.gov/pubmed/21167700

176. Chang P V, Hao L, Offermanns S, Medzhitov R. The microbial metabolite butyrate regulates intestinal macrophage function via histone deacetylase inhibition. Proc

Natl Acad Sci U S A. 2014 Feb 11;111(6):2247–52. Available from: http://www.ncbi.nlm.nih.gov/pubmed/24390544

177. Trompette A, Gollwitzer ES, Yadava K, Sichelstiel AK, Sprenger N, Ngom-Bru C, et al. Gut microbiota metabolism of dietary fiber influences allergic airway disease and hematopoiesis. Nat Med. 2014;20(2):159–66.

178. Martin F, Chan AC. Pathogenic roles of B cells in human autoimmunity: Insights from the clinic. Immunity. 2004;20(5):517–27.

179. Kim M, Qie Y, Park J, Kim CH. Gut Microbial Metabolites Fuel Host Antibody Responses. Cell Host Microbe. 2016;20(2):202–14. Available from: http://dx.doi.org/10.1016/j.chom.2016.07.001

180. Kim DS, Woo JS, Min HK, Choi JW, Moon JH, Park MJ, et al. Short-chain fatty acid butyrate induces IL-10-producing B cells by regulating circadian-clock-related genes to ameliorate Sjögren's syndrome. J Autoimmun. 2021 May 1;119. Available from: https://pubmed.ncbi.nlm.nih.gov/33631650/

181. Zou F, Qiu Y, Huang Y, Zou H, Cheng X, Niu Q, et al. Effects of short-chain fatty acids in inhibiting HDAC and activating p38 MAPK are critical for promoting B10 cell generation and function. Cell Death Dis 2021 126. 2021 Jun 7;12(6):1–17. Available from: https://www.nature.com/articles/s41419-021-03880-9

182. Madan R, Demircik F, Surianarayanan S, Allen JL, Divanovic S, Trompette A, et al. Nonredundant Roles for B Cell-Derived IL-10 in Immune Counter-Regulation. J Immunol. 2009 Aug 15;183(4):2312–20. Available from: http://www.ncbi.nlm.nih.gov/pubmed/19620304

183. Oliveira LDM, Teixeira FME, Sato MN. Impact of Retinoic Acid on Immune Cells and Inflammatory Diseases. Vol. 2018, Mediators of Inflammation. Hindawi Limited; 2018.

184. Pone EJ, Lou Z, Lam T, Greenberg ML, Wang R, Xu Z, et al. B cell TLR1/2, TLR4, TLR7 and TLR9 interact in induction of class switch DNA recombination: modulation by BCR and CD40, and relevance to T-independent antibody responses. Autoimmunity. 2015 Feb 1;48(1):1. Available from: /pmc/articles/PMC4625915/

185. Rosser EC, Oleinika K, Tonon S, Doyle R, Bosma A, Carter NA, et al. Regulatory B cells are induced by gut microbiota–driven interleukin-1β and interleukin-6 production. Nat Med. 2014 Nov 1;20(11):1334–9.

186. Pendergrass W, Wolf N, Pool M. Efficacy of MitoTracker Green™ and CMXRosamine to measure changes in mitochondrial membrane potentials in living cells and tissues. Cytom Part A. 2004 Oct;61(2):162–9. Available from: http://www.ncbi.nlm.nih.gov/pubmed/15382028

187. Ehrenberg B, Montana V, Wei MD, Wuskell JP, Loew LM. Membrane potential can be determined in individual cells from the nernstian distribution of cationic dyes. Biophys J. 1988;53(5):785–94.

188. Scaduto RC, Grotyohann LW. Measurement of mitochondrial membrane potential using fluorescent rhodamine derivatives. Biophys J. 1999;76(1 I):469–77.

189. Nicholls DG, Ward MW. Mitochondrial membrane potential and neuronal glutamate

excitotoxicity: Mortality and millivolts. Vol. 23, Trends in Neurosciences. 2000. p. 166–74.

190. Cottet-Rousselle C, Ronot X, Leverve X, Mayol J-F. Cytometric assessment of mitochondria using fluorescent probes. Cytom Part A. 2011 Jun 1;79A(6):405–25. Available from: http://doi.wiley.com/10.1002/cyto.a.21061

191. Mitra K, Lippincott-Schwartz J. Analysis of mitochondrial dynamics and functions using imaging approaches. Curr Protoc Cell Biol. 2010;CHAPTER(SUPPLO. 46):4251–42521.

192. Batandier C, Fontaine E, Kériel C, Leverve XM. Determination of mitochondrial reactive oxygen species: Methodological aspects. J Cell Mol Med. 2002;6(2):175–87.

193. Kudin AP, Bimpong-Buta NYB, Vielhaber S, Elger CE, Kunz WS. Characterization of Superoxide-producing Sites in Isolated Brain Mitochondria. J Biol Chem. 2004;279(6):4127–35.

194. Kauffman M, Kauffman M, Traore K, Zhu H, Trush M, Jia Z, et al. MitoSOX-Based Flow Cytometry for Detecting Mitochondrial ROS. React Oxyg Species. 2016;2(5):361.

195. Mullis K, Faloona F, Scharf S, Saiki R, Horn G, Erlich H. Specific enzymatic amplification of DNA in vitro: The polymerase chain reaction. Cold Spring Harb Symp Quant Biol. 1986;51(1):263–73.

196. BLAST: Basic Local Alignment Search Tool [Internet]. Available from: https://blast.ncbi.nlm.nih.gov/Blast.cgi

197. UCSC In-Silico PCR [Internet]. Available from: https://genome.ucsc.edu/cgi-bin/hgPcr

198. Bartsch YC, Eschweiler S, Leliavski A, Lunding HB, Wagt S, Petry J, et al. IgG Fc sialylation is regulated during the germinal center reaction following immunization with different adjuvants. J Allergy Clin Immunol. 2020;146(3):652-666.e11.

199. Lardy HA, Johnson D, McMurray WC. Antibiotics as tools for metabolic studies. I. A survey of toxic antibiotics in respiratory, phosphorylative and glycolytic systems. Arch Biochem Biophys. 1958 Dec 1;78(2):587–97.

200. Jastroch M, Divakaruni AS, Mookerjee S, Treberg JR, Brand MD. Mitochondrial proton and electron leaks. Essays Biochem. 2010;47:53–67.

201. Terada H. Uncouplers of oxidative phosphorylation. Environ Health Perspect. 1990;87:213–8.

202. Horgan DJ, Singer TP, Casida JE. Studies on the respiratory chain-linked reduced nicotinamide adenine dinucleotide dehydrogenase. 13. Binding sites of rotenone, piericidin A, and amytal in the respiratory chain. J Biol Chem. 1968 Feb 25;243(4):834–43. Available from: http://www.ncbi.nlm.nih.gov/pubmed/4295606

203. Slater EC. The mechanism of action of the respiratory inhibitor, antimycin. Vol. 301, BBA Reviews On Bioenergetics. 1973. p. 129–54.

204. XF Cell Mito Stress Test Report Generator User Guide [Internet]. Agilent Seahorse. p. 1–9. Available from: https://www.agilent.com/cs/library/usermanuals/public/Report_Generator_User_

Guide_Seahorse_XF_Cell_Mito_Stress_Test_Single_File.pdf

205. Traba J, Miozzo P, Akkaya B, Pierce SK, Akkaya M. An optimized protocol to analyze glycolysis and mitochondrial respiration in lymphocytes. J Vis Exp. 2016 Nov 21;2016(117).

206. Recaldin T, Fear DJ. Transcription factors regulating B cell fate in the germinal centre. Clin Exp Immunol. 2016;183(1):65–75.

207. Shukla V, Lu R. IRF4 and IRF8: Governing the virtues of B Lymphocytes. Front Biol (Beijing). 2014 Aug;9(4):269–82. Available from: http://www.ncbi.nlm.nih.gov/pubmed/25506356

208. Carotta S, Willis SN, Hasbold J, Inouye M, Pang SHM, Emslie D, et al. The transcription factors IRF8 and PU.1 negatively regulate plasma cell differentiation. J Exp Med. 2014;211(11):2169–81.

209. Collison LW, Workman CJ, Kuo TT, Boyd K, Wang Y, Vignali KM, et al. The inhibitory cytokine IL-35 contributes to regulatory T-cell function. Nature. 2007 Nov 21;450(7169):566–9. Available from: https://www.nature.com/articles/nature06306

210. Poniatowski LA, Wojdasiewicz P, Gasik R, Szukiewicz D. Transforming Growth Factor Beta Family: Insight into the Role of Growth Factors in Regulation of Fracture Healing Biology and Potential Clinical Applications. Mediators Inflamm. 2015;2015. Available from: /pmc/articles/PMC4325469/

211. Fillatreau S. Regulatory functions of B cells and regulatory plasma cells. Vol. 42, Biomedical Journal. Elsevier B.V.; 2019. p. 233–42.

212. Fillatreau S. Regulatory plasma cells. Curr Opin Pharmacol. 2015;23:1–5. Available from: http://dx.doi.org/10.1016/j.coph.2015.04.006

213. Epp A, Hobusch J, Bartsch YC, Petry J, Lilienthal GM, Koeleman CAM, et al. Sialylation of IgG antibodies inhibits IgG-mediated allergic reactions. J Allergy Clin Immunol. 2018 Jan 1;141(1):399-402.e8. Available from: https://pubmed.ncbi.nlm.nih.gov/28728998/

214. Petry J, Rahmöller J, Dühring L, Lilienthal GM, Lehrian S, Buhre JS, et al. Enriched blood IgG sialylation attenuates IgG-mediated and IgG-controlled-IgE-mediated allergic reactions. J Allergy Clin Immunol. 2021 Feb 1;147(2):763–7. Available from: http://www.jacionline.org/article/S0091674920308873/fulltext

215. Luu M, Visekruna A. Short-chain fatty acids: Bacterial messengers modulating the immunometabolism of T cells. Eur J Immunol. 2019 Jun 17;49(6):842–8. Available from: https://onlinelibrary.wiley.com/doi/abs/10.1002/eji.201848009

216. Kim MH, Kang SG, Park JH, Yanagisawa M, Kim CH. Short-chain fatty acids activate GPR41 and GPR43 on intestinal epithelial cells to promote inflammatory responses in mice. Gastroenterology. 2013;145(2).

217. Wang Y, Jiao X, Kayser F, Liu J, Wang Z, Wanska M, et al. The first synthetic agonists of FFA2: Discovery and SAR of phenylacetamides as allosteric modulators. Bioorg Med Chem Lett. 2010 Jan 15;20(2):493–8. Available from: https://www.sciencedirect.com/science/article/pii/S0960894X09016825?via%3Dih

ub

218. Rooks MG, Garrett WS. Gut microbiota, metabolites and host immunity. Nat Rev Immunol. 2016;16(6):341–52. Available from: http://www.ncbi.nlm.nih.gov/pubmed/27231050

219. Clark A, Mach N. The crosstalk between the gut microbiota and mitochondria during exercise. Vol. 8, Frontiers in Physiology. Frontiers Media S.A.; 2017. p. 319.

220. Chi Z, Chen S, Xu T, Zhen W, Yu W, Jiang D, et al. Histone Deacetylase 3 Couples Mitochondria to Drive IL-1β-Dependent Inflammation by Configuring Fatty Acid Oxidation. Mol Cell. 2020;80(1):43-58.e7. Available from: https://doi.org/10.1016/j.molcel.2020.08.015

221. Swindle EJ, Hunt JA, Coleman JW. A Comparison of Reactive Oxygen Species Generation by Rat Peritoneal Macrophages and Mast Cells Using the Highly Sensitive Real-Time Chemiluminescent Probe Pholasin: Inhibition of Antigen-Induced Mast Cell Degranulation by Macrophage-Derived Hydrogen Pero. J Immunol. 2002;169(10):5866–73.

222. Wang Y, Biswas G, Prabu SK, Avadhani NG. Modulation of mitochondrial metabolic function by phorbol 12-myristate 13-acetate through increased mitochondrial translocation of protein kinase Cα in C2C12 myocytes. Biochem Pharmacol. 2006;72(7):881–92.

223. Huang R, Zhao L, Chen H, Yin RH, Li CY, Zhan YQ, et al. Megakaryocytic differentiation of K562 cells induced by PMA reduced the activity of respiratory chain complex IV. PLoS One. 2014 May 9;9(5).

224. LeBien TW, Tedder TF. B lymphocytes: how they develop and function. Blood. 2008 Sep 1;112(5):1570–80. Available from: https://doi.org/10.1182/blood-2008-02-078071

225. Sanderson RD, Lalor P, Bernfield M. B lymphocytes express and lose syndecan at specific stages of differentiation. Cell Regul. 1989;1(1):27–35. Available from: https://pubmed.ncbi.nlm.nih.gov/2519615/

226. McCarron MJ, Park PW, Fooksman DR. CD138 mediates selection of mature plasma cells by regulating their survival. Blood. 2017 May 18;129(20):2749. Available from: /pmc/articles/PMC5437827/

227. Wilmore JR, Jones DD, Allman D. Improved resolution of plasma cell subpopulations by flow cytometry. Eur J Immunol. 2017 Aug 1;47(8):1386. Available from: /pmc/articles/PMC5584378/

228. Tan J, McKenzie C, Potamitis M, Thorburn AN, Mackay CR, Macia L. The Role of Short-Chain Fatty Acids in Health and Disease. Adv Immunol. 2014 Jan 1;121:91–119. Available from: https://www.sciencedirect.com/science/article/pii/B9780128001004000039

229. Tao R, de Zoeten EF, Özkaynak E, Chen C, Wang L, Porrett PM, et al. Deacetylase inhibition promotes the generation and function of regulatory T cells. Nat Med. 2007 Nov 7;13(11):1299–307. Available from: http://www.nature.com/articles/nm1652

230. Lucas JL, Mirshahpanah P, Haas-Stapleton E, Asadullah K, Zollner TM, Numerof RP.

Induction of Foxp3+ regulatory T cells with histone deacetylase inhibitors. Cell Immunol. 2009 Jan 1;257(1–2):97–104.

231. Zhou L, Zhang M, Wang Y, Dorfman RG, Liu H, Yu T, et al. Faecalibacterium prausnitzii Produces Butyrate to Maintain Th17/Treg Balance and to Ameliorate Colorectal Colitis by Inhibiting Histone Deacetylase 1. Inflamm Bowel Dis. 2018 Aug 16;24(9):1926–40. Available from: http://www.ncbi.nlm.nih.gov/pubmed/29796620

232. Matt SM, Allen JM, Lawson MA, Mailing LJ, Woods JA, Johnson RW. Butyrate and dietary soluble fiber improve neuroinflammation associated with aging in mice. Front Immunol. 2018 Aug 14;9(AUG):1832.

233. Xu Z, Pone EJ, Al-Qahtani A, Park SR, Zan H, Casali P. Regulation of aicda expression and AID activity: Relevance to somatic hypermutation and class switch DNA recombination. Crit Rev Immunol. 2007;27(4):367. Available from: /pmc/articles/PMC2994649/

234. Klein U, Dalla-Favera R. Germinal centres: role in B-cell physiology and malignancy. Nat Rev Immunol 2008 81. 2008 Jan;8(1):22–33. Available from: https://www.nature.com/articles/nri2217

235. Avery DT, Kalled SL, Ellyard JI, Ambrose C, Bixler SA, Thien M, et al. BAFF selectively enhances the survival of plasmablasts generated from human memory B cells. J Clin Invest. 2003 Jul 15;112(2):286–97.

236. Hall JA, Grainger JR, Spencer SP, Belkaid Y. The Role of Retinoic Acid in Tolerance and Immunity. Immunity. 2011 Jul 22;35(1):13. Available from: /pmc/articles/PMC3418663/

237. Shen P, Fillatreau S. Antibody-independent functions of B cells: A focus on cytokines. Vol. 15, Nature Reviews Immunology. Nature Publishing Group; 2015. p. 441–51.

238. Fillatreau S. Natural regulatory plasma cells. Curr Opin Immunol. 2018 Dec 1;55:62. Available from: /pmc/articles/PMC6290076/

239. Matthews AJ, Zheng S, DiMenna LJ, Chaudhuri J. Regulation of Immunoglobulin Class-Switch Recombination. 2014. 1–57 p.

240. Arpaia N, Campbell C, Fan X, Dikiy S, van der Veeken J, DeRoos P, et al. Metabolites produced by commensal bacteria promote peripheral regulatory T-cell generation. Nature. 2013 Dec 19;504(7480):451–5. Available from: http://www.ncbi.nlm.nih.gov/pubmed/24226773

241. Furusawa Y, Obata Y, Fukuda S, Endo TA, Nakato G, Takahashi D, et al. Commensal microbe-derived butyrate induces the differentiation of colonic regulatory T cells. Nature. 2013 Dec 13;504(7480):446–50. Available from: http://www.nature.com/articles/nature12721

242. Arpaia N, Rudensky AY, Offermanns S, Medzhitov R. Microbial metabolites control gut inflammatory responses. Proc Natl Acad Sci U S A. 2014 Feb 11;111(6):2058–9. Available from: http://www.ncbi.nlm.nih.gov/pubmed/24434557

243. Grunstein M. Histone acetylation in chromatin structure and transcription. Nature. 1997;389(6649):349–52. Available from:

https://pubmed.ncbi.nlm.nih.gov/9311776/

244. Lee SC, Bottaro A, Insel RA. Activation of terminal B cell differentiation by inhibition of histone deacetylation. Mol Immunol. 2003;39(15):923–32.

245. Tay RE, Olawoyin O, Cejas P, Xie Y, Meyer CA, Weng QY, et al. Hdac3 is an epigenetic inhibitor of the cytotoxicity program in CD8 T cells. J Exp Med. 2020 Jul 6;217(7). Available from: https://doi.org/10.1084/jem.20191453

246. Scharer CD, Barwick BG, Guo M, Bally APR, Boss JM. Plasma cell differentiation is controlled by multiple cell division-coupled epigenetic programs. Nat Commun 2018 91. 2018 Apr 27;9(1):1–14. Available from: https://www.nature.com/articles/s41467-018-04125-8

247. Stengel KR, Barnett KR, Wang J, Liu Q, Hodges E, Hiebert SW, et al. Deacetylase activity of histone deacetylase 3 is required for productive VDJ recombination and B-cell development. Proc Natl Acad Sci U S A. 2017 Aug 8;114(32):8608–13.

248. Stengel KR, Bhaskara S, Wang J, Liu Q, Ellis JD, Sampathi S, et al. Histone deacetylase 3 controls a transcriptional network required for B cell maturation. Nucleic Acids Res. 2019 Oct 5; Available from: https://academic.oup.com/nar/advance-article/doi/10.1093/nar/gkz816/5581732

249. Mochizuki K, Hayashi Y, Sekinaka T, Otsuka K, Ito-Matsuoka Y, Kobayashi H, et al. Repression of Somatic Genes by Selective Recruitment of HDAC3 by BLIMP1 Is Essential for Mouse Primordial Germ Cell Fate Determination. Cell Rep. 2018 Sep 4;24(10):2682-2693.e6. Available from: https://pubmed.ncbi.nlm.nih.gov/30184502/

250. Huang S, Chen G, Sun J, Chen Y, Wang N, Dong Y, et al. Histone deacetylase 3 inhibition alleviates type 2 diabetes mellitus-induced endothelial dysfunction via Nrf2. Cell Commun Signal. 2021 Dec 1;19(1):1–16. Available from: https://biosignaling.biomedcentral.com/articles/10.1186/s12964-020-00681-z

251. Martin F, Chan AC. Pathogenic Roles of B Cells in Human Autoimmunity: Insights from the Clinic. Immunity. 2004 May 1;20(5):517–27. Available from: http://www.cell.com/article/S1074761304001128/fulltext

252. O'Neill SK, Glant TT, Finnegan A. The role of B cells in animal models of rheumatoid arthritis. Front Biosci. 2007;12(5):1722–36.

253. Constantinescu CS, Farooqi N, O'Brien K, Gran B. Experimental autoimmune encephalomyelitis (EAE) as a model for multiple sclerosis (MS). Br J Pharmacol. 2011 Oct;164(4):1079. Available from: /pmc/articles/PMC3229753/

254. Banasiewicz T, Domagalska D, Borycka-Kiciak K, Rydzewska G. Determination of butyric acid dosage based on clinical and experimental studies – a literature review. Przegląd Gastroenterol. 2020;15(2):119. Available from: /pmc/articles/PMC7294979/

8 APPENDIX

8.1 Abbreviations

2-ME	Dimercaptoethanol
AA	Antimycin A
AB	Antibody
AF488	Alexa Fluor 488
AICDA	Activation-induced cytidine deaminase
APC	Allophycocyanin
APRIL	A proliferation-inducing ligand
ATP	Adenosine triphosphate
atRA	All-trans Retinoic Acid
BAFF	B cell-activating factor
BCL6	B-cell lymphoma 6 protein
BCMA	B cell maturation antigen
BCR	B cell receptor
BLIMP1	B lymphocyte-induced maturation protein-1
Br1	B regulatory 1
Breg	Regulatory B cell
BV	Brilliant Violet
CD	Cluster of differentiation
CTP	Cytidine triphosphate
DC	Dendritic cell
DMSO	Dimethyl sulfoxide
DW	Drinking water
EBI3	Epstein-Barr virus-induced gene 3
ECAR	Extracellular Acidification Rate
EDTA	Ethylenediaminetetraacetic acid
ELISA	Enzyme-linked Immunosorbent Assay
Fab	Antigen-binding fragment
FACS	Fluorescence Activated Cell Sorting
FBS	Fetal Bovine Serum
Fc	Crystallizable fragment

FCCP	Carbonyl cyanide-*4*-(trifluoromethoxy)phenylhydrazone
FFAR	Free fatty acid receptor
GFP	Green fluorescent protein
GPR	G-protein-coupled receptor
GTP	Guanosine triphosphate
HDAC	Histone deacetylase
HDACi	Histone deacetylase inhibition
HEPES	4-(2-hydroxyethyl)-1-piperazineethanesulfonic acid
i.p.	Intraperitoneal
Ig	Immunoglobulin
IL	Interleukin
Irf4	Interferon regulatory factor 4
Irf8	Interferon regulatory factor 8
IVIg	Intravenous immunoglobulin
MACS	Magnetic Activated Cell Sorting
MHC	Major histocompatibility complex
MMP	Mitochondrial membrane potential
MS	Multiple Sclerosis
mtROS	Mitochondrial reactive oxygen species
MZ	Marginal zone
NK	Natural killer
OCR	Oxygen Consumption Rate
OXPHOS	Oxidative phosphorylation
PAX5	Paired box protein Pax-5
PB	plasma blast
PBS	Phosphate-buffered saline
PC	plasma cell
PD-L1	Programmed cell death 1 ligand 1
PerCP-Cy5.5	Peridinin-chlorophyll protein Cyanine5.5
PPs	Peyer's Patches
PRDM1	PR domain zinc finger protein 1
qPCR	Real-time quantitative polymerase chain reaction
RA	Rheumatoid arthritis
Rot	Rotenone

RT	Room temperature
SLE	Systemic Lupus Erythematosus
T2-MZP	Transitional 2 marginal zone precursor
TACI	Transmembrane activator and CAML interactor
Tfh	T follicular helper CD4+ cell
Tfr	T follicular regulatory CD4+ cell
TGF1β	Transforming growth factor 1β
TIM1	T-cell immunoglobulin and mucin domain 1
TMB	3,3', 5,5' tetramethylbenzidine
TMRE	Tetramethylrhodamine-ethylester
Treg	Regulatory T cell
TSA	Trichostatin A
TTP	Thymidine triphosphate
XBP1	X-box binding protein 1

8.2 List of peer-reviewed publications

Bär F*, **Föh B***, Pagel R, Schröder T, Schlichting H, Hirose M, Lemcke S, Klinger A, König P, Karsten CM, et al. Carboxypeptidase E modulates intestinal immune homeostasis and protects against experimental colitis in mice. *PLoS One* (2014) **9**:1–9. doi:10.1371/journal.pone.0102347

* These authors contributed equally

- This study established the role of Carboxypeptidase E in the pathophysiology of intestinal inflammation during experimental DSS-colitis. The enzyme was shown to be involved in regulating intestinal immune homeostasis by processing and sorting neuropeptides and affecting intestinal cytokine levels. Expression of Carboxypeptidase E in enteroendocrine cells protected mice from intestinal inflammation, underlining the relevance of enteroendocrine cells in the microbiota-gut-immune axis.

Föh B, Schröder T, Oster H, Derer S, Sina C. Seasonal Clock Changes Are Underappreciated Health Risks—Also in IBD? *Front Med* (2019) **6**: doi:10.3389/fmed.2019.00103

- This publication evaluated the effects of seasonal clock changes on IBD. Medical leave frequencies due to ulcerative colitis and Crohn's disease before and after seasonal time shifts throughout the years 2010 to 2013 were analyzed. Data were obtained from a large cohort of more than 10 million insurance holders of a German health insurance company. As a result, seasonal clock changes during winter were associated with increased medical leave frequencies. In this article, possible molecular mechanisms and the broader political, biological, and medical perspectives on seasonal clock changes were discussed extensively.

Föh B*, Borsche M*, Balck A, Taube S, Rupp J, Klein C, Katalinic A. Complications of nasal and pharyngeal swabs – a relevant challenge of the COVID-19 pandemic? *Eur Respir J* (2020) **2004004**. doi:10.1183/13993003.04004-2020

* These authors contributed equally

- During the COVID-19 pandemic deep nasal and oropharyngeal swabs quickly became one of the most conducted medical procedures worldwide. According to the WHO, more than 645 million tests involving swab procedures were performed from the beginning of the worldwide pandemic in March 2020 until mid-November 2020. However, no reliable data were available on the rate and severity of complications of this procedure. Within the ELISA-study framework, we analyzed the adverse events from approximately 11,500 swab procedures conducted on more than 3,000 participants. The results showed that swab procedures are generally very safe with a rate of severe adverse events requiring immediate medical attention of only 0.026%. However, due to the vast number of swab procedures performed the absolute number of adverse events is relevant and needs to be taken into account when evaluating test strategies during the COVID-19 pandemic.

Borsche M, Reichel D, Fellbrich A, Lixenfeld AS, Rahmöller J, Vollstedt E-J, **Föh B**, et al. Persistent cognitive impairment associated with cerebrospinal fluid anti-SARS-CoV-2 antibodies six months after mild COVID-19. *Neurol Res Pract* (2021) **3**. doi:10.1186/S42466-021-00135-Y

- We report the case of a 57-year-old female exhibiting cognitive impairment that persisted at least six months after mild COVID-19 and was associated with antibodies against SARS-CoV-2 in her cerebrospinal fluid. The case reports shows that significant neurological Long-COVID symptoms can arise even after mild courses of COVID-19 and might be associated with anti-SARS-CoV-2-antibodies.

Föh B, Danneberg S, Czauderna C, Marquardt JU. Acute esophageal tear in eosinophilic esophagitis. *Oxford Med case reports* (2021) **2021**. doi:10.1093/OMCR/OMAB056

- We report the case of a 28-year-old female with pre-existing eosinophilic esophagitis exhibiting an acute esophageal tear after ingesting a large bolus. We describe a conservative approach encompassing intravenous treatment with antibiotics, proton-pump-inhibitors, and fasting for seven days leading to complete healing of the injury.

Skibbe K, Brethack A-K, Sünderhauf A, Ragab M, Raschdorf A, Hicken M, …, **Föh B**, et al. Colorectal Cancer Progression Is Potently Reduced by a Glucose-Free, High-Protein Diet: Comparison to Anti-EGFR Therapy. *Cancers* (2021) **13**, Page 5817. 2021;13: 5817. doi:10.3390/CANCERS13225817

- In this animal study, glucose-free high-protein diet is shown to reduce cancer progression in a murine model of colorectal cancer with similar efficacy as the established anti-EGFR-antibody therapy. The dietary intervention was accompanied by a metabolic shift toward lower glycolysis activity presenting a possible underlying mechanism.

Schmelter F*, **Föh B***, Mallagaray A, Rahmöller J, Ehlers M, Lehrian S, et al. Metabolic and Lipidomic Markers Differentiate COVID-19 From Non-Hospitalized and Other Intensive Care Patients. *Front Mol Biosci* (2021) **8**: 1–12. doi:10.3389/fmolb.2021.737039

* These authors contributed equally

- In this article, metabolic markers for severe COVID-19 infections were identified. Notably, intensive care patients with COVID-19 show a severely disturbed lipoprotein profile compared to healthy controls, but also to intensive care patients suffering from cardiogenic shock. Furthermore, associations of antibody titers against SARS-CoV-2 antigens were associated with metabolic parameters after mild

COVID-19 infections. The identified metabolic markers show a potential to stratify patients for risk of severe disease but need further investigation.

Föh B, Sieren MM, Both M, Seeger M, Günther R. Extensive intrathoracic and intraperitoneal splenosis mimicking mesothelioma: a case report. *J Med Case Rep* (2022) **16**. doi:10.1186/S13256-022-03288-9

- In this case report, a rare case of extensive intrathoracic and intraabdominal splenosis decades after obtaining an abdominal gunshot wound is presented.

Föh B, Buhre JS, Lunding HB, Moreno-Fernandez ME, König P, Sina C, et al. Microbial metabolite butyrate promotes induction of IL-10+IgM+ plasma cells. *PLoS One* (2022) **17**: e0266071. doi:10.1371/JOURNAL.PONE.0266071

- In this article, the main results of the present study are summarized and published for the scientific community.

Klein C*, Borsche M*, Balck A*, **Föh B***, Rahmöller J, Peters E, et al. One-year surveillance of SARS-CoV-2 transmission of the ELISA cohort: A model for population-based monitoring of infection risk. *Sci Adv* (2022) **8**: 5016. doi:10.1126/SCIADV.ABM5016

* These authors contributed equally

- Here, we report the results of the first prospective cohort for surveillance of SARS-CoV-2 transmission. Data from a representative group of approximately 1% of the inhabitants of the catchment area over a period of one year, is presented. We provide an analysis of occupational and behavioral risk factors for SARC-CoV-2 infection and provide a transferable model for the surveillance of future pandemics.

8.3 Conference contributions

8.3.1 Talks

06/2013 – 26th Annual Meeting of the German Working Group on Inflammatory Bowel Diseases (DACED), Mainz, Germany. **Föh B**, Bär F, Sina C. Effect of Carboxypeptidase E deficiency on the intestinal inflammatory reaction.

01/2018 – 28th Annual Meeting of the Northern German Society for Gastroenterology (NDGG e.V.), Hannover, Germany. **Föh B**, Seeger M, Guenther R. Presentation of the special gastroeneterologic case: "Frankfurt is a dangerous place".

10/2019 – Annual Retreat of the IRTG1911, Heiligenhafen, Germany. **Föh B**, Sina C, Divanovic S. Microbial metabolite Butyrate promotes differentiation of regulatory plasma cells.

8.3.2 Posters

04/2013 – 119th Congress of the German Society for Internal Medicine (DGIM), Wiesbaden, Germany. **Föh B**, Baer F, Lehnert H, Fellermann K, Ibrahim S, Sina C. Effect of Carboxypeptidase E deficiency on the intestinal inflammatory reaction of mice.

09/2018 – 2nd International Symposium "Allergy Meets Infection", Lübeck, Germany. **Föh B**, Schroeder T, Derer S, Divanovic S, Sina C. Immunomodulatory properties of bacterial metabolites on L- and B-cells.

02/2020 – Keystone Symposia Conference "Obesity and NAFLD: Mechanisms and Therapeutics", Banff, Canada. **Föh B***, Mitchell P.L.*, Nachbar R., Trottier J., Barbier O., Marette A. Docosapentaenoic Acid alone or in combination with Atorvastatin alleviates NAFLD in dyslipidemic mice.

* These authors contributed equally

10/2020 – Joint Annual Immunology Retreat of the University of Cincinnati and the Cincinnati Children's Medical Center, Cincinnati, USA. **Föh B**, Sina C, Divanovic S. Microbial metabolite Butyrate promotes differentiation of antigen-specific plasma cells with a regulatory phenotype.

8.4 Acknowledgments

I want to sincerely thank my mentor Prof. Christian Sina. Years ago, I was able to finish my M.D. thesis at your research lab, when I just finished my medical studies. After spending a year of clinical work in Kiel, you gave me the opportunity to pursue my Ph.D. in the Institute of Nutritional Medicine, where I not only had the necessary resources and conditions to continue my research until now but where I also met a lot of great people who sometimes became great friends. I also want to thank you for the important ideas and the advice I got, when working on this specific project and putting my results into a clinical context.

Furthermore, I want to express my deep gratitude to Prof. Marc Ehlers, who was essential in providing immunological expertise and experimental setups that I used for large parts of this study. I thank you for all the discussions, comments, and hard work that were absolutely necessary to complete this thesis, as well as for providing materials, without some of the experiments would not have been possible.

Furthermore, I want to thank my supervisor in the U.S. Senad Divanovic for his guidance, humor, and valuable scientific input, especially on immunometabolic analyses. I also want to thank Maria Fields, Jarren Oates, Pablo Alarcon, Michelle Damen, Jessica Doll, and Traci Stankiewicz for welcoming me with open arms to the group and Cincinnati. My gratitude belongs to the IRTG1911 and all its members for giving me the opportunity to work on this project with such great collaborators.

I distinctly want to thank Jana Sophia Buhre from the Ehlers lab. You are the person that helped with a lot of the experimental efforts, that were put into this project and were one of the most important partners for discussing results and data. Without your help, this project would not have taken its current form.

I also want to thank all the other fellow Ph.D. colleagues from the Institute of Nutritional Medicine, who were there to share experimental advice, stories, and sometimes frustrations. In particular, I want to express my gratitude to Hanna Lunding from the Ehlers lab, who was there for a large part of my work and became not only a colleague but one of my best friends.

My deepest gratitude belongs to my family. Everything I can possibly achieve is a reflection of the support I have and always had from Heinke, Torsten, and Fabian Föh, as well as my partner Katharina Mitzlaff. Nothing is possible without you.

8.5 Curriculum vitae

Personal Data

Date of birth	February 17th, 1990
Place of birth	Kiel
Address	Moltkestraße 6, 23564 Lübeck
Phone	+49 160 1542 704
Email	bandik.foeh@outlook.com

Education

08/2000 – 06/2009	High School Diploma (Grade 1.1) at the Klaus-Groth Schule, Neumünster, Germany
10/2009 – 12/2015	Studies in Medicine at the University of Lübeck, Germany
12/2015	Medical License
2016	MD thesis on "Carboxypeptidase E Modulates Intestinal Immune Homeostasis and Protects against Experimental Colitis in Mice" at the University of Lübeck, *summa cum laude*

Work Experience

08/2016 – 07/2017	Resident, Department of Internal Medicine I, University Hospital Schleswig-Holstein, Campus Kiel, Germany

Since 01/2018	Research Associate/PhD project at the Institute of Nutritional Medicine, University Hospital Schleswig-Holstein, Campus Lübeck, Germany, and the Division of Immunobiology, Cincinnati Children's Hospital Medical Center, Cincinnati, USA
Since 01/2021	Clinician Scientist at the Department of Internal Medicine I, University Hospital Schleswig-Holstein, Campus Kiel, Germany
Since 2018	Reviewer for scientific journals, including: Scientific Reports, *Nature Publishing Group* Frontiers in Endocrinology, *Frontiers Media S.A.* Frontiers in Cellular and Infection Microbiology, *Frontiers Media S.A.*

Experience Abroad

03/2010 – 04/2012	Internship at the Department of Internal Medicine, Dornbirn Hospital, Dornbirn, Austria
09/2012 – 10/2012	Internship at the Emergency Hospital and the Cardiology Center of Kaliningrad, Russia
09/2019 – 12/2019	Visiting researcher at the Marette Lab, Université Laval, Québec City, Canada
01/2020 – 03-2021	Visiting researcher (as part of the PhD project) at the Divanovic Lab, Division of Immunobiology, Cincinnati Children's Hospital Medical Center, Cincinnati, USA

Particular Knowledge

Certificates	02/2018 – Lab Animal Science (mouse, rat), EU Function A 09/2018 – Ethics in Science, University of Lübeck, Germany

	11/2018 – Good Scientific Practice, University of Lübeck, Germany
	03/2019 – Biostatistics Workshop, University of Lübeck, Germany
	07/2019 – Scientific Writing, University of Lübeck, Germany
	11/2020 – Basic and advanced courses for principal investigators of clinical trials of medicinal products for human use, EU No. 536/2014
Languages	English (Proficient, C2) French (Elementary, A2) Friesian (Proficient, C2)
Data processing	MS Office (Excel), ImageJ, Flowjo, BioEdit, GraphPad, MetaboAnalyst

Lübeck, June 20th, 2022